Distribution Category:
Energy Storage—Electrochemical--
Near-Term Batteries (UC-94ca)

ANL/OEPM-81-14

ANL/OEPM--81-14

DE82 021216

Annual Report for 1981 on

RESEARCH, DEVELOPMENT, AND DEMONSTRATION OF NICKEL-IRON BATTERIES FOR ELECTRIC-VEHICLE PROPULSION

Prepared for

The Office for Electrochemical Project Management
Argonne National Laboratory
Under Contract No. 31-109-38-4141

by

Westinghouse Electric Corporation
Pittsburgh, Pennsylvania

March 1982

TABLE OF CONTENTS

		Page
	ABSTRACT	viii
1.0	EXECUTIVE SUMMARY	1-1
2.0	TECHNICAL STATUS	2-1
	2.1 NICKEL ELECTRODE	2-1
	2.1.1 NICKEL ELECTRODE SUBSTRATE	2-3
	2.1.1.1 HIGH-STRENGTH REACTIVELY SINTERED DESIGN	2-3
	2.1.1.2 CORRUGATED FIBER PLAQUE DESIGN	2-11
	2.1.1.3 "BRUSH" ELECTRODE SUBSTRATE	2-15
	2.1.1.4 HIGH DENSITY DESIGN	2-15
	2.1.1.5 NICKEL SUBSTRATE STRUCTURE DEVELOPMENT	2-15
	2.1.2 EPP NICKEL ELECTRODE	2-16
	2.1.2.1 COBALT SUBSTITUTION	2-17
	2.1.2.2 NICKEL ELECTRODE EXPANSION	2-17
	2.1.2.3 NICKEL-PLATING EXPERIMENT	2-17
	2.1.2.4 EPP PROCESSING SPECIFICATION	2-18
	2.1.2.5 GAS PRESSURE RELIEF EXPERIMENTAL DESIGN	2-18
	2.1.2.6 NICKEL ELECTRODE POLARIZATION	2-18
	2.1.2.7 NICKEL ELECTRODE ELECTROLYTE EFFECTS	2-20
	2.1.3 PASTED NICKEL ELECTRODES	2-20
	2.1.3.1 ACTIVE MATERIAL FORMULATION AND ELECTRODE SWELLING TESTS	2-23
	2.1.3.2 USE OF NICKEL CARBONATE	2-26
	2.2 IRON ELECTRODE	2-29
	2.2.1 IRON ELECTRODE SUBSTRATE	2-30
	2.2.1.1 SINGLE SINTER EVALUATION	2-30
	2.2.1.2 MANUFACTURING PROCESS	2-30
	2.2.2 COMPOSITE ELECTRODE ACTIVE MATERIAL	2-31
	2.2.2.1 IRON ELECTRODE ELECTROLYTE EFFECTS	2-32
	2.3 CELL HARDWARE COMPONENT DEVELOPMENT	2-32

TABLE OF CONTENTS (Continued)

		Page
2.3.1	SEPARATORS	2-32
2.3.2	ELECTRICAL CONNECTORS	2-34
2.3.2.1	TAB TO COLLECTOR	2-36
2.3.2.2	TERMINAL POST	2-36
2.3.3	CASE/COVER	2-38
2.3.3.1	PROTOTYPE CELL CONTAINERS	2-38
2.3.3.2	SEALING TECHNIQUES	2-40
2.3.3.3	MODULE CONCEPT	2-40
2.3.4	ELECTROLYTE MANAGEMENT SYSTEM	2-40
2.4	CELL TESTING	2-43
2.5	PILOT PLANT OPERATIONS	2-44
2.5.1	GRID FABRICATION	2-47
2.5.2	IRON ELECTRODE PRODUCTION	2-47
2.5.3	NICKEL ELECTRODE PRODUCTION	2-49
2.5.4	CELL ASSEMBLY	2-49
2.5.5	MODULE ASSEMBLY	2-53
2.5.6	BATTERY ASSEMBLY	2-53
2.6	QUALITY ASSURANCE	2-55
2.6.1	DOCUMENT REVIEW AND CONTROL	2-55
2.6.2	INSTRUCTIONS AND PROCEDURES	2-55
2.6.3	CONTROL OF MEASURING AND TEST EQUIPMENT	2-55
2.6.4	PROCUREMENT CONTROLS	2-57
2.6.5	INSPECTION AND TEST CONTROLS	2-57
2.6.5.1	ROUTE CARD 001	2-57
2.6.5.2	ROUTE CARD 002	2-57
2.6.5.3	NIBP 011	2-57
2.6.5.4	ROUTE CARD 003	2-58
2.6.5.5	ROUTE CARD 004	2-58
2.6.5.6	NIBP 008	2-61
2.6.6	CELL ASSEMBLY	2-61
2.6.7	AUDITS	2-64

TABLE OF CONTENTS (Continued)

	Page
2.6.7.1 ANL AUDIT	2-64
2.6.7.2 AESD AUDIT	2-64
3.0 TECHNICAL PERFORMANCE	3-1
3.1 THREE-PLATE CELL TESTS	3-1
3.1.1 EPP NICKEL ELECTRODE TESTS	3-3
3.1.2 PASTED NICKEL ELECTRODE TEST	3-5
3.1.3 BRIQUET IRON ELECTRODE TESTS	3-5
3.1.4 COMPOSITE IRON ELECTRODE TESTS	3-5
3.1.5 SUMMARY OF THREE-PLATE TEST RESULTS	3-8
3.2 ELECTROLYTE CONCENTRATION EVALUATION	3-9
3.2.1 NICKEL ELECTRODE ELECTROLYTE EFFECTS	3-9
3.2.2 IRON ELECTRODE ELECTROLYTE EFFECTS	3-15
3.3 FULL-SIZE CELL TESTS	3-18
3.3.1 FULL-SIZE TEST RESULTS	3-18
3.3.2 LOW TEMPERATURE TESTS	3-23
3.3.3 DISCUSSION OF RESULTS	3-30
3.3.4 CELL POST OPERATION EXAMINATION	3-34
3.4 MODULE TESTS	3-35
3.4.1 TEST EQUIPMENT	3-39
3.4.2 MODULE TEST DATA	3-41
4.0 FUTURE WORK	4-1
4.1 GRID STRUCTURE DEVELOPMENT	4-1
4.2 MULTICELL MODULE DESIGN	4-3
4.3 SEPARATOR EVALUATION	4-3
4.4 PERFORMANCE EVALUATION	4-4
4.5 CHARGE OPTIMIZATION	4-4
4.6 MODULE FABRICATION AND DEVELOPMENT SUPPORT	4-4
4.7 PROGRAM MANAGEMENT	4-4
5.0 PUBLICATIONS AND PRESENTATIONS	5-1
6.0 ACKNOWLEDGEMENTS	6-1

LIST OF TABLES

Table	Title	Page
2.1	Plaque Properties	2-8
2.2	Formation Bench Results	2-10
2.3	3-Plate Characterization Test Program	2-22
2.4	Expansion of Various Nickel Active Materials	2-25
2.5	Performance and Expansion of Nickel Carbonate Hydroxide	2-28
2.6	Quality Control Measurements on Celgard K-501	2-33
2.7	Comparison of W. R. Grace and Celanese Separator	2-35
2.8	Nickel-Iron Battery Procedures	2-56
3.1	Nickel-Iron Battery Goals	3-2
3.2	EPP-Type Nickel Electrode 3-Plate Test Results	3-4
3.3	Iron Electrode 3-Plate Test Results	3-7
3.4	Construction Details of Full-Size Nickel-Iron Cells	3-20
3.5	Full-Size Cell Test Results	3-22
3.6	Summary of Nickel-Iron Cell Post Operations Examination	3-36
3.7	Post Operations Analysis Procedure for Nickel-Iron Cells in Modules	3-38
3.8	Module ANL-1 Test Data	3-43
3.9	Module ANL-2 Test Data	3-44
3.10	Module ANL-1 Charge Efficiency	3-45
4.1	FY '82 Proposed Task Milestones	4-2

LIST OF ILLUSTRATIONS

Figure	Title	Page
2.1	Nickel Iron Battery Technical Goals	2-2
2.2	Nickel Electrode Plaque Design	2-4
2.3	State-of-the-Art Fiber Plaque in Cross Section	2-5
2.4	Reactively-Sintered Fiber Plaque in Cross Section	2-6
2.5	Positive Plate Process Flow	2-9
2.6	New Design, Method	2-12
2.7	Corrugated Fiber "Cross-Corrugated" Design	2-13
2.8	New Design Metal Fiber Plaque	2-14
2.9	Nickel Plate Performance	2-21
2.10	Comparison of Expansion and Output	2-24
2.11	Method of Spot Welding Bar Stock to Plate	2-37
2.12	Case Cover for the Nickel-Iron Cell	2-39
2.13	6-Cell Nickel-Iron Module Monoblock Design	2-41
2.14	Electrolyte Management System	2-42
2.15	Module Tester	2-45
2.16	Tester Controls and Instrumentation	2-46
2.17	Automatic Pasting Line	2-48
2.18	Batch Drying Ovens	2-50
2.19	250 Ton Press Air-Hydraulic Press	2-51
2.20	Semi-Automatic Electrode Enveloper	2-52
2.21	21-Cell Module	2-54
2.22	Iron Electrode QC Test Electrode Preparation	2-59
2.23	QC Electrode Test Data Form	2-60
2.24	Nickel Electrode QC Test Electrode Preparation	2-62
2.25	Cell QC Test Preparation Procedure	2-63
3.1	Three-Plate Test Results	3-6
3.2	Nickel Electrode Reaction	3-10
3.3	Nickel Electrode Electrolyte Concentration Effects	3-13
3.4	Iron Electrode Electrolyte Concentration Effects	3-16

LIST OF ILLUSTRATIONS (Continued)

Figure	Title	Page
3.5	Nickel-Iron Cell Configuration	3-19
3.6	Cell 270 CE Life Test Results	3-24
3.7	Cell 270 CE Cycle 52 Full Discharge Curve	3-25
3.8	Cell 270 CE Cycle 366 Full Discharge Curve	3-26
3.9	Cell 270 CE Cycle 510 Full Discharge Curve	3-27
3.10	Cell 270 CE Cycle 659 Full Discharge Curve	3-28
3.11	Cell 270 CE Cycle 366 80% Depth of Discharge	3-29
3.12	Thermal Effects on Wh Capacity	3-31
3.13	Thermal Effects Normalized to 25°C	3-32
3.14	Module EMS Test Loop	3-40
3.15	Alarm Panel Schematic	3-42

ABSTRACT

The FY '81 program continued to involve full-size, prototype cell, module and battery fabrication and evaluation, aimed at advancing the technical capabilities of the nickel-iron battery, while simultaneously reducing its potential cost in materials and process areas. Improved Electroprecipitation Process (EPP) nickel electrodes of design thickness (2.5 mm) are now being prepared that display stable capacities for the C/3 drain rate with less than 10% capacity decline for greater than 1000 test cycles. Iron electrodes of the composite-type are delivering 24 Ah at the target thickness (1.0 mm). Iron electrodes also are displaying capacity stability for greater than 1000 test cycles in continuing 3-plate cell tests. Finished cells have delivered 57 to 63 Wh/kg at C/3, and have demonstrated cyclic stability up to 1200 cycles at 80 percent depth of discharge profiles. Modules evaluated at the National Battery Test Laboratory (NBTL), Argonne National Laboratory, have exceeded 580 test cycles and remain on test.

Reduction in nickel electrode swelling (and concurrent stack starvation), to improve cycling, continues to be an area of major effort to reach the final battery cycle life objectives. Pasted nickel electrodes continue to show promise for meeting the life objectives while, simultaneously, providing a low manufacturing cost. Two full-size pasted nickel electrode cells have exceeded 700 cycles at C/3 rates to 80-100 percent depth of discharge.

Refinements have occurred in the areas of cell hardware, module manifolding and cell interconnections as a result of a related DOE/JPL battery demonstration program. These improvements have been incorporated into the construction and testing of the cells and modules for this ANL/DOE program.

1.0 EXECUTIVE SUMMARY

The basic program objective is to accelerate the development of nickel-iron batteries and demonstrate improved performance features in electric vehicle battery systems. The primary performance goals established by Westinghouse are:

60 Wh/kg	gravimetric energy density
120 Wh/l	volumetric energy density
110 W/kg	power density at 50 percent DOD
1200 cycles	life at 80 percent DOD cycles
100 $/kWh	1981 $ OEM selling price

The development approach was to utilize established Westinghouse technology that is capable of meeting the performance, life and cost objectives. The primary features of the Westinghouse design are the use of low cost raw materials, minimal use of nickel, and utilization of established manufacturing processes. A typical example is the use of sintered steel fiber electrode substrates that provide for a cell design with less than 50 percent the nickel content of other nickel-alkaline batteries.

Performance improvements achieved since initiation of contract, and demonstrated at Westinghouse in cells and multicell modules, include: 1) 30 percent increase in gravimetric energy density to 57 Wh/kg, 2) 70 percent increase in volumetric energy density to 120 Wh/l, and 3) a 5 percent increase in power density to 105 W/kg. These performance values do not include the weight and volume impact of auxiliary equipment. In addition, a conceptual design has been established for a multi-cell modular package that can further enhance these performance parameters by providing additional 9 percent weight and 15 percent volume reductions.

The demonstrated performance has indicated that an electric vehicle with characteristics similar to DOE ETV-1, with a Westinghouse nickel-iron battery, could attain a 100 mile range on the SAE J227a "D" cycle.

Additional accomplishments have been made in process development by operating pilot line facilities to demonstrate the potential for $80/kWh OEM selling price. This line was transferred in FY '81 from the R&D Center to the Advanced Energy Systems Division. Process procedures were specified to incorporate division manufacturing and quality assurance procedures. New equipment was installed to automate various segments of the processes.

Cycle life objectives remain to be demonstrated for modules and batteries. The potential for meeting the 1000 cycle goal has been enhanced by demonstration of the following: 1) iron electrode life of >1000 cycles at 80 percent depth of discharge (DOD), 2) nickel electrode life of >1000 cycles at 80 percent DOD, 3) cell life of >1000 cycles at 80 percent DOD, and 4) 5-cell module life of >580 cycles at 80 percent DOD.

Progress during FY '81 has been substantial in the areas of performance improvements and identified cost reductions. A solid base has been established to demonstrate cycle life and performance in electric vehicle systems during the next year.

2.0 TECHNICAL STATUS

The technical effort on the Nickel-Iron Battery Program during FY '81 was aimed at meeting the performance objectives as summarized in Figure 2.1.

The objective of the development task was to demonstrate improved performance capability in prototype cells, modules, and batteries. The improvements include: attaining 53-60 Wh/kg and 120-135 Wh/L in the overall cell, under a 4-8 hour charge and 2-4 hour discharge condition, while exhibiting short term, stable cycling capability.

The system development task encompasses the following major subtasks:

- o Nickel Electrode Development
- o Iron Electrode Development
- o Cell Component Development
- o Cell Testing
- o Pilot Plant Operations

The progress toward meeting the objectives of the subtasks and their status will be covered in this report.

2.1 NICKEL ELECTRODE

The nickel electrode development consists of:

- o Controlling electrode swelling
- o Improving active material utilization
- o Improving the load factor and porosity

		DOE 1986 GOALS	ANL 1981 OBJECTIVES	W 1986 GOALS
Specific Energy (at C/3 Rate)	Wh/kg	56	54	60
Volumetric Energy (at C/3 Rate)	Wh/L	120	NS	120
Peak Specific Power (30 sec. at 50% dod)	W/kg	104	110	110
Energy Efficiency (including auxiliaries)	%	70	NS	70
OEM Cost (1981 Dollars)	$/kWh	70	NS	100
Cycle Life (80% dod to 75% cap.)	Cycles	800	400	1200

Figure 2.1. Nickel-Iron Battery Technical Goals

The development of both EPP and pasted nickel electrodes is aimed at reduced material and processing costs.

2.1.1 NICKEL ELECTRODE SUBSTRATE

The electrode substrate refers to the current collector structure that is used both to contain the nickel electrode active material and to provide electrical conductivity to and from the electrode active material to the cell positive terminal. Presently, a double plaque is processed (Figure 2.2), and is cut in half to produce the final electrode substrate. The substrate consists of steel wool that is nickel plated to provide corrosion protection to the steel fibers during the EPP process. The nickel electrode substrate contains 2 vertical grooves that serve as electrolyte flow channels when the nickel electrode is installed into the cell stack.

2.1.1.1 HIGH-STRENGTH REACTIVELY-SINTERED DESIGN

Effort on the EPP nickel electrode substrates dealt with experimentation related to a new electrode design, employing a greater strength fiber plaque.

The state-of-the-art steel wool fiber plaque is comprised of mild steel fibers which are sintered in hydrogen; then electroplated with nickel metal. The result is a plaque body having a multiplicity of sintered interconnections. Figure 2.3 shows how these interconnections appear as slender "necks" joining adjacent fibers; the whole being plated with a protective coating of nickel.

When the state-of-the-art plaque with the nickel coating applied is brought to temperature in a hydrogen atmosphere for the second time, then reactive sintering occurs between fibers.

This additional, new type of sintering is due to the increased coalescence of the previously sintered joints during nickel film diffusion and the formation of nickel-iron alloys (Figure 2.4).

These fibers improve plaque strength while maintaining good conductance and corrosion resistance. Measurements confirmed that a four-fold increase in

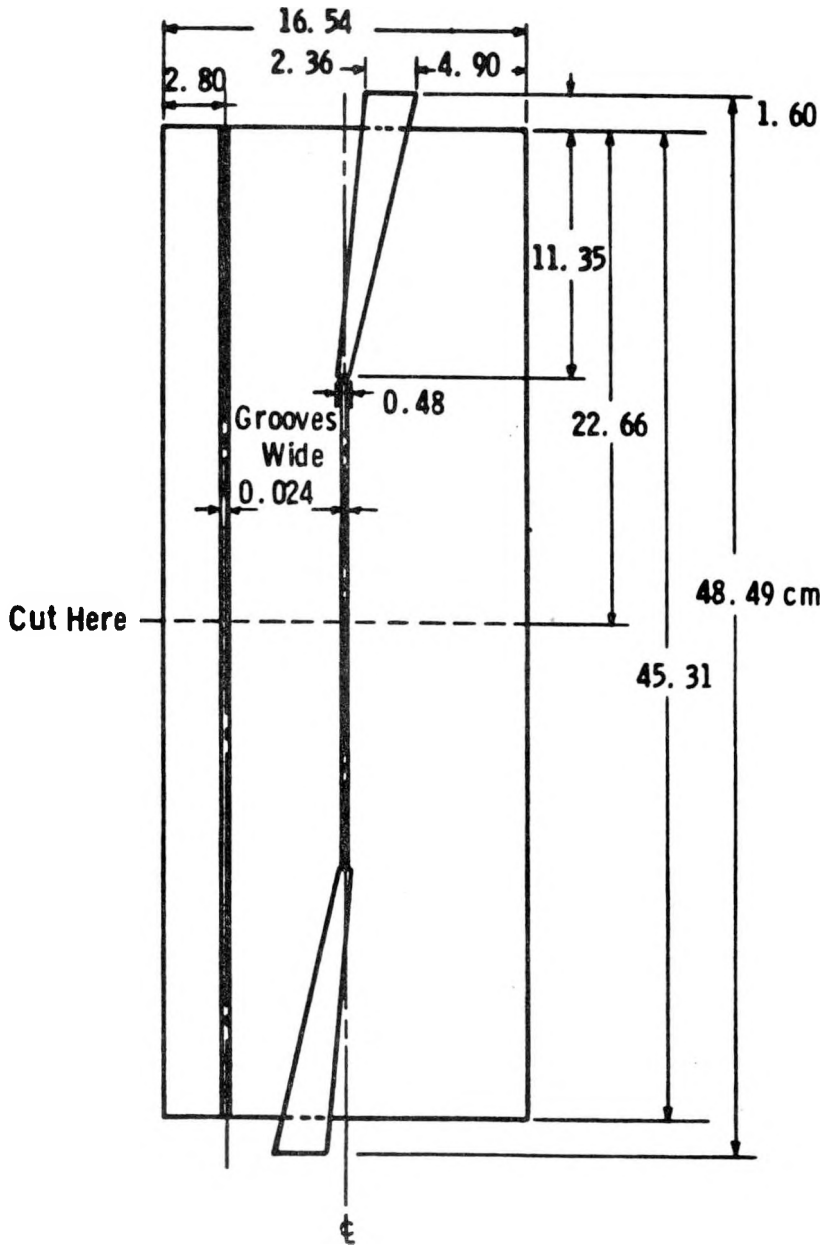

Figure 2.2. Nickel Electrode Plaque Design

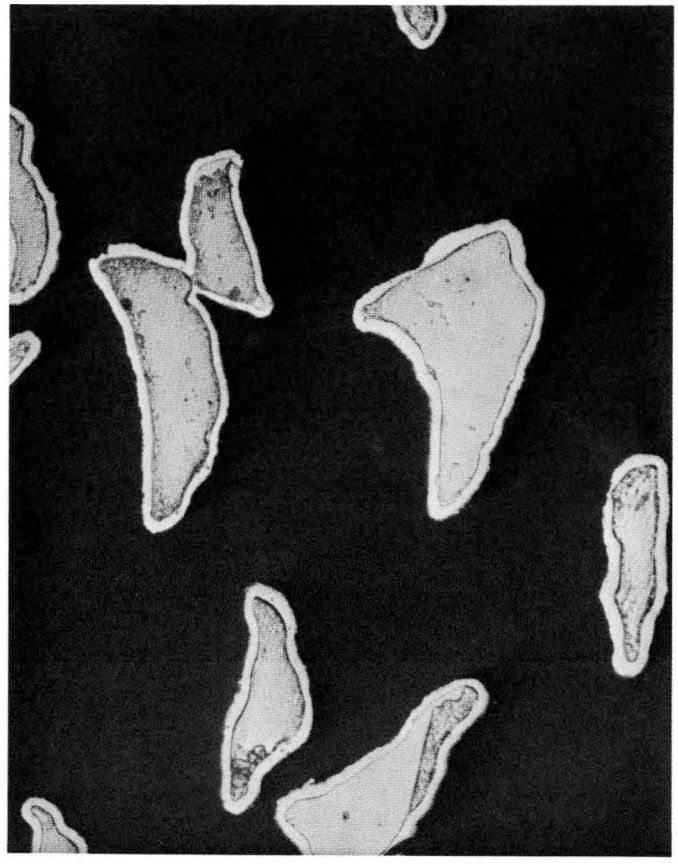

Figure 2.3. State-of-the-Art Fiber Plaque in Cross-Section (500X)

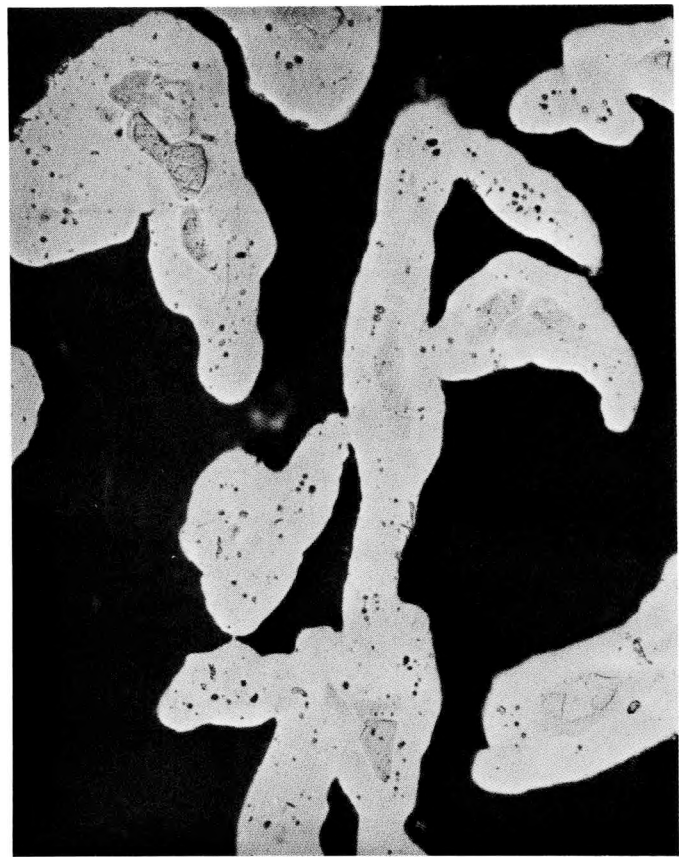

Figure 2.4. Reactively-Sintered Fiber Plaque in Cross Section (500X)

strength resulted. Further, electrical resistance of the plaque of high fiber weight, approached the resistance of plaques made in the prior art. Also, when replated with a light flash coat of nickel, the plaque exhibited excellent corrosion resistance. These results are summarized in Table 2.1.

Diffusing nickel into mild steel fibers in this way produces alloys of the genre known as "valve metal", which comprises 70 percent iron and 30 percent nickel. The compositions actually obtained probably vary around this general region, depending on the relative amounts of iron-vs-nickel plate thickness involved.

The merit of this process and design change comprises the added strength achieved through the enhanced inter-fiber sintering due to the activation energy provided by Ni-Fe alloy formation. The new alloy formed provides more strength.

As the electrical resistance and corrosion test criteria show, the fiber substrate, particularly when subsequently replated, is appropriate for use as a current collector in the nickel-iron cell.

This type of electrode is processed as outlined in Figure 2.5. The reactive sintering for increased fiber strength is the major process advantage. In addition, nickel plating is carried out before coining and before application of the tabs. The tabs also are nickel plated before welding to the fiber plate body. These nickel plating modifications were made to address the plating defects in the tab and coined areas.

Eight cells incorporating reactive sintered nickel electrode substrates were fabricated and initially cycled with the results noted in Table 2.2. Resistance of the cells equals the resistance of standard production cells, illustrating that the current collector fiber resistance is a minor component of total cell resistance.

TABLE 2.1: PLAQUE PROPERTIES

Type	Fiber Weight	Strength (psi)	Resistivity ($\mu\Omega$-cm)	Fe Corrosion (16 Hours in De-Ion H_2O mg/l, Fe)
Prior Art Plaque	Low	800 ± 60	100-200	0.4
Reactive-Sintered	High	3,500 ± 670	300	0.4

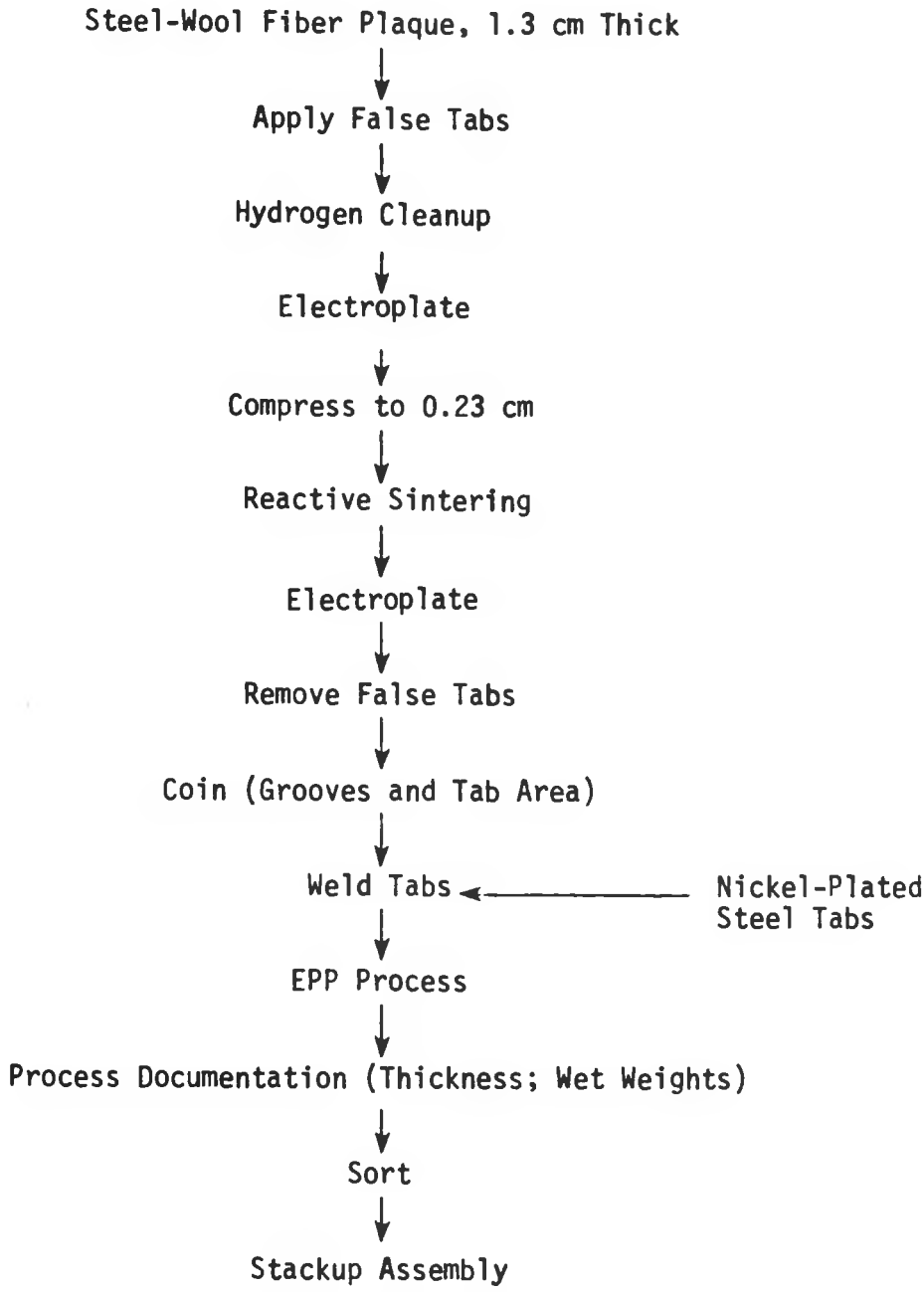

Figure 2.5. Positive Plate Process Flow

TABLE 2.2: FORMATION BENCH RESULTS

Cell No.	Maxi Run No.	Electrolyte Flow (psi, Cycle #3)	Capacity (Ah) Cycle #1	Capacity (Ah) Cycle #2	Capacity (Ah) Cycle #3	Ah/g of Active Material (Cycle #3)	Milli-Ohm Resistance (100-200A)
95	8	1.5	188	201	211	0.22	0.64
96	8	2.5	188	201	207	0.22	0.77
97	8	4.0	185	199	196	0.21	0.64
98	8	4.0	185	199	200	0.22	0.64
99	8	2.5	188	201	196	0.22	0.65
100	9	1.0	188	225	230	0.23	0.64
101	9	4.0	200	230	248	0.24	0.68
102	9	3.0	200	230	248	0.24	0.62

Tests evaluating this concept are presently in progress on an additional 21-plate cell. This cell, employing reactively sintered fibers plus nickel flash coat in the positive current collectors, was placed on cycle-life testing. Companion three-plate cells were also charge-discharge cycle tested. Preliminary cycling tests show capacity stability through 630 cycles with only 17 percent capacity decline for the 21-plate cell. A companion 3-plate cell is still on cycle-life test beyond 700 cycles with 25 percent capacity loss.

2.1.1.2 CORRUGATED FIBER PLAQUE DESIGN

The strength of the sintered metal positive fiber plaque is of the order of 4000 psi in the (x-y) plane of the plaque (length direction and width direction). It is estimated that strength in the thickness (Z) direction (normal to the plane of the plaque) is less than 100 psi, however, because the fibers are essentially lying the x-y plane.

Depending on the type of plaque "layup", many of the fibers can be made to be oriented in the "Z" direction, thus providing needed strength to the plate structure and restraining the plate expansion during cycle life. This expansion is perceived to play a critical role in cell loss of performance, therefore a stronger plaque should provide significant extension of the cell lifetime. By employing a technique which first corrugates the fiber plaque, then squeezes the corrugations to effect a better alignment with the "Z" direction, fiber alignment is provided that accomplishes an increase in "Z" direction strength to the order of 1000 psi. It is expected that electrode shape change and stackup pressure stresses can be reduced by employing this new design.

An additional benefit deriving from the new design is that the performance of the new plate should be enhanced, particularly at high rates due to the new plate being, in effect, of much higher surface area. The doubled-over 40 mil starting material also provides built-in electrolyte channels and expansion spaces for the "X" direction.

Figures 2.6 and 2.7 depict the corrugation methods being developed. The grid design being developed is shown in Figure 2.8.

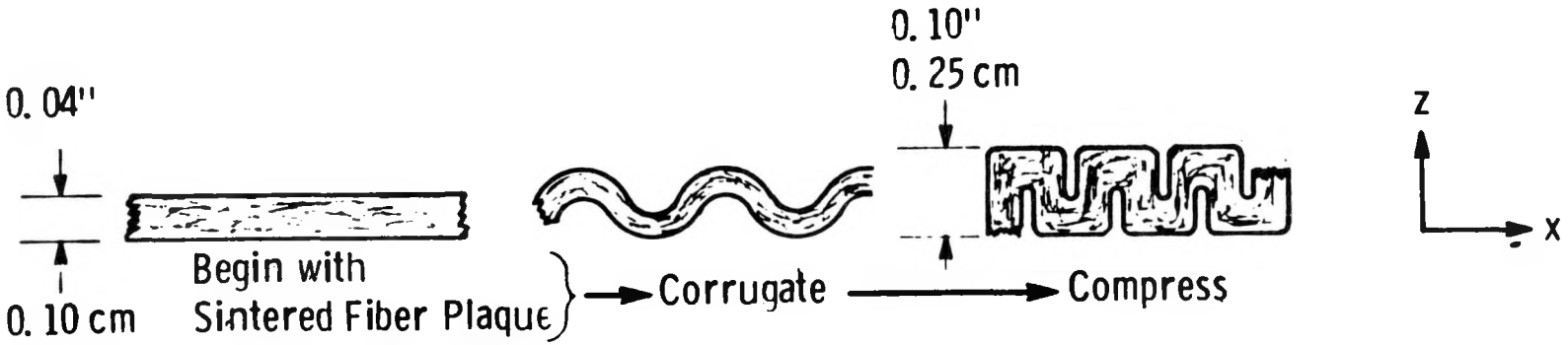

Figure 2.6. New Design, Method

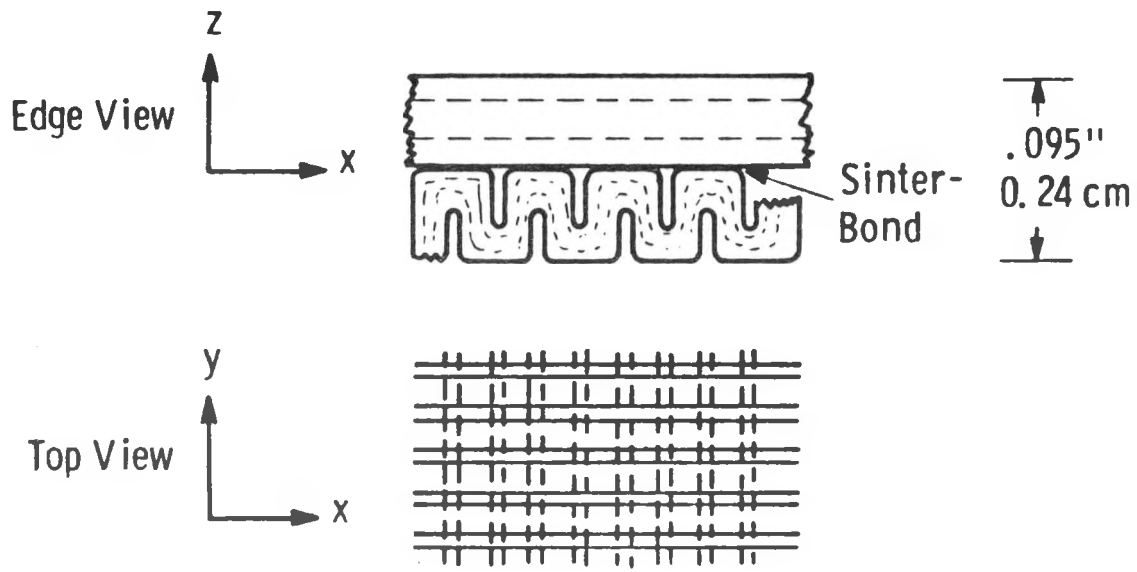

Figure 2.7. Corrugated Fiber "Cross-Corrugated" Design

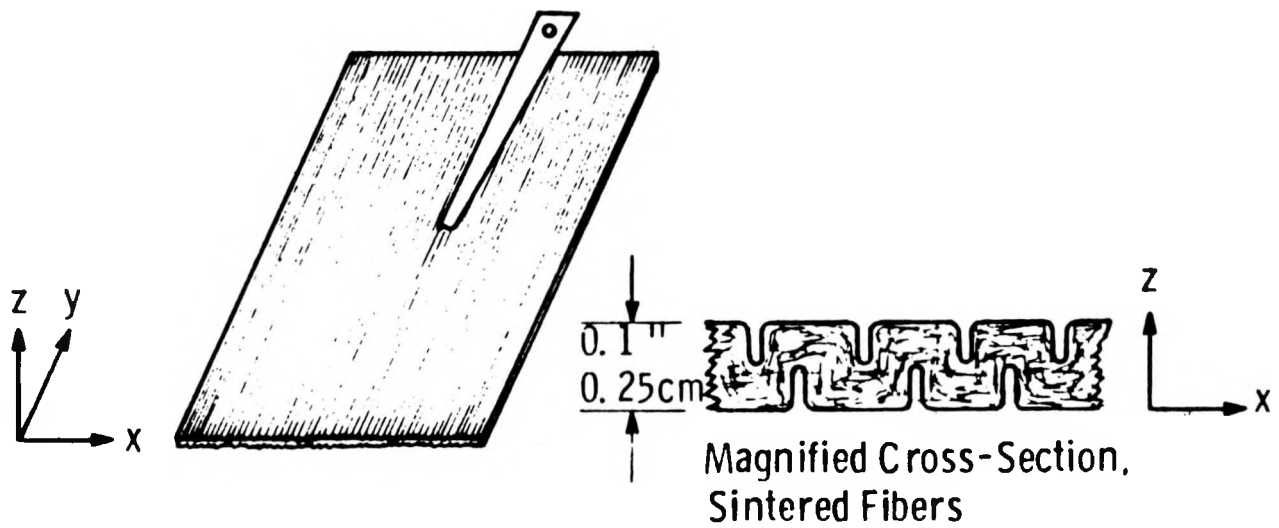

Figure 2.8. New Design Metal Fiber Plaque

Grids were produced for subsequent EPP processing to evaluate active material parameters and cycle life. Sufficient electrodes were produced for evaluation in a full size 19-plate cell and in a comparison 3-plate cell. Preliminary results show that these cells are performing at approximately a 10 percent capacity decline after 370 cycles.

2.1.1.3 "BRUSH" ELECTRODE SUBSTRATE

No further technical effort was expended on the Brush Electrode during FY '81. Refer to the "Annual Status Report for FY '80" for detailed study information.

2.1.1.4 HIGH DENSITY DESIGN

Substrate fiber density has been incrementally raised. The results, discussed in the "Annual Status Report for FY '80", demonstrated that more active material efficiency results when higher fiber density (low AM + GRID) plaques are employed.

Cells, employing high fiber density, were constructed and cycled to establish the relative merit of high fiber density on performance, particularly, electrode swelling. The results indicated that, with respect to swelling, the effect of high fiber density was minor.

2.1.1.5 NICKEL SUBSTRATE STRUCTURE DEVELOPMENT

Test and evaluation of alternative substrate materials for the nickel electrode has been initiated. The key element in the evaluation is material recently developed by National Standard Corporation. The parameters investigated under the development program are:

- Resistivity versus weight of substrate
- Electrode performance
- Economic trade offs

Comparisons were made between standard commercially available steel wool to extruded iron fiber (National Standard) samples which were sintered in hydrogen atmosphere. The following measurements were taken:

- Resistance versus weight
- Thickness versus weight

The resistance measurements were taken using a Keithly Model 503 milliohm meter with a test fixture having 1 inch square copper block contactors spaced 4 inches apart under a 1 kilogram load. The extruded iron fiber samples currently under investigation are the result of trying to duplicate steel wool presently in production. Preliminary data indicates that extruded iron fiber is more conductive than steel wool.

Based on preliminary results the National Standard resistance is lower than comparable commercially available steel wool. This can be partly attributed to the pure iron fiber which is more conductive than alloy steel of comparable fiber diameter.

2.1.2 EPP NICKEL ELECTRODE

The objective of this subtask is to improve upon the well-established Westinghouse EPP process for preparing nickel electrodes. Specifically, this effort is aimed at developing 25 Ah nickel electrodes with 0.25 Ah/g active material, 0.14 Ah/g total electrode and 0.075 Ah/cm^3, all at the 3h discharge rate. These goals are to be attained in plates of 2.54 mm maximum thickness. The EPP process technology, at the onset of this program, made 343 cm^2, <3.3 mm thick electrodes of the following specifications: 0.20 Ah/g active material, 0.12 Ah/g total electrode and 0.07 Ah/cm^2 at the 3h discharge rate.

In addition, electrode design and process techniques are being investigated to improve plate dimensional stability during operation in a nickel-iron cell.

Experiments conducted to date show EPP, as applied to fiber plaque substrates, is most consistently accomplished by employing two levels of impregnation. These levels are: a) "high" current, followed by b) "low" current.

According to the concept arising from experiments, the "high" current step reaches a saturation level with respect to accomplished impregnation with nickel in a short time. The "low" current step, which is required to complete the nickel loading to the densities needed for target capacity, can take from 16 to 20 hours to reach completion, as presently executed.

A charge step in Potassium Hydroxide is employed between the two levels of EPP processing. Total elapsed processing time is approximately 48 hours. This process has been employed for all nickel electrodes manufactured in the pilot plant during 1981.

2.1.2.1 COBALT SUBSTITUTION

No further technical effort was expended on the Cobalt Substitution during FY '81. Refer to the "Annual Status Report for FY '80" for detailed study information.

2.1.2.2 NICKEL ELECTRODE EXPANSION

An important design problem related to cycle life of the nickel-iron cell is the stack electrolyte starvation resulting from an increase in the nickel electrode thickness on cycling. The design approach under development and evaluation to circumvent and/or minimize EPP electrode swelling utilizes a high-strength substrate (Reference 2.1.1) and low-loading, high active material utilization electrode, via a high fiber density plaque design.

2.1.2.3 NICKEL-PLATING EXPERIMENT

No further technical effort was expended on the Nickel Plating Experiment during FY '81. Refer to the "Annual Status Report for FY '80" for detailed study information.

2.1.2.4 EPP PROCESSING SPECIFICATION

No further technical effort was expended on EPP Processing Specifications during FY '81. The processing specifications developed and reported in the "Annual Status Report for FY '80" are used in present processing.

2.1.2.5 GAS PRESSURE RELIEF EXPERIMENTAL DESIGN

No further technical effort was expended on the Gas Pressure Relief Experiment during FY '81. Refer to the "Annual Status Report for FY '80" for detailed study information.

2.1.2.6 NICKEL ELECTRODE POLARIZATION

When a cell employing nickel electrodes delivers current to an electric load, the voltage of the cell drops as a function of time. The voltage loss due to the nickel electrode can be divided into three components:

(1) Polarization voltage losses associated with the reaction at the nickel oxide electrode. It has been determined* that alkali metal ions and protons are incorporated into the nickel electrode during the charge reaction, and released during the discharge reaction. Such diffusion-related losses depend on the structure, e.g., porosity, of the electrode and on the current density (reaction rate) at which the electrodes are operated. The nickel electrode in the cell increases in polarization as discharge proceeds, starting with an initial nominal value of 10 mV per electrode at the C/3 rate; increasing to much more at the end of discharge. Polarization is responsible for much of the decay in loaded voltage for any given discharge as a function of discharge time. A major objective in electrode design is to provide sufficient permeability to minimize these polarization voltage losses due to diffusion.

---

*O. G. Malandin, et. al., Elektrokhimiya, 14, No. 1, 91 (1978)

(2) Resistive voltage losses associated with the ohmic resistance of the plate. These losses are dependent on the lengths and cross-sections of the electrical paths.

The resistance of the plate is made up of contributions from three components:

(a) A composite of metal fiber current collector, a semiconducting solid active material phase, and pores filled with electrolyte comprising an aqueous KOH, LiOH solution.

(b) The inter-electrode space, consisting of a porous polymeric separator and pores filled with electrolyte.

(c) Electrode leads, joining the electrode to the external circuit.

(3) Voltage loss due to the state-of-charge depends on open-circuit electrode potential. This potential, which must be evaluated by experiment, can change up to 200 mV from beginning to end of discharge.

In order to identify the polarization of the nickel electrode, all three voltage loss components must be measured. Electronic resistance was identified on an oscilloscope as the instantaneous component of the voltage drop during current interruption. The polarization contribution was observed as a slowly-decaying curve, typically requiring many seconds, or even minutes to register a stable open-circuit electrode potential. As a cell discharges, diffusion processes become progressively more hindered, so that the "polarization" component of the voltage drop increases.

Thus, the performance of the nickel positive plate is a complex mechanism involving electronic (ohmic) voltage drop, a state-of-charge dependent "polarization" voltage drop, and a state-of-charge dependent open circuit potential.

The effective voltage drop of nickel electrodes was measured as a function of discharge current density based on projected electrode area. The dependence of

resistance corrected voltage drop on current was examined over the full range of current anticipated in vehicular operation. Figure 2.9 depicts the polarization behavior of a plate comprising the corrugated fiber concept.

It illustrates electrode response when the measured generalized polarization is plotted versus a logarithmic scale of discharge current. The results indicate that these nickel electrodes may not be diffusion-limited even at the higher discharge rates corresponding to vehicle acceleration modes. Indication of possible linearity due to an activation polarization region is noted from approximately 8 to 46 amperes.

2.1.2.7 NICKEL ELECTRODE ELECTROLYTE EFFECTS

A program was initiated to determine the performance of two uniform groups of pilot production electrodes (Table 2.3).

These two groups of test cells had initially been on a schedule of 4 hours charge at 8.33A, and discharge at 8.33 amps to 3.0 hours maximum, or 1.00V minimum. These conditioning cycles were carried out through cycle No. 35.

Subsequently, the cells were modified to evaluate changes in KOH and LiOH concentration; then cycled as before, up to cycle No. 55. The response of these cells to these electrolyte compositions are displayed in Figure 3.3 in Section 3.0, "Technical Performance".

2.1.3 PASTED NICKEL ELECTRODES

The performance goals for the pasted nickel electrode are the same as those described for the electroprecipitation process (EPP) nickel electrode. However, purchase of commercially available material and subsequent pasting into the fiber metal plaque offers a reduction in total electrode manufacturing cost, a significant decrease in capital equipment expenditure and a more reliable control over final electrode thickness and weight. Effort this past year has centered on formulation of an optimum paste composition and pilot manufacture of full size electrodes. Extended life testing of a limited number of full size cells containing pasted nickel electrodes has also been accomplished.

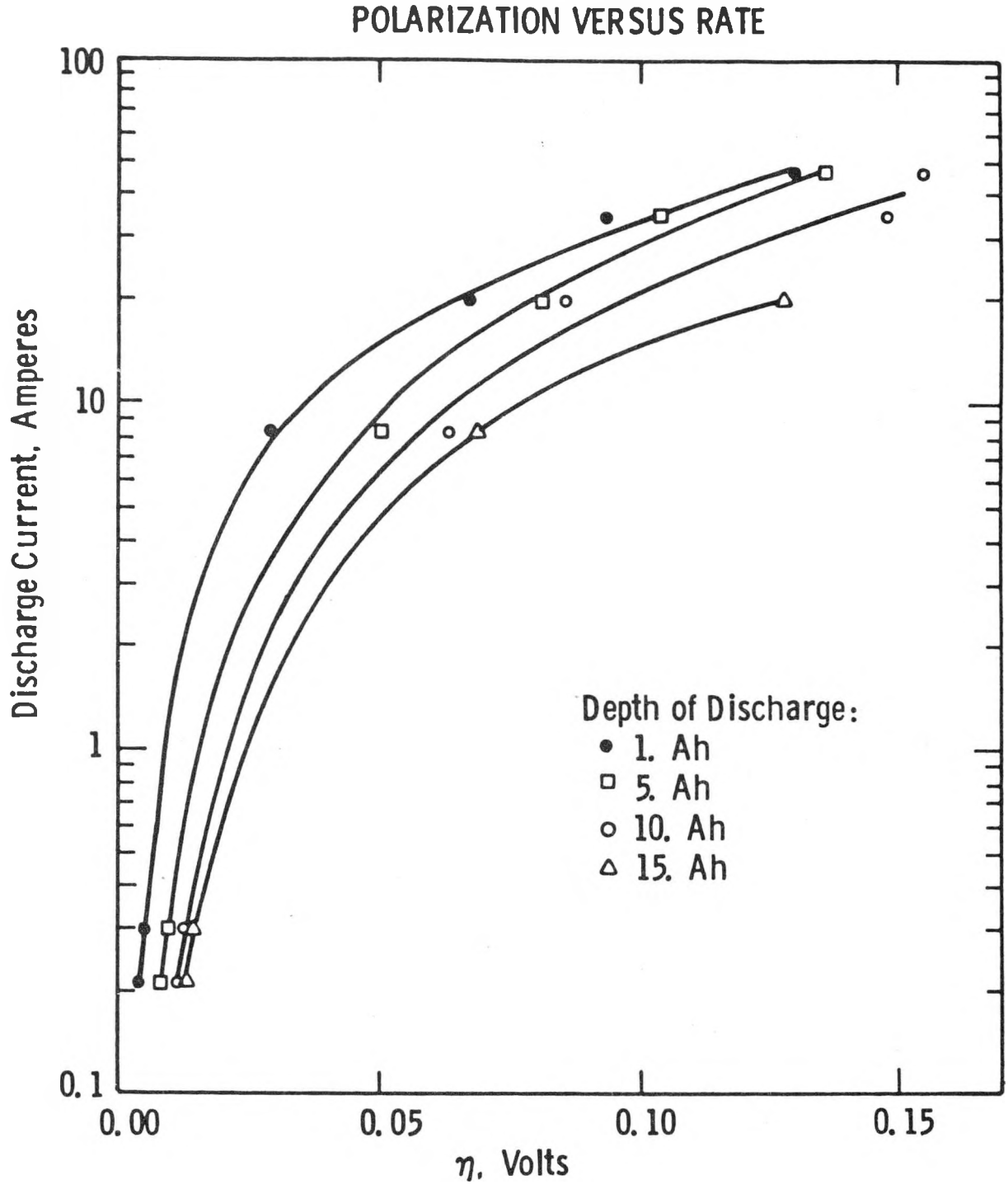

Figure 2.9. Nickel Plate Performance

TABLE 2.3: 3-PLATE CHARACTERIZATION TEST PROGRAM

Data Information:

- Capacity - Versus - Electrolyte Concentration
- Capacity - Versus - Li Concentration
- Charge Efficiency
- Self Discharge
- Polarization (IR)
- Expansion - Versus - Concentration
- Expansion - Versus - Li
- Capacity - Versus - Rate
- Charge Acceptance
- Capacity - Versus - Temperature
- Resistance - Versus State-of-Charge
- Taper Versus Constant Current Charge
- Float Service
- Driving Cycle Tests

2.1.3.1 ACTIVE MATERIAL FORMULATION AND ELECTRODE SWELLING TESTS

Initial experiments quantitatively determined the degree of nickel electrode expansion for several types of nickel active materials. Laboratory size (1 in) electrodes were used and the materials tested were commercially available green nickel hydroxide, ozonized nickel hydroxide slurry, nickel carbonate and electro-precipitated nickel hydroxide (EPP). All were tested with cobalt hydroxide additive. Several pairs of each type electrode were cycled and removed periodically for thickness measurement. For each starting material, the initial electrode thicknesses were about equal. The electrolyte used was 25 w/o KOH with 15 g/l LiOH and cycling was kept at the three hour rate. All electrodes were given a 50 percent overcharge for all cycles. The results for the four active material types are given in Figure 2.10. Electrodes pasted with green nickel hydroxide (Curve B) show the greatest expansion after 60 cycles while those pasted with nickel carbonate (Curve C) do not expand significantly after the same cycling period. Electrodes, pasted with ozonized nickel hydroxide and cobalt additive (Curve A), show a degree of expansion similar to our current EPP electrode (Curve D). Electrochemical outputs from the four materials were similar as shown in Figure 2.10. For all types of electrodes, the major portion of the total expansion occurred in the first 30 cycles.

Expansion of nickel electrodes after continuous cycling results primarily from density changes of the active material. Addition of water of hydration and interlayer cations during the charging cycle results in a volume increase of the nickel active material. For pure nickel hydroxide, addition of two water molecules per nickel atom accompanied by oxidation in an alkaline medium, can increase the material volume nearly 30 percent. Density changes for the four active materials studied are shown in Table 2.4. Pycnometer measurements were made on the initial powders and material extracted from the cycled electrodes after charging. The final densities measured for all four cycled materials were found to be the same. This occurs since the electrolyte chemistry and cycling regime were the same for each electrode thus dictating the same final structure and stoichiometry regardless of starting material. Predicted expansion of the electrodes based on measured density changes are reasonably close to the observed values. The data suggest that control of the initial density

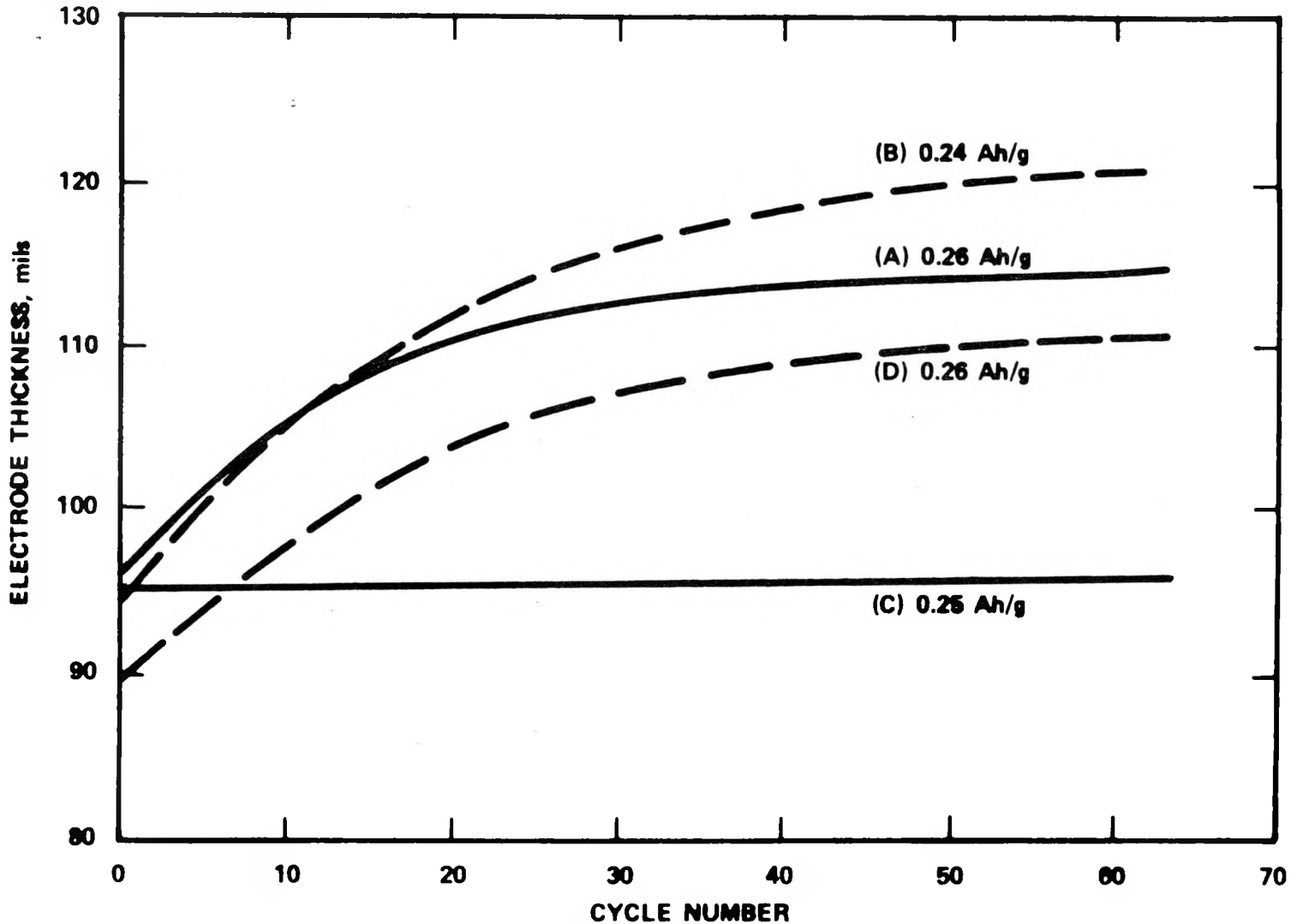

Figure 2.10. Comparison of Expansion and Output

TABLE 2.4: EXPANSION OF VARIOUS NICKEL ACTIVE MATERIALS

Active Material	Dry Active Loading g/cm^2	Initial Active Density g/cm^3	Final Active* Density g/cm^3	Predicted Expansion %	Observed Expansion %
EPP	1.95	3.10	2.65	15	15
$Ni(OH)_2$-$Co(OH)_2$	1.90	3.49	2.65	24	21
Ozonized $Ni(OH)_2$-$Co(OH)_2$					
$NiCO_3$-$Co(OH)_2$	1.95	2.72	2.65	3	<5

*Final density is a function of electrolyte chemistry and number of cycles.

of the active material can prevent electrode expansion and lead to increased electrode life.

2.1.3.2 USE OF NICKEL CARBONATE

Laboratory size (1 in^2) nickel electrodes prepared using nickel carbonate as the initial active material showed insignificant expansion on cycling. Consequently, this material was explored to determine conditions for maximum electrochemical utilization. Variables considered were electrode thickness, electrode porosity, and electrolyte concentration.

Electrode thickness was kept in the 2.0 to 2.4 mm range since, from past experience, this range was found to be optimum for best electrode performance. Also, these electrodes fit conveniently into the present design 250 Ah cells. Electrolyte was varied from standard 25 percent KOH + 15 g/l LiOH to 30 percent KOH + 10 g/l LiOH. Expansion of the carbonate-based nickel electrodes was negligible in the 30 percent KOH electrolyte while outputs were consistently higher than for the lithiated standard type.

Initial experiments involved using pure nickel carbonate as the starting active material. Paste was prepared using commercial grade nickel carbonate with cobalt hydroxide additive.

In this formulation, the materials were blended into a paste using a ball mill. The paste was rolled into a fiber metal grid support at 0.29 g/cm^2 dry loading and the initial thickness was 2.4 mm (94 mils). The finished electrode was cycled in 25 percent KOH + 15 g/l LiOH electrolyte and performance is shown in Figure 2.10 curve (C). The initial forming cycle consisted of 5 mA/cm^2 for 72 hours followed by a booster charge of 25 mA/cm^2 for four hours. Additional charge cycles were 25 mA/cm^2 for four hours. All discharges were at 25 mA/cm^2 which corresponds to the three hour rate in full size cells. During the initial charge cycle, the decomposition of nickel carbonate results in evolution of carbon dioxide which is gettered by the electrolyte to form potassium carbonate according to the equations:

$$NiCO_3 + 1/2\ O_2 + H_2O \rightarrow NiO_2 \cdot H_2O + CO_2$$

$$2KOH + CO_2 \rightarrow K_2CO_3 + H_2O$$

Presently, it is deemed necessary to change electrolyte after this initial forming cycle.

After the 60 cycle performance shown in Figure 2.10, curve (C), the electrode was taken off test for a thickness measurement. The value obtained was 2.45 mm (96 mils) showing insignificant increase over the initial 2.40 mm (94 mils) thickness.

For comparison purposes, Figure 2.10 also shows performance values for two other types of nickel electrodes. One of these is a standard electroprecipitation process (EPP) type which had an active loading of about 0.30 g/cm^2 at an initial thickness of 2.3 mm (90 mils) (Curve D). This electrode was cycled under the same conditions as the above pasted carbonate example and achieved a maximum 0.28 Ah/g output in the first few cycles. Examination of this electrode after 50 cycles showed that it had expanded to 2.8 mm (110 mils), an increase of about 20 percent over its initial value.

The other electrode included in Figure 2.10 for comparison purposes is pasted $Ni(OH)_2$ containing $Co(OH)_2$ additive (Curve A). The paste was rolled into a fiber metal grid support at 0.28 g/cm^2 at a thickness of 2.3 mm (90 mils). The cycling regime was identical to the others shown in Figure 2.11. After 50 cycles, this electrode had expanded to 2.9 mm (114 mils) or an increase of about 25 percent from its initial value.

Electrode performance and expansion data for several laboratory size (1 in^2) nickel carbonate-nickel hydroxide mixtures are shown in Table 2.5. Data were terminated at 25 cycles since previous surveys have shown that most of the expansion observed for nickel electrodes occurs within this cycling period. Active material loadings were in the 0.26 to 0.31 g/cm^2 (1.7 to 2.0 g/in^2) range and initial thicknesses were 2.26 to 2.40 mm (89 to 95 mils).

TABLE 2.5: PERFORMANCE AND EXPANSION OF NICKEL CARBONATE HYDROXIDE

Electrode No.	Dry Loading g/cm^2	Thickness, mm Initial	Final	Performance Ah/g at Cycle 1	Cycle 25
JJB	0.26	2.40	2.45	0.27	0.24
1023A	0.27	2.28	2.40	0.22	0.24
1023B	0.28	2.30	2.40	0.22	0.24
1030A	0.31	2.26	2.40	0.24	0.25
1030B	0.31	2.27	2.40	0.24	0.24
1229A	0.29	2.30	2.48	0.20	0.24
1229B	0.30	2.32	2.55	0.20	0.24
0.120	0.28	2.29	2.79	0.20	0.25

All electrodes contained $Co(OH)_2$ in the active materials. Electrolyte used for all tests was 30% KOH + 10 g/l LiOH.

Performance data show that no advantages in electrode outputs are achieved with mixtures relative to pure carbonate or hydroxide. However, an advantage with the mixtures is obtained in the initial forming cycle relative to pure carbonate, in that less contamination of the electrolyte is experienced in the initial forming cycle. Electrode expansion follows a trend from less than 3 percent for the pure carbonate to about 22 percent for the pure hydroxide. Best balance between expansion and forming electrolyte considerations is obtained using a 50-50 w/o mixture of carbonate and hydroxide.

Full size electrodes (341 cm^2) were constructed initially using a mixture containing $Ni(OH)_2$, $NiCO_3$, and $Co(OH)_2$. By milling the material with excess water, acceptable loading was attained and performance paralleled closely the parameters obtained for the laboratory sized electrodes. Loadings for the large plates was about 0.28 g/cm^2 at a final pressed thickness of 2.35 mm which follows closely the values in Table 2.5. Outputs achieved for the full size plates were in the 24-25 Ah range at the C/3 rate corresponding to 0.25 Ah/g of loaded active material. The electrodes show stable output for continuing test cycles.

It must be noted that the full size plates showed a greater degree of swelling than the small laboratory test electrodes. This was attributed to variations in testing procedures and is not expected to have a significant effect in full size cells where restraining fixtures are used. Full size electrodes containing the nickel hydroxide-nickel carbonate-cobalt hydroxide mixture have been prepared and are being assembled into cells for life and performance tests. Life test results for nickel-iron cells containing pasted nickel electrodes are included later in this report. These cells contained only nickel hydroxide and cobalt hydroxide as the active material. The addition of nickel carbonate to the active material is expected to increase performance and life relative to these initial cells.

2.2 IRON ELECTRODE

The composite-type iron electrode contains a fiber metal-expanded metal combination as the current carrier. The connection tab is spot welded firmly to the

expanded metal screen and results in good power characteristics for the iron electrode. The present battery design requires an electrode of 345 cm^2 active area and approximately 1 mm (40 mils) thickness having an output of 25 Ah at the C/3 discharge rate. The final program goal is to achieve 0.25 Ah/g of total electrode (30 AH) entirely on the upper voltage discharge plateau. During this past year, research and development on the iron electrode was discontinued due to heavy emphasis on pasted nickel electrode development. Effort on the iron electrode was restricted to pilot manufacture of the standard composite type with commercially available red iron oxide as the starting material.

2.2.1 IRON ELECTRODE SUBSTRATE

The current collector for the iron electrode continues to be a porous structure formed from a combination of steel fibers and an expanded metal iron sheet. The expanded metal is the center layer for the fiber structure which is sintered to both faces. The plaque is sintered in hydrogen and a vertical tapered tab is seam welded into the plaque body. The open pattern in the expanded metal is diamond-shaped and the long direction is aligned with the axis of the fiber. The expanded metal center provides integrity in handling and improves the current collecting property of the electrode.

2.2.1.1 SINGLE SINTER EVALUATION

Presently, evaluations are being conducted on the iron substrate to eliminate the second high temperature sintering operation. Iron plaques were processed for three-plate testing and process evaluation. Test results on fifty cycles may be found in Section 3.1.4. Single sintering would reduce costs and improve pilot line productivity by eliminating a process operation. Long life cyclic stability remains to be verified.

2.2.1.2 MANUFACTURING PROCESS

The basic manufacturing steps of full size electrodes are as follows: (1) roll loading of the grid structure with an aqueous paste of red iron oxide and carbon additive, (2) the reduction of this air dried mixture at in pure hydrogen, and (3) pressing of the electrode to an approximate final thickness of 1.0 mm.

Control of the amount and uniformity of the loading is based on the expansive structure of the steel wool matrix and the water content of the paste. The paste is readily incorporated into the plaque in a continuous manner using rubber rolls. The loaded plaque is then sized to using hard rolls so that the controlled volume of the retained paste is uniformly loaded into the voids.

After pasting, a drying step is used to rapidly remove all of the paste water. An open structure results which offers access for the hydrogen during the subsequent reducing step. A continuous belt hydrogen furnace is used for reduction of the iron oxide. The dimensions of the electrode are not measurably affected during the reduction step. The final electrode contains 70-74 g loading and is readily sized to 1.0 mm thickness using shim-stops and a fabric interface between the press platens and the iron electrode surface.

2.2.2 COMPOSITE ELECTRODE ACTIVE MATERIAL

The starting material for the composite-type iron electrode consists of red iron oxide and a carbon producing additive. These components are entered as an aqueous paste into the steel wool grid, as described previously.

In the past year, red iron oxide has been exclusively obtained in quantity from the Pfizer Corp. Electrodes prepared from this material consistently exceed 24 Ah per full size plate at the C/3 discharge rate. Life tests of randomly selected samples showed stable performance after 500 continuous cycles. Iron electrode specifications continue to be those given in the 1980 report.

The following are measured for QA/QC during production of iron electrodes:

- plaque weight,
- pasted weight,
- reduction factor,

These parameters allow complete qualification of electrodes for eventual assembly into full size cells.

2.2.2.1 IRON ELECTRODE ELECTROLYTE EFFECTS

A program was initiated to determine the performance of two uniform groups of selected, high-quality production electrodes (refer to Section 2.1.2.7 Table 2.3 for additional details).

These two groups of test cells had initially been on a schedule of four hours charge at 8.33A, and discharge at 8.33 amps to three hours maximum, or 1.00V minimum. These conditioning cycles were carried out through Cycle No. 35.

Subsequently, the cells were modified to evaluate changes in KOH and LiOH concentration; then cycled as before, up to Cycle No. 55. The response of these cells to these electrolyte compositions are displayed in Figures 3.6 to 3.10 in Section 3.0, "Technical Performance".

These cells are now being cycled on the following schedule to approach the minimum over-charge necessary to maintain capacity: 3.5 hours at 8.33A charge; discharge as before.

2.3 CELL HARDWARE COMPONENT DEVELOPMENT

Development work on cell components includes: separator(s), cell and intercell connectors, cell case and cover, and cell auxiliaries that deal with automatic water feeding and/or the electrolyte circulating system.

2.3.1 SEPARATORS

A decision was made to use Celgard K-501, supplied by Celanese Fibers Company, as the standard separator. This decision was made because of the satisfactory performance of cells in which it was used and because of its good handling properties. In particular, since it is laminated into one sheet, adoption of a serpentine method of wrapping electrodes in the stack assembly was possible.

The resistance measurements made on incoming material are given in Table 2.6. One shipment of separator material was received from Celanese with high

TABLE 2.6: QUALITY CONTROL MEASUREMENTS ON CELGARD K-501

Roll No.	Thickness Mils	Weight g/yd^2	Resistance(1) $m\Omega\text{-}in^2$
(2)			
6723	13.3	69.9	77
21846	14.3	69.9	29.5
21847	14.2	70.1	31.5
(2)			
6721	13.1	72.5	646
(2)			
832-7-1	10.9	70.5	889
(2)			
839-1-2	13.3	82.4	1136
(2)			
839-4-1	13.1	74.8	1106
(2)			
874-4-2	14.0	88.3	674
(2)			
855-8-1	12.3	80.2	770
(2)			
854-4-1	12.8	70.1	816
(2)			
6727	13.1	75.6	677
23294	14.2	70.0	32.5
23295	13.8	70.7	34.6
23296	14.9	71.9	30.6
23297	13.0	74.1	29.3
23298	13.9	72.0	29.6
23299	13.1	71.4	29.8

(1) Separator resistance is measured by the ac method, described in Alkaline Storage Batteries, by Falk and Salking, pp 257-260.

(2) Returned to supplier.

resistance. This was caused by the addition of an excessive wetting agent during manufacturing. This was replaced by Celanese with acceptable material.

Alternate separator materials from W. R. Grace Company were evaluated. This was done by comparing measurements and performance of the W. R. Grace materials with those of Celgard K-501 and its components, Celgard 3401 and Fibertex. An advantage of W. R. Grace barrier is that it has, potentially, a much lower price than Celgard 3401. The thickness, weight and resistance measurements are shown in Table 2.7.

Two 21-plate cells were assembled with the W. R. Grace materials, and two control cells were assembled with Celgard K-501. The serpentine method of assembly is too difficult to use with the unlaminated W. R. Grace materials, so that the bag type of construction was used. These bags were made with one layer of absorber and one layer of barrier, the absorber being inside the barrier; the bags were assembled on the iron electrodes. Bags were also made of K-501 for the iron electrodes of the control cells, so that the type of assembly used for separators in all four of the test cells was the same.

On the initial charge-discharge test cycles the capacities of the cells were similar but, by Cycles 7 and 8, the average capacity of the control cells was 20 Ah greater than the capacity of the cells with W. R. Grace separators. Internal resistance and pressure readings on the cells with W. R. Grace separators tended to be higher than on the cells with Celgard K-501. The capacity of the experimental cells was limited by the iron electrodes, which may have been affected by reduced access of electrolyte to these electrodes.

Examination of other candidate separator materials as they become available from commercial suppliers will continue.

2.3.2 ELECTRICAL CONNECTORS

The continuing objective of this subtask is the development of reliable, easily manufactured and highly conductive electrical connectors. The connectors interface with two types of environment--the internal connections (requiring

TABLE 2.7: COMPARISON OF W. R. GRACE AND CELANESE SEPARATOR

Supplier	Material	Thickness (mils)	Weight (g/yd^2)	Resistance ($m\ \Omega\text{-}in^2$)
W. R. Grace	90921-BC-1 barrier	7	136	20
W. R. Grace	114 absorber	6	63	10
Celanese	K-501 laminate	13.2	71	30
Celanese	3401 barrier	1	11.3	5-10
Crown Zellerbach	Fibertex absorber	5.8	26.4	7.1

caustic resistant components) and the connections external to the cell (in air). The present internal design for the cell terminal assembly is a four component system, involving three joints: (1) electrode-to-tab, (2) tab-to-collector, and (3) collector-to-terminal post, with experimentation being conducted on joining materials and/or techniques. The external intercell connections are lengths of flexible cables, with mechanical fastener joints at each end, that clamp onto the cell terminal posts.

2.3.2.1 TAB TO COLLECTOR

The internal connections between the electrode tab and the terminal post have received much attention during the past year. Here development work was focused in two major areas: (1) cost reductions in comb fabrication, and (2) elimination of the tab and comb. Significant results were obtained when the combs rather than being machined from blanks were assembly welded with bar stock pieces. Preliminary work in (2) involved a technique that utilized cables and a through-the-cover cable collection terminal.

The cost savings achieved in the assembly welding of combs led to the method now being used. Here a bar stock piece is first spot welded to each electrode tab in an operation that eliminates the melt down of separator at the tab region on top of the plates, which was always a problem when the machined comb was welded to each electrode tab, despite various heat sinking schemes that were employed. Later, during cell stack assembly the electrodes are gathered and welded to the collector assembly (see Figure 2.11). This not only reduced the cost of the assembly but improved the stacking operation. The second development activity was no longer necessary and was discontinued.

2.3.2.2 TERMINAL POST

During FY '81 a cost reduction was implemented substituting a "Brazing Technique" versus the "Hot Isostatic Pressing" (HIP) for the terminal post manufacturing. The new technique substantially reduced the cost of the terminal post. The HIP technique uses a copper rod encased with steel cladding. The ends of the rod are welded and the rod placed into the Isostatic Pressing furnace. The encased rod is cut to length, threads machined into the casing, and

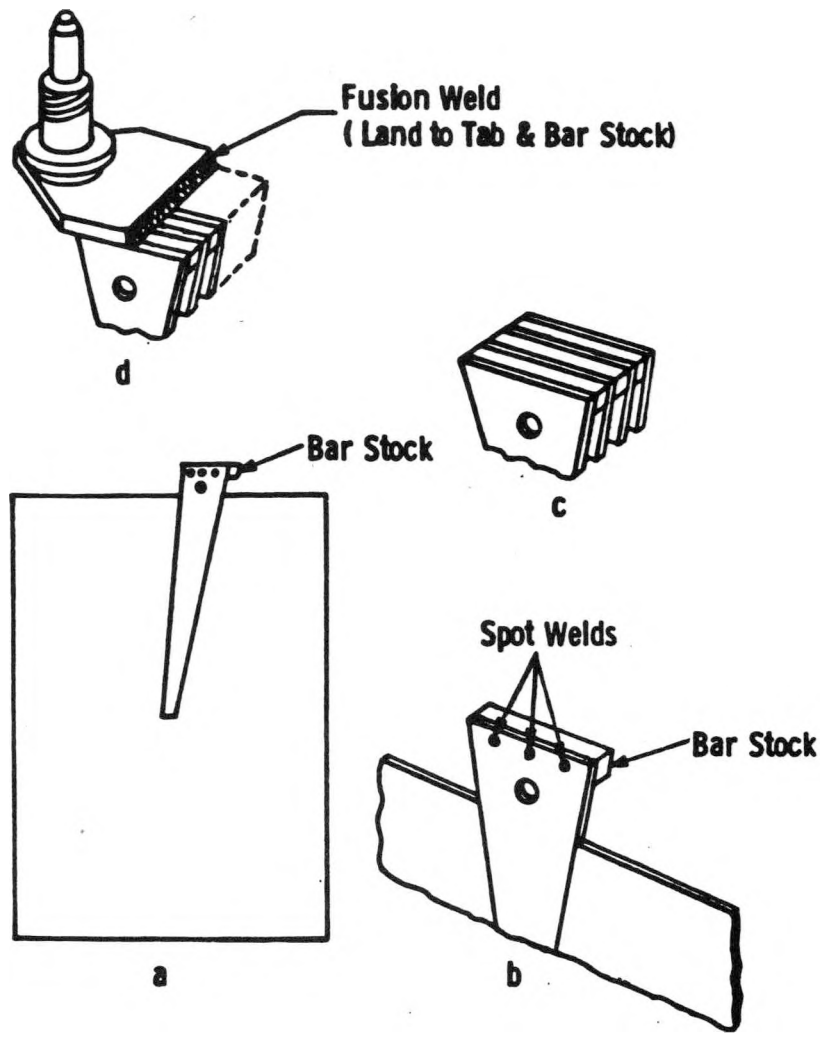

Figure 2.11. Method of Spot Welding Bar Stock to Plate Vertical Tab (a) and (b), of Assembling Plates in Stack (c) and of Welding Post and Land to Tab (d)

the upper 5/8" of casing removed exposing the copper rod. The part is welded to the collector plate and with a washer welded to the lower post. The finished terminal is then nickel plated.

The Brazing Technique takes the washer and threaded steel jacket, manufactured as one piece, and welds them to the steel collector plate. The copper rod is then soldered into the threaded steel jacket. The finished assembly is then nickel plated. The cost of the pilot manufacturing costs were reduced from $27/piece for HIP to $3/piece for the brazing method resulting in a 800 percent cost reduction for this part.

2.3.3 CASE/COVER

Work in this area included: (1) design and procurement of molded prototype cell containers and covers, (2) development of new joining and sealing techniques, having compatability to a multicell module case and cover, and (3) development of a multicell module concept for manufacturing cost estimates.

2.3.3.1 PROTOTYPE CELL CONTAINERS

A new design of case and cover is being utilized. Improvements in the circulation ports and the external connections associated with them necessitate changes in the cover, which resulted in the cover configuration as shown in Figure 2.12. At the same time, structural changes were made to strengthen and improve the seal integrity of the area around the terminals. The case design finally selected remains very close to the original. Previous core shift problems were resolved by tighter alignment during the mold setup.

An action plan has been implemented to resolve the cover cracking problem encountered over the past six months. The following items have been initiated:

- The molding die has undergone several modifications in an attempt to increase the quality of the parts.
- Resin material was changed from General Electric Noryl N2-25 to 844.

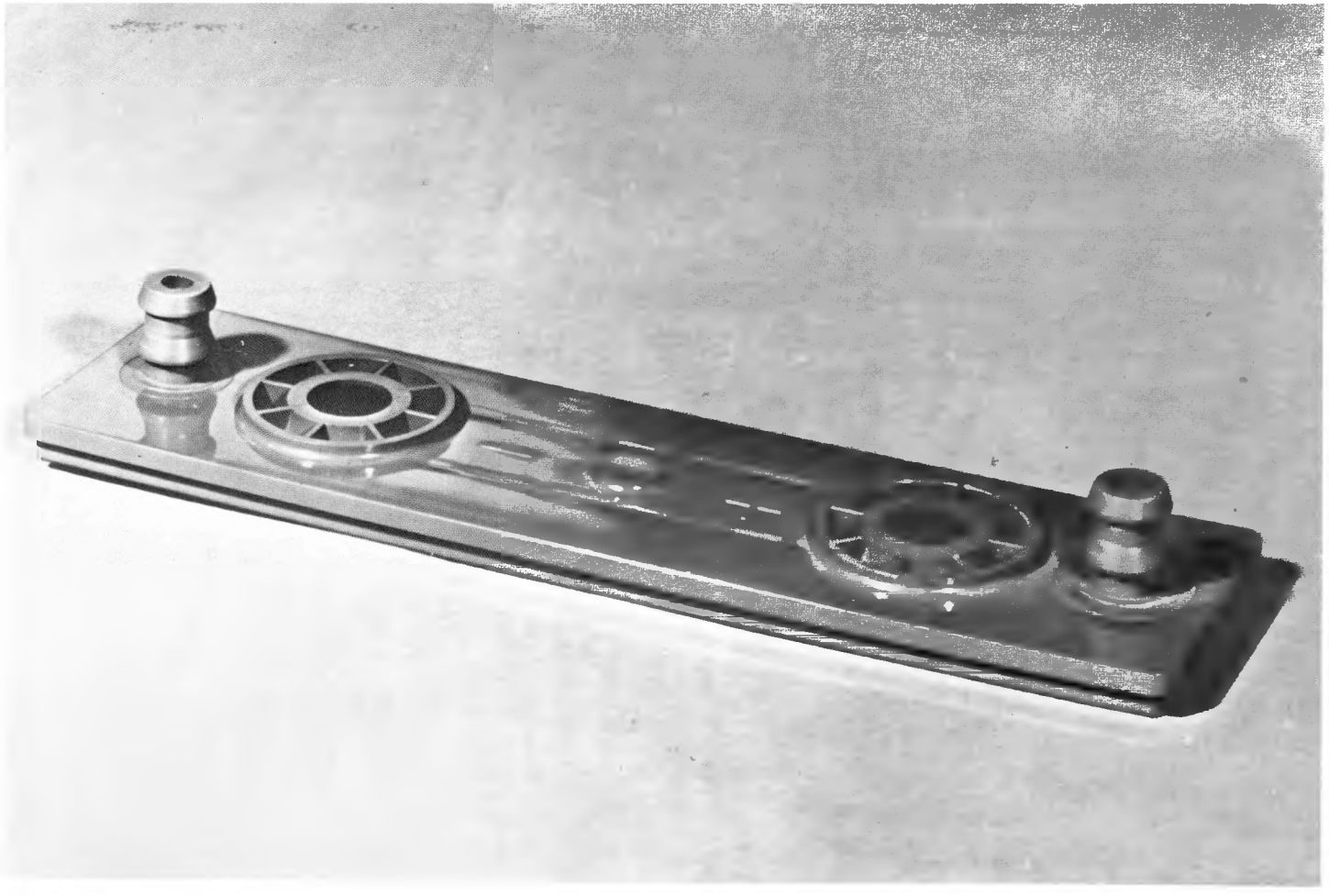

Figure 2.12. Case Cover for the Nickel-Iron Cell

- o Resin temperature was increased to 580°F.
- o Mold temperature was raised to 200°F.
- o Pressure increased from 1100 psi to 1400 psi.

The above conditions have all but eliminated the knit line on the cover where the cracking was occurring.

2.3.3.2 SEALING TECHNIQUES

The induction weld sealing process (cover-to-case) was also abandoned. Present dimensional variations in the adjoining pieces, although satisfactory for an adhesive method, proved too large for this process induction equipment.

2.3.3.3 MODULE CONCEPT

A conceptual design for a multicavity module was completed. The aim was to reduce the volume and weight of a six-cell module by packaging all as a group. Additionally, manifolding and intercell connections were made internally. Figure 2.13 shows a conceptual design which provides a projected 9 percent reduction in weight and 14 percent in volume.

2.3.4 ELECTROLYTE MANAGEMENT SYSTEM

An improved Electrolyte Management System for EV application was designed, built, and tested. The new design features include: (1) a reservoir and integral gas separator made from Chlorinated Polyvinyl Chloride Plastic (CPVC) with welded construction, (2) a stainless steel heat exchanger coil within the reservoir, (3) a collapsible reservoir bladder made from molded neoprene that minimizes the amount of hydrogen and oxygen in the reservoir, and (4) CPVC plumbing on the EMS. The salient features of the EMS are shown in Figure 2.14.

The EMS is designed to have a 40 liter electrolyte storage capacity and a heat removal capability of 1 kW/hr. Cooling is accomplished by water circulation through the heat exchanger which maintains the electrolyte temperature within 20°F of the cooling water temperature. Instrumentation on the EMS includes a low and a low-low level switch, a thermocouple to measure the electrolyte

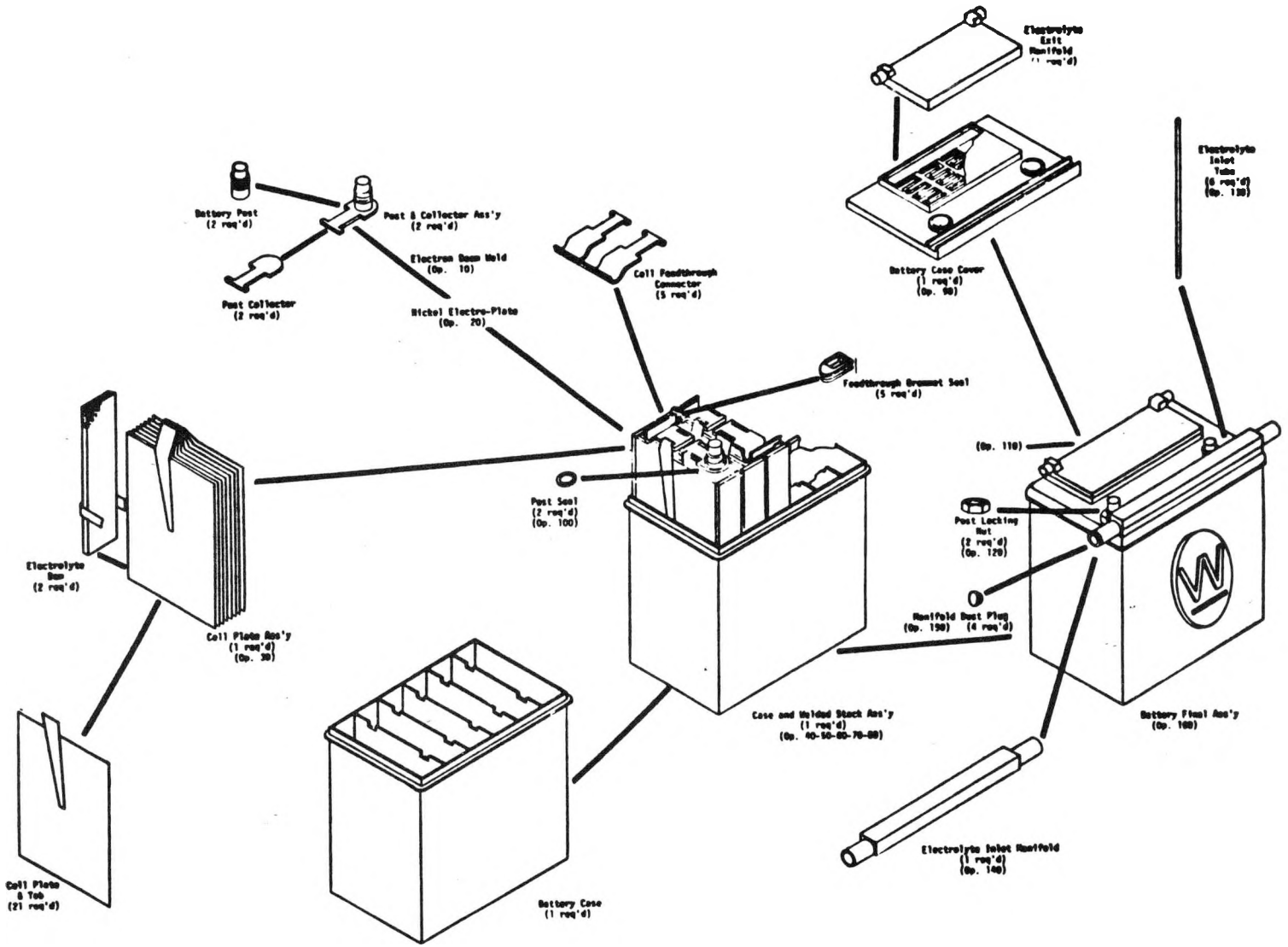

Figure 2-13. 6-Cell Nickel-Iron Module Monoblock Design

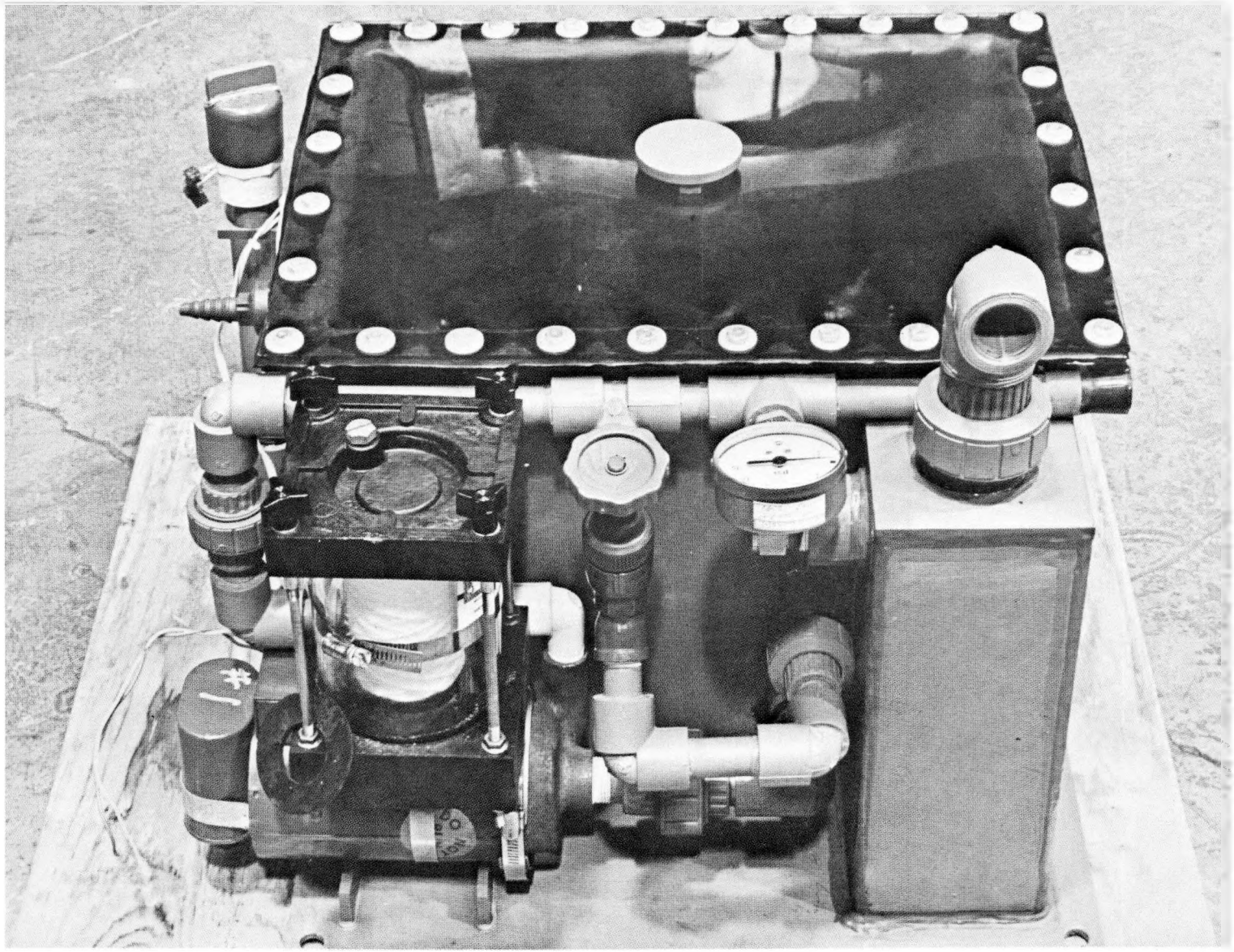

Figure 2.14. Electrolyte Management System

temperature in the reservoir and a pressure gauge to measure the electrolyte pressure to the battery.

Significant improvements were made in space requirements and weight for the EMS assembly. The reservoir is 18.5 in. x 19.75 in. x 13.5 in. or 50 percent smaller than the earlier design. The empty weight of the EMS is 54 pounds and this represents a 45 percent reduction in weight over the earlier designed stainless steel EMS.

Future work on the EMS will be directed toward the use of alternate plastic materials, improve molded construction, and more compact pumps which improve the battery volumetric and gravimetric energy densities.

2.4 CELL TESTING

The purpose of the testing program is to demonstrate the state of technological advancement, with respect to the overall nickel-iron battery goals. The ultimate purpose of the testing program is two-fold: (1) provide performance information for use by the developer as feed-back to determine operating characteristics, suggest modifications, and improve design, (2) provide information of interest to potential users, who have a need to know performance, environmental and safety aspects of the system.

For Task 2, the System Development portion of the contract, testing continues to concentrate in several areas. Prototype-size iron and nickel electrode tests are still being performed, to assist in evaluating design, materials and process changes and to determine their effect(s) on improving performance. Also, full size nickel-iron cells are being tested in finished, molded containers. Multi-cell modules are also being tested for performance and design evaluation. Testing of full size batteries is now part of the DOE/JPL program of near term electric vehicle evaluation. Two 90-cell batteries, including electrolyte management systems, were supplied to the JPL upgraded demonstration vehicle test program during FY '81.

The testing is to provide information on the operational and performance characteristics in the following areas: (1) pre-test, (2) charging and charge efficiency, (3) capacity, (4) power, (5) charge retention, (6) life, and (7) environmental aspects, such as temperature.

Developmental cells, modules, and batteries are tested with circulation of electrolyte during both charge and discharge. Up to five charge/discharge 80 percent DOD cycles can be run each day, with 20 full-size cell test positions available. Up to 25 full-size iron and/or nickel electrodes can also be tested at this same rate.

A special, variable depth-of-discharge test station was designed to simultaneously test up to three 12-cell, full-size modules. The system was chosen in an effort to cease the practice of testing cells at 100 percent DOD and to provide information on cells tested in a condition more closely approximating battery usage. These stations can assist in obtaining added depth-of-discharge and life data. The system is capable of cycling the modules at different DOD's and can also be used in temperature/life tests.

The 3-station, full-size module tester is shown in Figure 2.15. Here three modules are shown under test, complete with the electrolyte circulation system. A typical control and instrumentation panel is shown in Figure 2.16.

2.5 PILOT PLANT OPERATIONS

The transfer of the pilot line and all related manufacturing equipment from the R&D Center to the Advanced Energy Systems Division at Large, PA was completed in 1981. The equipment was installed and is operational with a current production rate exceeding twenty-five 250 Ah cells per day. Manufacturing processes employed are basically those developed at the R&D Center and were described in previous reports. Production methods and tooling are being refined and developed to increase productivity, produce consistent product, and improve the quality of the nickel-iron system.

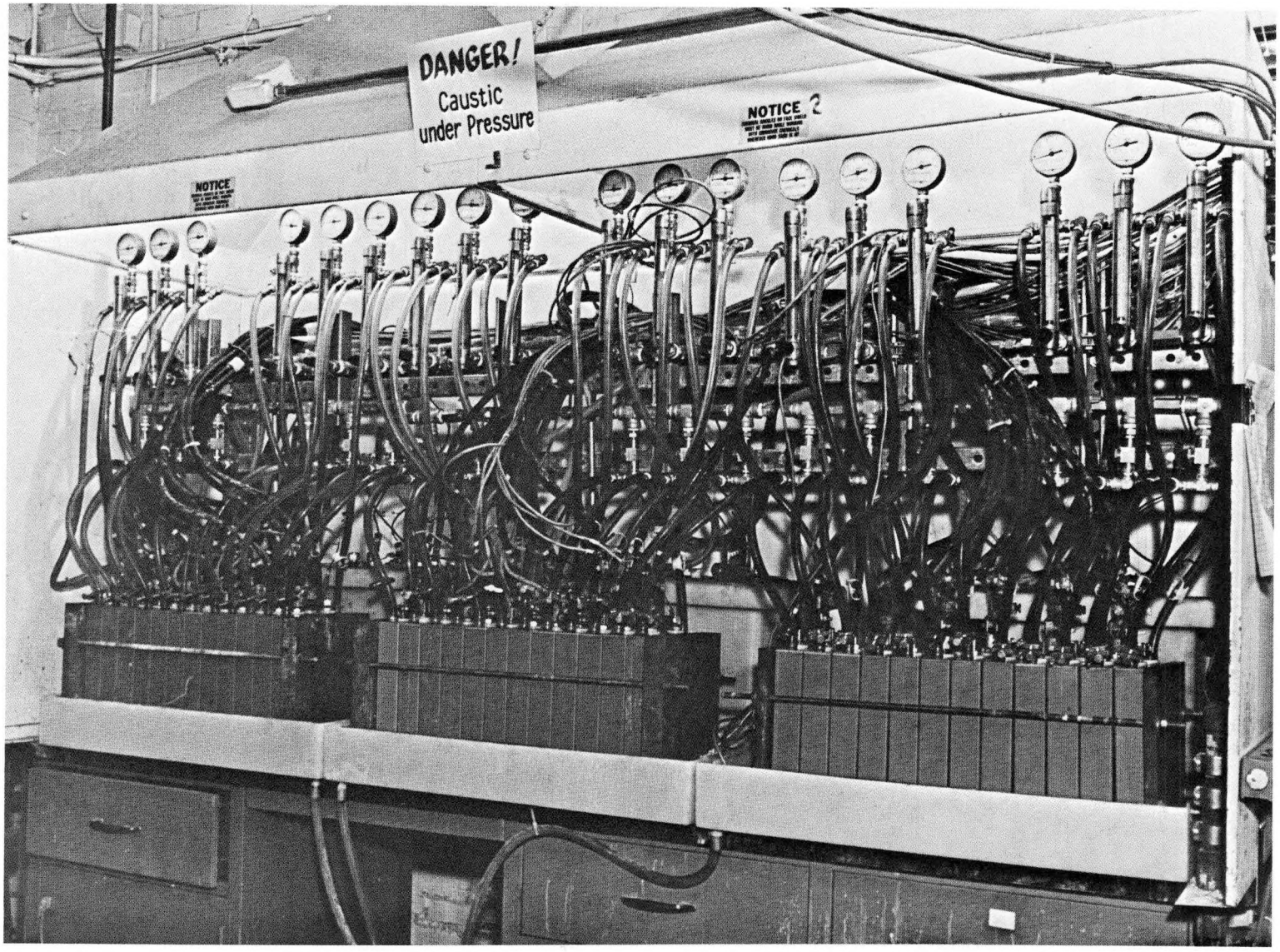

Figure 2.15. Module Tester

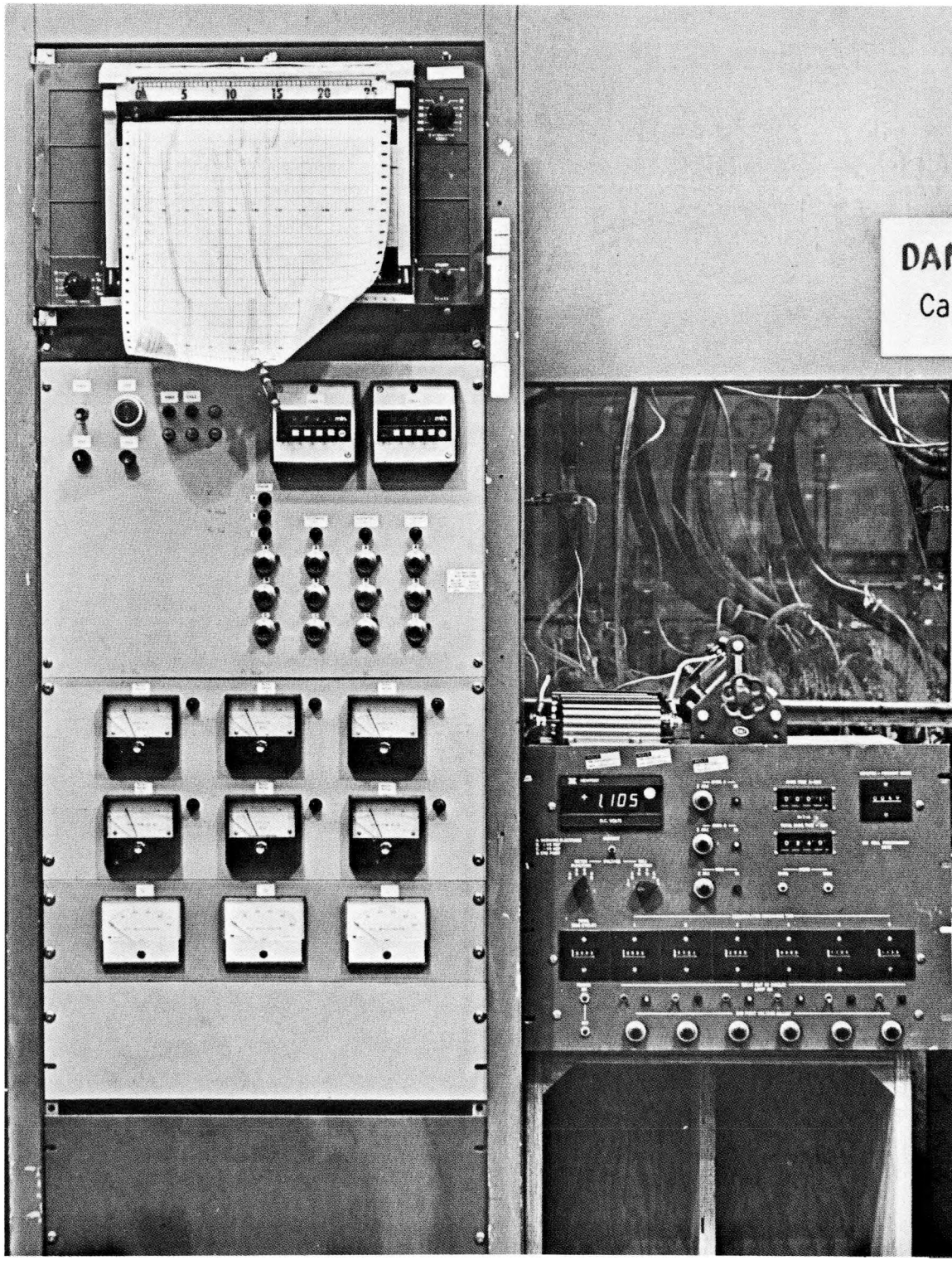

Figure 2.16. Tester Controls and Instrumentation

2.5.1 GRID FABRICATION

The following manufacturing concepts are underway to reduce the labor content for manufacturing electrode grids and improve the quality by lessening operator handling and skill requirements.

A punch press has been obtained and dies are being developed to size, emboss, and shear the periphery of the grids with a single stroke of the press. The press will replace the current manual operations for sizing, embossing, and shearing.

The current tab presently joined to the electrode by resistance seam welding method requires four seam welds to complete this assembly. A procedure is being developed that will utilize a resistance spot welding machine with projection weld technique to fuse the tab to the electrode with a single stroke of the machine.

Sintering of the electrode is now performed in a furnace that is also used for activation of the iron electrodes. The different operating temperatures and cover gases required for the sintering and activation processes reduces the efficiency of the furnace. A furnace designed for and dedicated to activation of iron electrodes will be installed this year. The existing furnace will be used exclusively for sintering grids and will increase the production rate for the sintering operation.

2.5.2 IRON ELECTRODE PRODUCTION

Active material is presently loaded into the electrode by passing the electrode manually through a roll coater three times and then through a rolling mill to remove excess material from the electrode. An automatic pasting line has been developed and installed to replace the manual operations. The automatic pasting line, shown in Figure 2.17, consists of three in-line roll coaters followed by a rolling mill. The new line has substantially increased production, improved product quality, and reduced processing time.

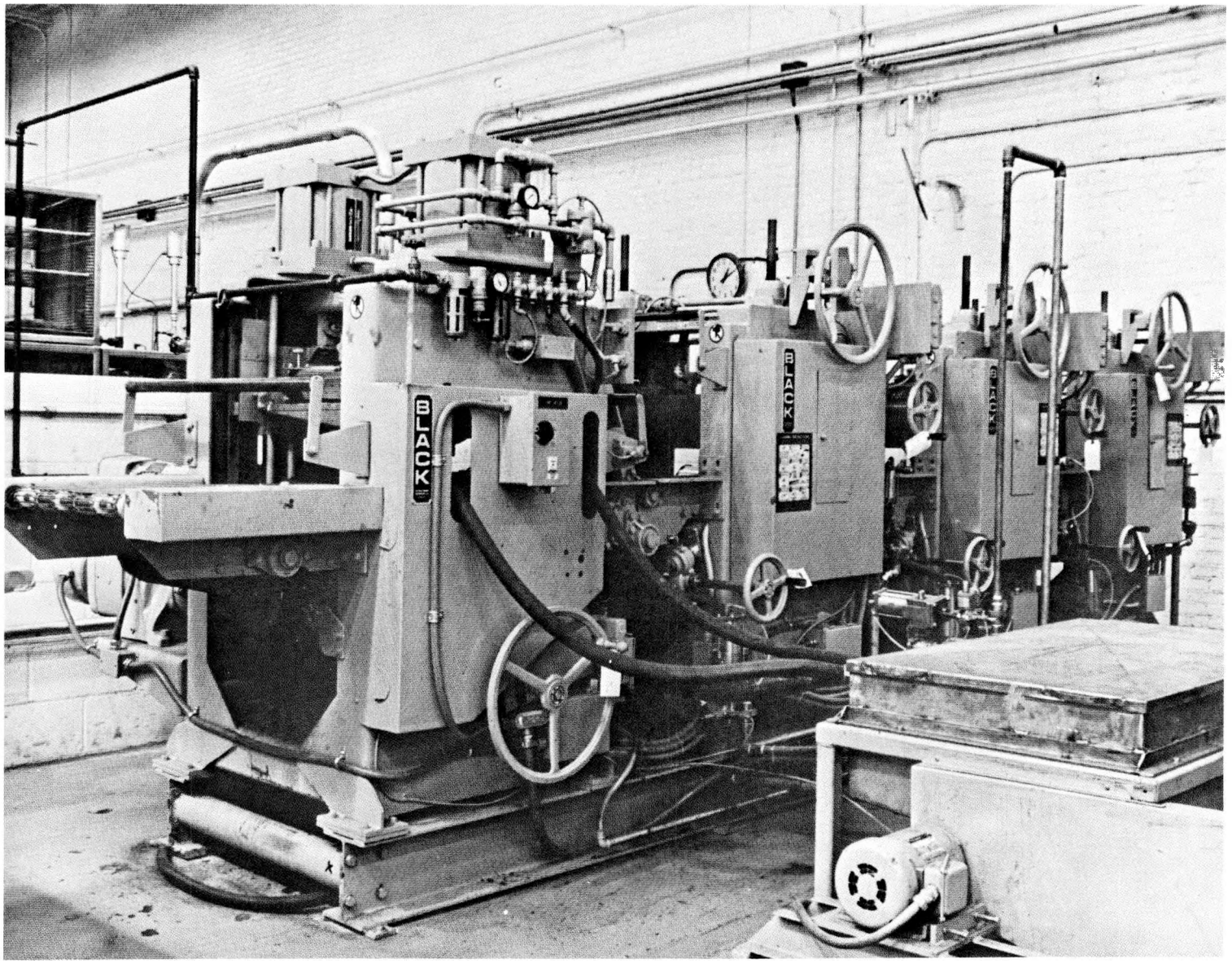

Figure 2.17. Automatic Pasting Line

Two batch type drying ovens were purchased and installed, shown in Figure 2.18, to air dry the pasted electrodes. Prior operations allowed the electrodes to hang overnight for drying. The new ovens reduced that time to 1-1/2 hours, reduced the effect of atmospheric conditions on the product, improved quality, and reduced processing time.

A 250 ton air-hydraulic press was installed for sizing the thickness of electrodes after pasting. The new press, shown in Figure 2.19, increased the production rate of the sizing operation.

A reduction furnace will be installed for activation of the iron electrodes. The additional furnace will improve productivity of the activation process as well as the efficiency of the sintering furnace.

A semi-automatic electrode enveloper, shown in Figure 2.20, was designed and installed to bag iron electrodes. Bagging of electrodes will improve the quality of the product by reducing potential shorts by particulate matter, eliminate dusting of material into work area, and improve productivity.

2.5.3 NICKEL ELECTRODE PRODUCTION

The electroprecipitation process (EPP) utilized for producing nickel electrodes is essentially as described in 2.1.2.4, and detailed in Table 2.1.

2.5.4 CELL ASSEMBLY

Changes in cell fabrication were discussed in Section 2.3. Cells assembled fall into one of the following groups: (1) Developmental cells and modules, (2) ANL/NBTL modules, (3) Cell strings and cell spares for the two JPL batteries, and (4) modules for other test evaluations.

Fifty-six cells have been built and tested during this past program year for developmental purposes.

Other test cells, having experimental nickel electrodes for individual cell test or for modules, were fabricated in the pilot line. Several cells have

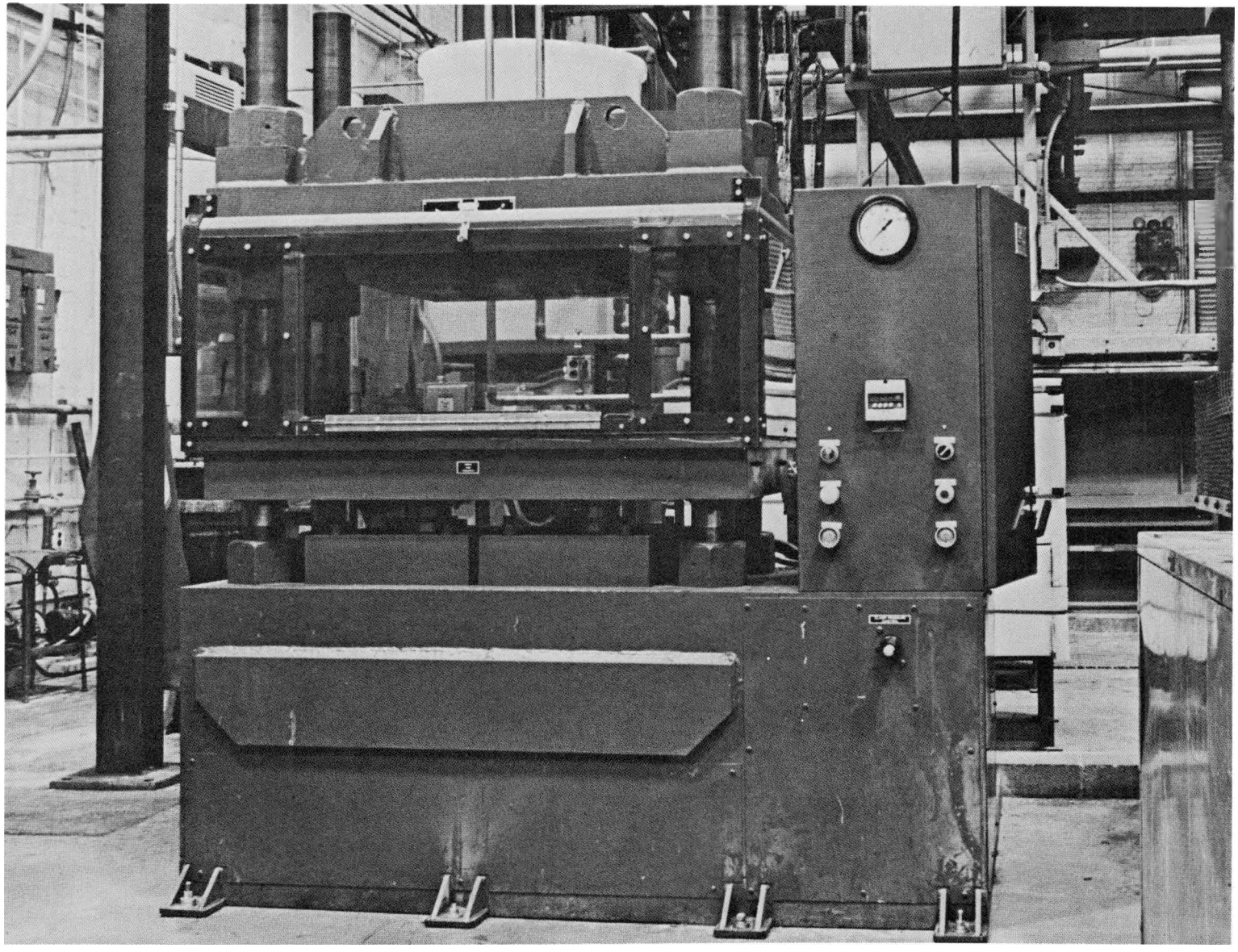

Figure 2.19. 250 Ton Air-Hydraulic Press

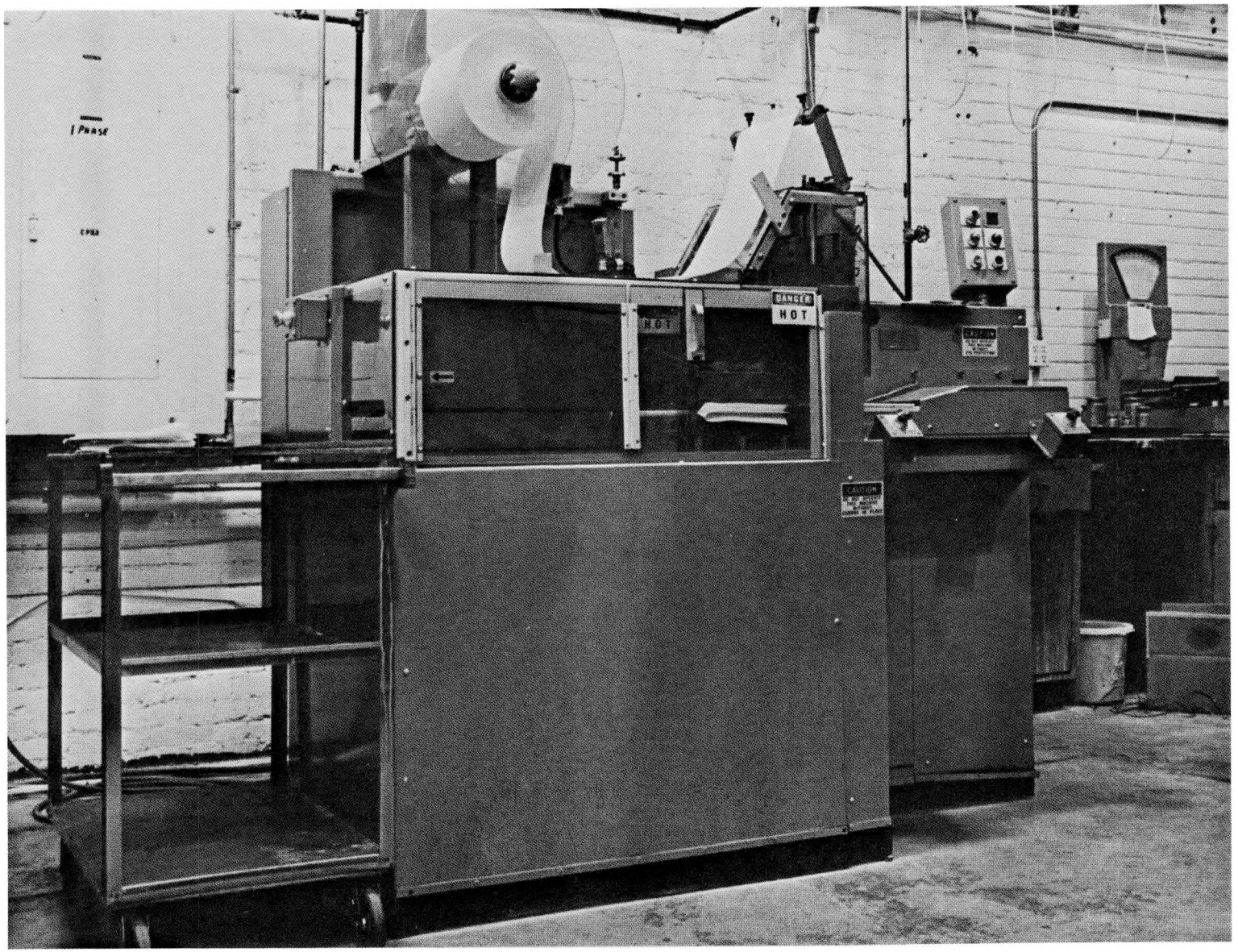

Figure 2.20. Semi-Automatic Electrode Enveloper

been made, incorporating changes in processing and materials, which reflect experience gained during development. These include:

1) High density fiber in the positive electrode (0.25 g/cm^2).
2) Reactively-sintered nickel-iron alloy fiber plaque.
3) Modified nickel plating processes.

Six modules have been tested on the DOD auto life cycler. An additional four modules were sent to the NBTL, two as part of this program and two as part of the JPL program.

2.5.5 MODULE ASSEMBLY

Figure 2.21 shows the present method of assembling full-size nickel-iron cells into strings. Strings of cells are designed in such a way as to efficiently use the particular vehicle battery compartment. In the figure, a 21-cell string is shown, complete with circulating system manifolding, end clamping plates and string binding.

The assembly procedure calls for obtaining the appropriate number of qualified cells, cleaning them with a boric acid solution and wire brushing the terminals. The cells are placed into the assembly fixture with retaining plates on each end and the assembly fixture tightened to the required dimension. The banding strap is covered with heat-shrinkable tubing and four straps placed around the module. The module is removed from the assembly fixture and bolted onto a fiberglass channel.

2.5.6 BATTERY ASSEMBLY

Three hundred twenty-nine (329) cells have been fabricated for the JPL program to permit building and delivering the two full-size batteries and spare cells required. One battery system was delivered in August 1980, the other December, 1980.

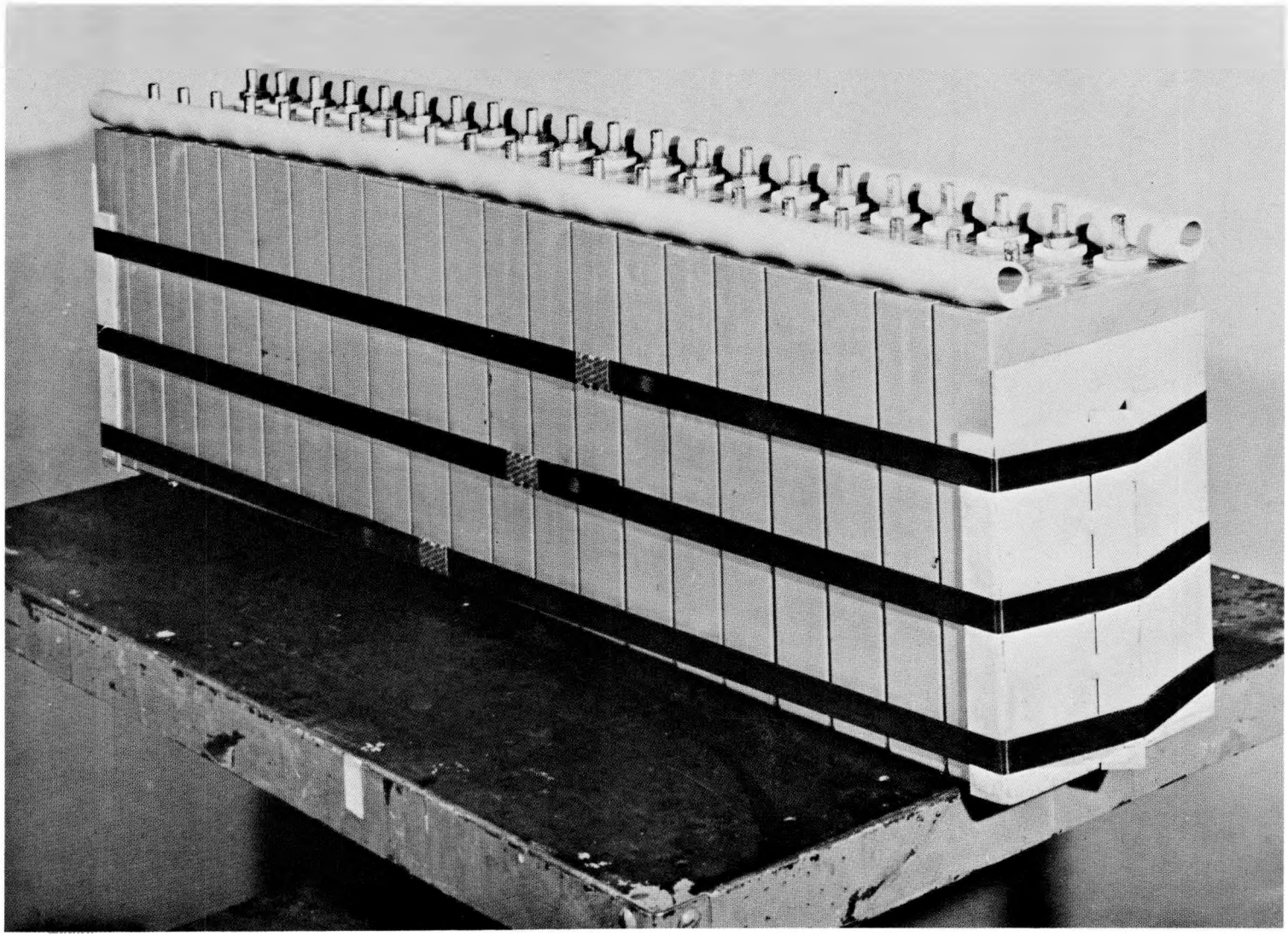

Figure 2.21. 21-Cell Module

2.6 QUALITY ASSURANCE

A Quality Assurance Plan (AESD-TME-3088) was prepared to describe the steps being taken to assure that the overall quality of the work being conducted on the battery line met all design requirements. This plan was designed to fulfill the requirements of ANL Quality Verification Program Description AQR-001 and ANL Quality Assurance Program Description AQR-002 as they apply to the battery program.

2.6.1 DOCUMENT REVIEW AND CONTROL

Engineering designs were incorporated into Cell Assembly Drawing 1691D62. Each of the eighteen parts making up this assembly was further defined on its own drawing, except for standard hardware items which are called out on the assembly drawing by part number and supplier. All drawings and/or Engineering Releases (ERCO) were reviewed and signed by the cognizant design engineer, the cognizant manufacturing engineer, and the cognizant quality engineer before their release for fabrication.

Additional drawings defining the components required for full module and battery assemblies were completed, reviewed and signed by the same three cognizant disciplines.

2.6.2 INSTRUCTIONS AND PROCEDURES

A total of seventeen processing and testing procedures (NIBP) were written, reviewed, approved and released for use. Table 2.8 lists these by title. Note that one is a safety plan.

2.6.3 CONTROL OF MEASURING AND TEST EQUIPMENT

All measuring and test equipment that is used to evaluate design requirements or control processes is maintained in a current calibrated state. Likewise all test instrumentation that controls or records input or output parameters is calibrated.

TABLE 2.8: NICKEL-IRON BATTERY PROCEDURES (NIBP)

NIBP No.	Title
001	Fe Grid Lamination
002	First Sinter
003	Coining and Trimming
004	Seam Welding Tab to Plaque
006	Second Sinter
007	Nickel Plate
008	Electroprecipitation Process (EPP)
009	Iron Paste Preparation
010	Iron Paste Loading
011	Iron Reduction - Activation and Pressing
014	Electroless Nickel Plating
018	Battery Module Assembly
019	Qualification Testing of EV Size 10-Cell Battery Module
024	Verification/Acceptance Testing for 180 Cell Battery
026	Formation of Pasted Nickel Electrodes
030	Nickel-Iron Battery Pilot Production Line Safety Plan
033	Cell Disassembly and Analysis

2.6.4 PROCUREMENT CONTROLS

All purchase requisitions for deliverable hardware were reviewed and signed by Product Assurance to assure that ordering information was complete. Upon receipt at AESD, each item was inspected for conformance to the purchase order requirements.

2.6.5 INSPECTION AND TEST CONTROLS

All electrodes processed are accompanied by a route card which shows the individual process steps and sequence which must be followed. In addition to the general surveillance of the operations, certain crucial inspection operations are performed.

2.6.5.1 ROUTE CARD 001 (IRON ELECTRODE)

This covers processing through the second sinter and has three specific inspection operations:

- Weight of the laminated grid
- Thickness after coining and trimming
- Weight after coining and trimming

2.6.5.2 ROUTE CARD 002 (IRON ELECTRODE)

This covers processing through the final operation and has two specific inspection operations:

- Final electrode weight
- Stack thickness (11 electrodes)

2.6.5.3 NIBP 011

This procedure requires the processing of four control electrodes with each day's reduction lot. These four electrodes are:

- o Stamped with an identification number
- o Weighed prior to pasting
- o Weighed as pasted and dried
- o Weighed as reduced.

The control electrodes are spaced in the continuous reduction furnace to monitor the reduction factor of the daily reduction lot.

Each reduction lot is qualified prior to use for production cells. (A lot consists of one day's continuous reduction of one paste batch.) A three-plate cell is assembled and tested per the procedure shown in Figure 2.22. The completed three plate cell is then tested by charging at 8.3 amps for a total of four hours and then discharging at 8.3 amps to a cut-off voltage of 0.8 volts Fe versus Hg/HgO reference electrode, or three hours whichever occurs first. Acceptance criteria is at least 22 amp hours after a minimum of three cycles. Test results are documented on the Quality Control Testing Report shown in Figure 2.23.

2.6.5.4 ROUTE CARD 003 (NICKEL ELECTRODE)

This covers processing through second sinter and identifies four specific inspection operations:

- o Weight of the needle punched blanket
- o Thickness after coining and trimming
- o Weight after coining and trimming
- o Groups by weight prior to nickel plating.

2.6.5.5 ROUTE CARD 004 (NICKEL ELECTRODE)

This covers processing through the final operation and contains two inspection operations:

Three Plate Cell Preparation Procedure

for

Iron Electrode Quality Control Testing

NEEDED: One Electrode form each reduction run.

Item		Done By: Initials - Date
1.	Identify electrode to reduction run:_____.	_____
2.	Measure average thickness (Four (4) measurements) after final pressing and record:_____mils. NOTE: must be within 36 to 44 mils spec. limits)	_____
3.	Weigh electrode and record:_____ grams (NOTE: must be within 113 to 128 grams spec. limits).	_____
4.	Spot weld extension tab to current collector tab, and stamp electrode ID on end of extension.	_____
5.	Obtain two counter electrodes (Ni) from DiCroce.	_____
6.	Spot weld extension tabs to counter electrodes if needed.	_____
7.	Stack electrodes in sandwich fashion with Celgarde separator between Fe and counter (Ni) electrodes. (NOTE: At no time are the Iron and Counter (Ni) electrodes to come in contact with each other, or their extension tabs. Counter (Ni) electrodes may touch each other.) Stacking Sequence: Counter electrode #1 (Ni), Celgarde, Fe electrode, Celgarde, counter electrode #2 (Ni).	_____
8.	Insert electrode stack in cell test case (provided by tester) assuring a tight fit. Use plexiglass shims if necessary.	_____
9.	Fill case with KOH 25 w/o + 15 gm/l LiOH electrolyte to ~ one inch past the top of the electrodes. This filling operation should be carried out as soon as possible after the electrodes are stacked and inserted in the case (Steps 7 and 8) to avoid drying out of nickel electrode(s).	_____
10.	Ascertain that cell is not shorted by measuring open circuit voltage ~10 minutes after electrolyte filling. With positive meter* lead on nickel and negative lead on Iron electrodes, voltage should be greater than 0.200 volts and rising. _____V	_____

*Use digital voltmeter with at least 10 megohm input impedance like Fluke's model #8010A or 8024A.

Test Results

☐ Qualified

☐ Not Qualified

Comments:

_____

_____

Figure 2.22. Iron Electrode QC Test Electrode Preparation

☐ Three Plate Test
☐ Cell Test
☐ Module/Battery Test

Test No. _____

Electrode(s)	Identification	Remarks

Grid Weight grms	Active Material Wt. grms	Total Weight grms	Nom. Thickness mils	Reduction Factor

Separator	Counter Electrode	Reference Electrode	Electrolyte Comp: 25 w/o KOH+15g/l LiOH Temp. Charge ____ °F Discharge ____ °F

Start Date End Date	Test Operator(s)	Tester and Station I. D.	D.A.S. ID	Test Results ☐ Qualified ☐ Not Qualified Comments	Init./Date

TEST PARAMETERS AND RESULTS

Cycle Number	Charge Rate A	Charge Limit T or V	Charge Fl. (GPM) / Pr. (PSI)	Discharge Rate A	Discharge Limit T or V	Discharge Cap. AH	Discharge Fl (GPM) / Pr. (PSI)	Imp. mΩ	Calculations and Remarks
1									
2									
3									
4									
5									
6									
7									
8									
9									
10									
11									
12									
13									
14									

Figure 2.23. QC Electrode Test Data Form

- o Thickness after cutting and cleaning
- o Wet weight after cutting and cleaning

2.6.5.6 NIBP 008

This procedure requires a three electrode qualification electrode from each EPP run. A three-plate cell is assembled and tested per the procedure shown in Figure 2.24. The completed cell is tested by charging at 8.3 amps for a total of four hours and then discharging to a cut off voltage of 1.0 volts or three hours, whichever occurs first. The acceptance criteria is at least 22 amp hours after a minimum of three cycles. Test results are documented on the Quality Control Testing Report shown in Figure 2.23. Only qualified EPP runs are released for assembly into cells.

2.6.6 CELL ASSEMBLY

Cells are assembled using iron and nickel electrodes from qualified runs and hardware that has been accepted by receiving inspection. A Preparation Procedure for QC Testing of Full Size EV-250 Cells Form (Figure 2.25) is completed for each cell assembled. Each cell is uniquely identified by the number permanently marked on the top of the cells. As shown on the form, the following inspections are completed prior to charging:

- o Polarity check
- o Open circuit voltage
- o Leak check at 7 psi
- o Weight.

The completed cell is then tested by charging at 83 amps for a total of four hours and then discharging to a cut off voltage of 1.0 volts or three hours, whichever occurs first. Acceptance criteria for each cell consists of:

Three Plate Cell Preparation Procedure

for

Nickel Electrode Quality Control Testing

NEEDED: One Electrode from each EPP run.

Item		Done By: Initials - Date
1.	Identify electrode to EPP run:_____	_____
2.	Measure average thickness (4 measurements) after final processing step and record: _____ mils. NOTE: Must be 100 mills or less.	_____
3.	Weigh electrode and record: _____grams. (NOTE: must be 145 gms or greater - suspended wet weight)	_____
4.	Spot weld extension tab to current collector tab, and stamp electrode I. D. on end of extension.	_____
5.	Obtain two counter electrodes (Fe) from DiCroce.	_____
6.	Spot weld extension tabs to counter electrodes, if needed.	_____
7.	Stack electrodes in sandwich fashion with Celgarde separator between Ni and counter (Fe) electrodes. NOTE: At no time are the Ni and counter (Fe) electrodes to come in contact with each other, or their extension tabs. Counter (Fe) electrodes may touch each other. Stacking Sequence: Counter electrode #1 (Fe) Celgarde Ni electrode, Celgarde, counter electrode #2 (Fe).	_____
8.	Insert electrode stack in cell test case (provided by tester) assuring a tight fit. Use plexiglass shims, if necessary.	_____
9.	Fill case with KOH 25 w/o + 15 gm/l LiOH electrolyte to ~ one inch past the top of the electrodes. This filling operation should be carried out as soon as possible after the electrodes are stacked and inserted in the case (Steps 7 and 8) to avoid drying out of nickel electrode(s).	_____
10.	Ascertain that cell is not shorted by measuring open circuit voltage ~ 10 minutes after electrolyte filling. With positive meter* lead on nickel and negative lead on iron electrodes, voltage should be greater than 0.200 volts and rising. _____V	_____
	*Use digital voltmeter with at least 10 megohm input impedance like Fluke's model #8010A or 8024A.	
	Test Results ☐ Qualified ☐ Not Qualified	_____ _____
	Comments:	

Figure 2.24. Nickel Electrode QC Test Electrode Preparation

PREPARATION PROCEDURE
for
Q. C. TESTING OF FULL SIZE EV-250 CELLS

Item #		Done By: (Initials/Date)
1.	Assign cell number_____.	_____
2.	Identify Fe electrodes used_____.	_____
3.	Identify Ni electrodes used_____.	_____
4.	Identify separator material used_____.	_____
5.	Stack cell in accordance with specifications and procedures described in drawings number: 3900451, 1691D62. GO_____. (Do not cover until steps 7 and 8 are complete.)	_____
6.	Weld tabs to terminal assembly.	_____
7.	Polarity check.	_____
8.	Ascertain that cell is not shorted by measuring open circuit voltage. With positive meter* lead on nickel (+) and negative meter lead on iron (-) electrodes, cell voltage should be greater than 0.200 volts and rising. _____V. *Use digital voltmeter with at least 10 megohm input impedence like Fluke's model 801DA or 8024A.	_____
9.	Case assembly.	_____
10.	Permanently mark assigned cell number on cell cover.	_____
11.	Leak-check at 7 psi in constraining fixture using Nitrogen gas.	_____
12.	Fill cell with KOH 25 w/o + 15 gm/l LiOH electrolyte to top of case. This filling operation should be carried out as soon as possible following final cell assembly to avoid drying out of the nickel electrodes.	_____
13.	Weigh cell_____kgs.	_____
14.	Measure open circuit voltage of a full cell and record _____.	_____
15.	End use_____.	_____

COVER _____	TEST RESULTS:
CASE _____	☐ Qualified _____
GROMMET _____	☐ Not Qualified _____

COMMENTS:

Figure 2.25. Cell QC Test Preparation Procedure

- o Electrolyte pressure between 1 and 5 psig
- o At least 220 ampere hours by Cycle 3
- o Internal impedance 0.9 m.

Qualified cells are held in storage for assembly into modules and batteries. Each final assembly configuration is tested again prior to shipment.

2.6.7 AUDITS

2.6.7.1 ANL AUDIT

The annual QA audit by ANL personnel was held on July 21 and 22, 1981. One audit finding was reported. Corrective action was implemented and a response to ANL submitted for the docketed nonconformance. By way of contract, four methods/systems/procedures reviewed during the course of the audit were cited for exceptional effectiveness.

2.6.7.2 AESD AUDIT

Paragraph 3.13 of the Quality Assurance Program Plan states that "at least one documented audit will be performed on the battery program during 1981 at both the R&D Center and AESD". The internal (Westinghouse) audit at AESD was conducted in August and a summary of the results are presented below. The audit at the R&D Center was cancelled because no input to the battery program was coming from R&D. The Quality Assurance internal audit conducted at AESD by C. L. Williams, et al, was part of a comprehensive, in-depth and critical audit of the program compliance to AESD Division Procedures. The Argonne QA contract requirements were included as a part of this larger audit. The audit team indicated that some general policy issues in the overall division quality program should be addressed.

At the conclusion of this audit, a concentrated effort was launched to assure that all battery program administration is conducted in accordance with existing Division Procedures. AESD finds it important to fix lack of conformances to established procedures even though it did not impact the quality of the ANL program. Corrective action for the specific nonconformances was completed. A

somewhat longer term program is addressing the more general quality program policy questions raised by the audit.

3.0 TECHNICAL PERFORMANCE

Initial program goals and projected demonstration values are presented in Table 3.1. Full-size cells and three plate cells were initially cycled to 100 percent depth of discharge each cycle. These cycling tests were more stringent than those required for long life cycle testing, which are now conducted on cells in finished molded case/covers, to 80 percent depth of discharge, based on rated capacity. The cycle life test cells employ electrolyte circulation, electrolyte composition and temperature control, and minimization of CO formation in the electrolyte. All these controls have been incorporated into the auto cycler, single cell test system and into the "closed", 3-module test system, which is used to test up to 6 cells/module. The cell test system operates with twenty test stations in the auto cycle life tester. Twenty-five 3-plate cells can be simultaneously tested.

Full-size cells have always been on test in containers of the proper volumetric constraints, as per design specifications. Cells made with molded cases and covers are being rated on performance, based on their actual weights, including electrolyte. Cells are being fabricated with cases and covers made of GE Noryl 844.

Details of all the full-size cells that are on test, including those that have been modified to permit testing by a circulating electrolyte system, are provided throughout this section. Cells with experimental nickel electrodes that were tested or are on test include: 067CE, 068CE, 080CE, 082CE, 083CE, 092CE, 093CE, 094CE, 097CE, 098CE, 099CE and 103CE. Cells with pilot line electrodes include: 128CE, 169CE, 186CE, 270CE, 330CE and 336CE. Cells with pasted nickel electrodes include 731CP and 732CP.

3.1 THREE-PLATE CELL TESTS

Full size electrodes are tested in a 3-plate cell configuration to provide initial performance evaluation of design and processes prior to full size cell

TABLE 3.1: NICKEL-IRON BATTERY GOALS

		ANL - 1981 Objectives	Performance			
			Cells[a]	Modules[b]	Battery[c] With EMS	Battery[c] Without EMS
Specific Energy (at C/3 Rate)	Wh/kg	54	56	45	48	51
Volumetric Energy (at C/3 Rate)	Wh/L	NS	115	102	78	103
Peak Specific Power (30 sec. at 50% dod)	W/kg	110	105	98	94	100
Energy Efficiency (including auxiliaries)	%	NS	55	45	51	51
OEM Cost $/K (Projected based on 1981 $)	$/kWh	NS	NA	NA	105	100
Cycle Life (80% dod to 75%)	Cycles	400	>500	>600	TBD	TBD

a) Typical of cells tested at Westinghouse, w/o Auxiliary EMS weight.

b) ANL/NBTL 5 and 6 cell modules, w/o Auxiliary EMS weight.

c) 90 cell battery tested at Westinghouse.

evaluation. The following sub-sections summarize the results of this test program.

3.1.1 EPP NICKEL ELECTRODE TESTS

Table 3.2 summarizes 3-plate cell test results on EPP nickel electrodes. Electrodes comparable to a state-of-the-art technology deliver 21 to 26 Ah, depending on EPP processing conditions. From 6 to 33 percent decline in capacity is usually noted after 200-300 test cycles at 100 percent depth of discharge for standard technology plates (Table 3.2, annual report for FY '79). Electrodes 987E, 1028E and 2650E, driven to approximately 1100 test cycles, further demonstrates capacity stability; showing 10 to 22 percent decline.

Electrodes 987E, 1028E, and 2650E employing higher fiber density, demonstrated significant increase in cycle life and capacity stability. Driven to approximately 1100 cycles, these electrodes showed a 10-22 percent decline in capacity, demonstrating that some of the nickel in the electrode could be replaced with lower cost steel. This would yield a potentially lower cost electrode.

Treatment of the high density fibers in the reactive sintering process (987E, 2650E) further improved the electrode design by producing a stronger fiber plaque, showing less capacity decline while on cycle life. Cell 987E is continuing on test. Judgment is reserved on the need for nickel replating, however, until this continuing test is completed.

Electrodes 2702E, 2801E and 2902E are baseline cells employing pure nickel fiber current collectors, which will provide a comparison of the performance of nickel positive active material which is not affected by any possible iron contamination. Direct correlation to full cells is complicated because the 3-plate cells which are relatively loose and unrestrained can allow the ductile nickel fibers to expand more freely than steel fibers in the restrained cell configuration. This could account for a different failure mode for the pure nickel fibers, i.e., the active material loses contact with the fibers causing a capacity decline.

TABLE 3.2: EPP-TYPE NICKEL ELECTRODE 3-PLATE TEST RESULTS

Cell Description[a]	Initial Capacity[c] Ah	Life Characteristics: Cycles[d]	Life Characteristics: % Decline[e] Capacity	Construction
841[g]	20.2	598	33	Reactive Sinter, Nickel Replate, Run No. 8, EPP
987 E	21.6	>1100	25	Reactive Sinter, Nickel Replate, Run No. 9, EPP
1028 E	20.0	>1070	10	High Fiber Density, Needle Punch, EPP Mini Run 122
2650 E	20.5	>1090	22	Reactive Sinter, EPP
2707 E	20.3	730	36	Reactive Sinter, Nickel Replate, Companion to EPP Cell 094 CE
2801 E	35.0	381	60	Pure Nickel Fiber, EPP
2902 E	27.0	359	41	Pure Nickel Fiber, EPP
2903	27.0	359	26	Pure Nickel Fiber, EPP
PN 005	15.2	757	32	Paste Nickel
10-8 CN	25.0	> 422	16	Corrugated Fiber, 0.127" Thick Plate, EPP

a. Special Feature, Components, Weight (kg) and Volume (l)
b. C/3 Discharge, 4-8 Hour Charge
c. Based on at Least Five Consecutive Cycles
d. "Greater Than" Symbols Denote Continuing Operation
e. Percent Decline from Initial
f. Data Effective December 31, 1981
g. "E" = EPP Nickel Electrodes (Positives)
h. "CN" = Corrugated Nickel Fiber (Positive Plate)

3.1.2 PASTED NICKEL ELECTRODE TEST

Three plate tests were run to evaluate the present formulation of nickel active paste. This formulation consists of nickel hydrate, nickel carbonate and cobalt hydrate. These compounds were milled in deionized water with deflocculants. This paste formulation provided for a high density paste so that the requisite loading was obtained in 2.5 mm finished thickness electrodes.

Loading range for the three electrodes tested was 95-97g for 345 cm^2 active area (dried at 55°C). The electrolyte used for the tests was 32 percent KOH + 5 gpl LiOH. The initial charging cycle consisted of 1.6A x 72 hours followed by 8.3A x 4 hours. Each successive charging cycle was 8.3A x 4 hrs. Discharge for all cycles was 8.3A to a 1.0V cell cutoff. Composite iron electrodes were used as the counter electrodes for all tests.

Results for the three electrodes tested are shown in Figure 3.1. Electrodes F1 and F2 came from the same production lot while G100 was produced in a later production run. Electrode F1 was wrapped in separator, while the iron counter electrodes were wrapped in the tests involving F2 and G100. As shown, Electrode F1 gave about 20 Ah output over the 90 cycle test period while F2 produced 24 Ah under the same test conditions. Electrode G100 which was placed on test at a later date gave 24.5 Ah at Cycle 62. The original electrolyte was retained for the duration of each test. Also, the discharge voltage profiles were very similar for the three electrodes. The results of these tests show that separator configuration can affect electrode performance. This effect will be further studied in full size cell tests.

3.1.3 BRIQUET IRON ELECTRODE TESTS

All effort on the briquet type iron electrode has been deferred to enable concentration on improving the composite electrode approach.

3.1.4 COMPOSITE IRON ELECTRODE TESTS

Results on full-size test electrodes have been summarized in Table 3.3. The composite-type iron electrodes have demonstrated a stable capacity of 22-23 Ah

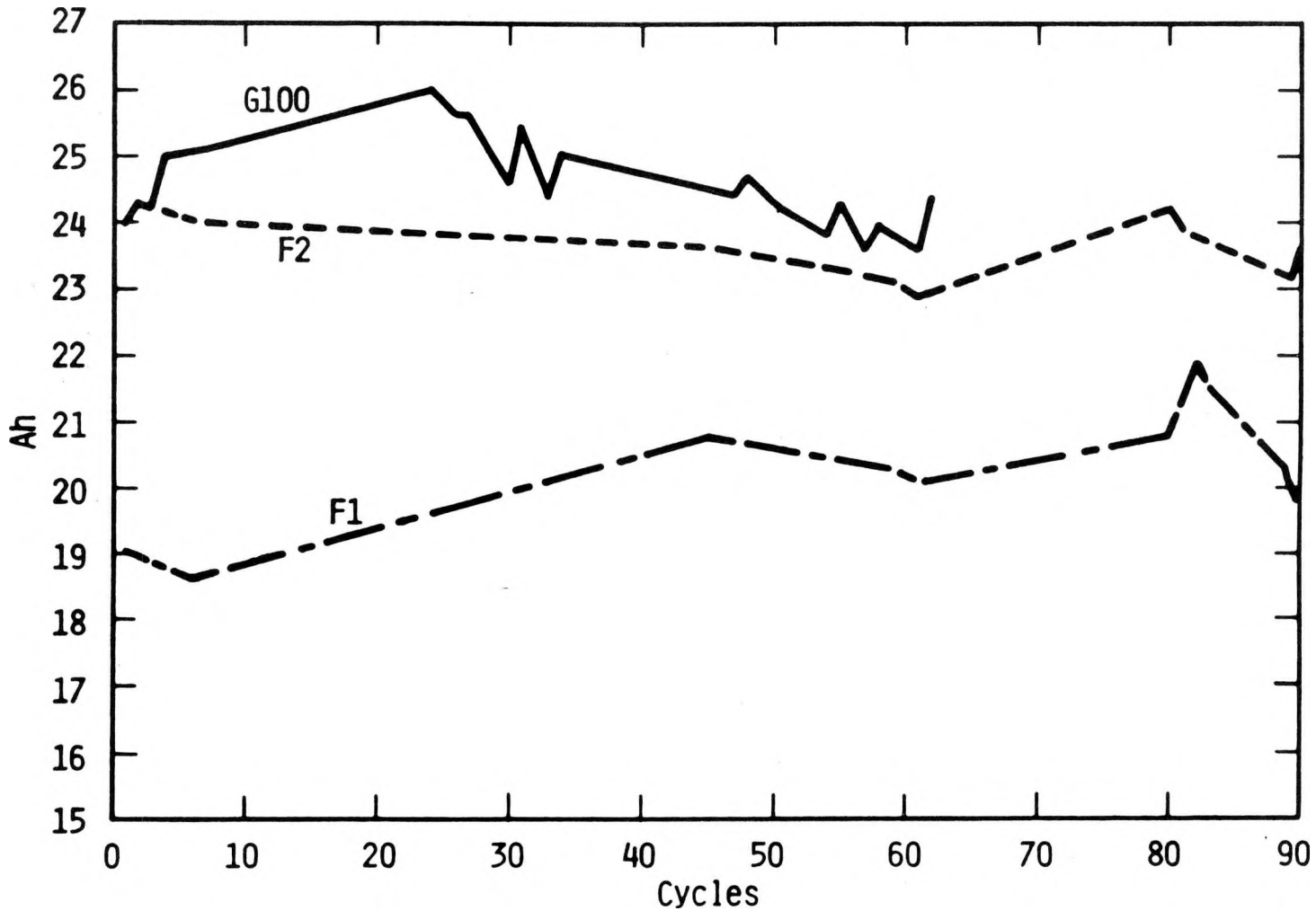

Figure 3.1. Three-Plate Test Results Nickel

TABLE 3.3: IRON ELECTRODE 3-PLATE TEST RESULTS

Cell Description[a]	Initial Capacity[c] Ah	Initial Capacity[c] Wh	Life Characteristics: Cycles[d,f]	Life Characteristics: % Decline[e] Capacity	Construction
345 C	25.8		1271	36	Pilot Line Production Control Electrodes
346 C	25.2		1004	31	Pilot Line Production Control Electrodes
388 C	23.0		921	38	Pilot Line Production Control Electrodes
389 C	24.0		904	40	Pilot Line Production Control Electrodes
390 C	24.0		724	45	Pilot Line Production Control Electrodes
391 C	25.0		>818	20	Pilot Line Production Control Electrodes
910 FX	27.0		693	39	Oxide Material Development
916 FX	21.0		573	39	Oxide Material Development
917 FX	23.0		623	44	Oxide Material Development
918 FX	21.0		649	25	Oxide Material Development
919 FX	21.0		359	24	Oxide Material Development
Q-7	25.0		50	3	Single Sinter Iron Electrodes
Q-9	25.0		50	0	Single Sinter Iron Electrodes

a. Special Feature, Components, Weight (kg) and Volume (l)
b. C/3 Discharge, 4-8 Hour Charge
c. Based on at Least Five Consecutive Cycles
d. "Greater Than" Symbols Denote Continuing Operation
e. Percent Decline from Initial
f. Data Effective December 31, 1981

at up to 1,200 test cycles to date at 100 percent depth of discharge cyclic life testing. This stability has been maintained in electrodes having variations in nickel plating, steel wool fiber type and phenolic content of the active material paste, suggesting none of these factors are critical to stable performance. This improved performance has been attained in 1.00 mm thick electrodes. Some electrodes have tested to 1,150 cycles to date, delivering 18.0 Ah/plate at that test level in the 3-plate test. Nickel plating is not necessary on the iron electrode grid structure for long cycle life.

3.1.5 SUMMARY OF THREE-PLATE TEST RESULTS

EPP electrodes are wet and therefore cannot be accurately weighed for active material content. However, based on electrodes of 23 Ah capacity, performance of EPP electrodes is estimated at 0.26 Ah/g active material and 0.11 Ah/g total electrode weight (target performance is 0.25 Ah/g active and 0.14 Ah/g electrode). EPP nickel electrodes indicate 6 percent loss in capacity in 300 test cycles in one of the better electrodes. At up to 1000 test cycles, a decline of up to 20 percent of the original capacity can occur in the unrestrained, 3-plate test. This capacity stability is due to the introduction of higher fiber density and higher strength in the substrate.

Full-size, pasted nickel electrodes deliver 20 to 23 Ah for several hundred cycles, to date. These loadings are 90-105g active material in electrodes of 1.80 to 2.30 mm thickness (0.22 Ah/g active material).

With respect to individual electrode gravimetric performance goals, some composite iron electrodes are approaching target performance (0.40 Ah/g active material and 0.27 Ah/g total electrode) at 0.40 Ah/g active and 0.25 Ah/g electrode, based on 29.0 Ah capacity obtained for the electrodes.

Initial evaluation of the single sinter iron electrode substrate, electrodes Q7 and Q9, indicated no distinguishable behavior from the double sinter process. Electrode capacity remains stable after 50 cycles, additional cycling is required to assess the substrate stability as compared to the double sinter electrodes.

3.2 ELECTROLYTE CONCENTRATION EVALUATION

Three-plate cell testing was utilized to evaluate electrolyte composition effects on each electrode type. Electrolyte concentration levels of 25 w/o, 35 w/o and 45 w/o were evaluated with lithium hydroxide levels of 0 g/l, 15 g/l and 25 g/l. The results of these tests are presented in the following sections.

3.2.1 NICKEL ELECTRODE ELECTROLYTE EFFECTS

Nickel electrodes, employing a sintered steel fiber metal grid structure, were prepared by electrolytic precipitation. This low-cost, porous grid was nickel plated; then cathodically impregnated[1] with nickel hydroxide containing approximately cobalt hydroxide.

When the nickel electrode is charged in KOH electrolyte, water molecules and stabilizing potassium ions take up positions in the interlayer space. Observing that such charged potassium-nickel oxyhydroxide conformed to 4 $NiO_{1.81}$ • 2.25 H_2O • 0.5 K_2O when analyzed, Bode[2] proposed an idealized formula of $[Ni_4O_4(OH)_4]\ O_{1.5}\ K$ based on crystal structure considerations. Jackovitz[3] observed that, when lithium ion is a component in the KOH electrolyte, it is preferentially absorbed in the interlayer relative to potassium ion.

The electrochemical oxidation mechanism to form this charged lithium-potassium-nickel oxyhydroxide occurs by abstraction of hydrogen from the brucite-type structure of the hydroxide[4]. Thus, the water molecules, and lithium and potassium ions, migrate into the active material on charge while hydrogen ions move in the opposite direction. This exchange is reversed on discharge (Figure 3.2).

---

[1] C. C. Hardman, U. S. Patent No. 3,600,227, 1971.

[2] H. Bode, K. Dehmelt and J. Witte, Electrochim. Acta, 11, 1079 (1966).

[3] J. F. Jackovitz and J. Seidel, Electrochem. Soc., Fall Meeting, Battery Divn., Abstract No. 23, 1981.

[4] J. F. Jackovitz, Westinghouse Report 81-1B6-NIPAT-P1, 1981.

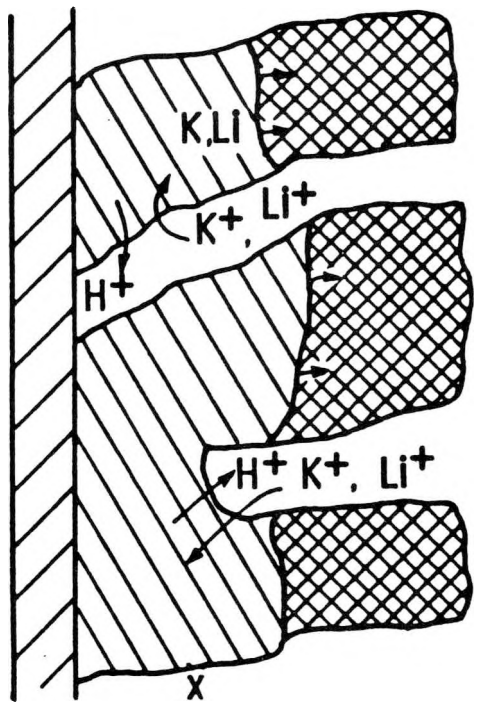

Nickel Oxyhydroxide
C-Axis Increasing:
4.6 Å → 7.4 Å

NICKEL ELECTRODE, DISCHARGE MODE

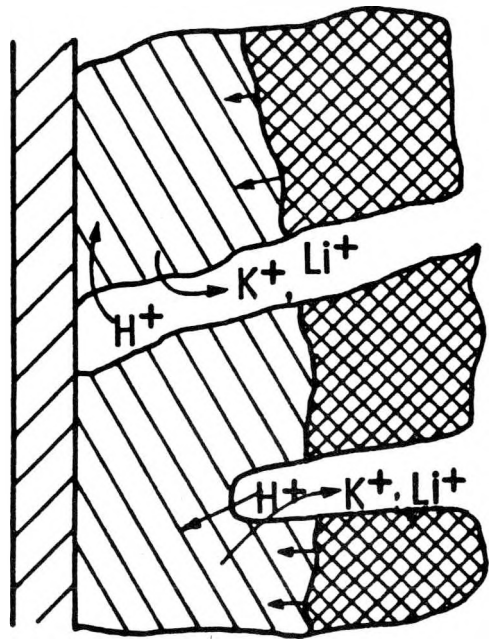

Nickel Oxyhydroxide
C-Axis Decreasing:
7.4 Å → 4.6 Å

NICKEL ELECTRODE, CHARGE MODE

Figure 3.2. Nickel Electrode Reaction

Maladin[1] further characterized this countercurrent movement of hydrogen ions versus hydrated alkali metal ions for the case of active material employing cobalt in addition to nickel. Maladin's analyses show an almost complete removal of potassium from a charged state of nickel oxyhydroxide with an aver- nickel valence of 3.22:$K_{0.21}$ $H_{0.57}$ NiO_2 • 0.04 CoO (OH) • 0.37 H_2O to a dis- charged state with nickel having an average valence of 2.14K:$_{0.01}H_{1.85}NiO_2$ 0.04 CoO (OH) • 0.32 H_2O.

This mobility of alkali metal ions, hydrogen ions and water molecules is vitally important in the charge-discharge behavior of the nickel active material. For instance, Maladin observed that removal of the cobalt affected the mobility of potassium ions and consequently decreased active material efficiency.

The crystal structure of the active material elongates from 4.6Å to 7.4Å along the C-axis on charge, and then contracts on discharge: an effect which could influence stability of performance over extended charge-discharge cyclic service.

This study attempted to isolate the effect of alkali metal ion concentration and to relate the influence of levels of lithium and potassium ions to electrode performance.

Three-plate cell testing was employed to establish nickel-limited cells for all of the electrolyte categories. The test matrix employed KOH levels of 25 w/o 35 w/o and 45 w/o and LiOH levels of 0.g/ℓ, 15 g/ℓ and 25 g/ℓ. The test plates were obtained from pilot production. All plates measured 22.66 cm in height, 16.54 cm in width. The nickel plates were 0.25 cm thick and were loaded with Ni and Co oxyhydroxide obtained by anodization in 25 w/o KOH.

---

[1] O. G. Maladin, et al, Elektrochimiya, 14, No 1, 91 (1978)

Nine 3-plate cells for the positive plate tests comprised one central nickel plate with an iron plate shimmed to a snug fit on each side. The two iron plates were wrapped with Celanese K-501 laminate. These cells operated in excess electrolyte, with 1 cm space at the plate edges and 2-3 cm of electrolyte above the plates.

All cells were initially filled with 25 w/o KOH electrolyte having 15 g/ℓ of LiOH. After 35 cycles to stabilize cell performance, each cell electrolyte was changed to evaluate one of the KOH and LiOH levels previously stated. The cells were repetitively charge-discharge cycled by charging at the C/3 rate (8.3A) for 3.3 hours, then discharging at the C/3 rate to a 1.0 OV cutoff. Cycling was continued through Cycle 355, at which time the cells were left on open circuit for approximately three months. After resumption of cycling through Cycle 358, all electrolyte was replaced with fresh material and some sediment shorts were removed. Continued cycling was carried out through Cycle 436, at which time the performance-versus-cycle life test was terminated.

The plots of C/3 rate ampere-hour capacity-versus-cycle life for these cells comprise Figure 3.3. The three cells employing 45 w/o KOH exhibited the greatest capacity loss during the first 250 cycles. Ultimately, these cells went to zero capacity due to internal electronic short circuits caused by sediment. Capacity loss was less for the three cells employing 35 w/o KOH. These particular cells were cycled 355 times without obvious internal shorting across the plate bottoms. However, buildup of sediment or loss of active material was appreciable. The particular cell having LiOH at 25 g/ℓ did not maintain capacity, as well as companion cells with LiOH at 0 or 15 g/ℓ.

KOH at 25 w/o allowed the nickel plates to exhibit the best capacity maintenance through 436 cycles. No significant difference in capacity-versus-cycle life performance could be attributed to the presence of LiOH. Within this group, charging efficiency also was uniform, at 87-88 percent, for discharges up to 80 percent of nominal C/3 capacity.

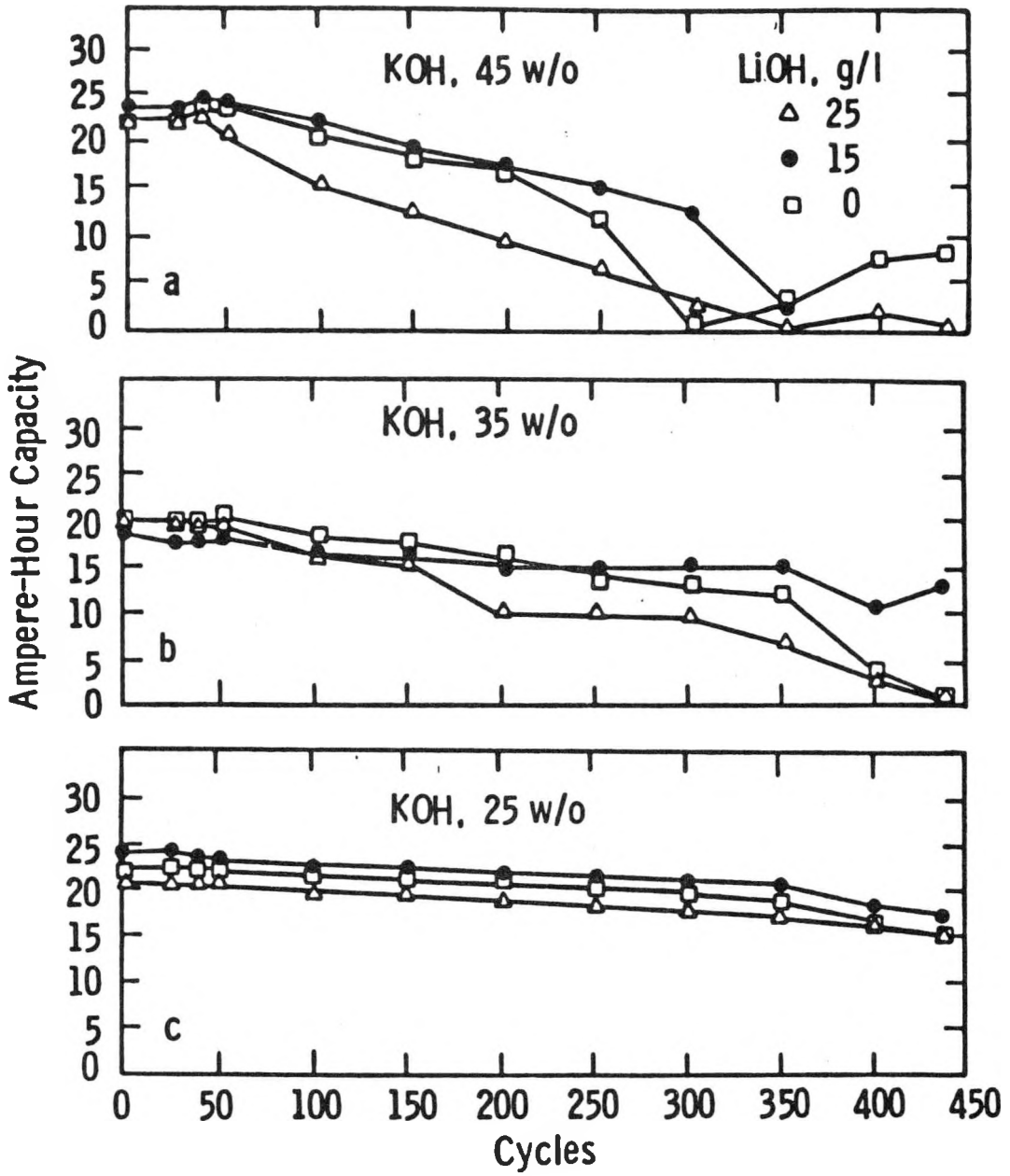

Figure 3.3. Nickel Electrode Electrolyte Concentration Effects

Positive plate expansion, ranging from 16 to 48 percent, could not be related to electrolyte parameters due to experimental scatter.

Loss of positive active material was greatest for the 45 percent KOH group and least for the 25 percent KOH group. Within the 45 w/o KOH concentration group, lithium also interacted strongly; further aggravating the active material losses.

Performance of the nickel electrode correlates well with active material loss. For minimum active material loss specimens, (all 25 w/o KOH with or without lithium), ampere-hour capacity is most stable over extended cycling in a high-stress, 100 percent DOD (depth of discharge).

Migration of K+ or Li+ into and out of the expanding and contracting nickel oxyhydroxide lattice should be concentration-dependent. These data can therefore be interpreted as meaning that mechanical stresses originating in the crystal structure lead to loosening and shedding of active material from the electrode. There is, however, little in the data to suggest that the absorption and desorption of either K+ or Li+ is strongly related to capacity. Only a very modest increase in ampere-hour capacity was noted for the 45 w/o KOH specimens early in cycle life, and this was soon negated by rapid loss of active material and consequent loss of capacity.

In 25 w/o KOH, approximately 400 cycles at 100 percent DOD can be expected from these electrodes before capacity loss exceeds 20 percent. Date by Francis[1] and Clark, et al[2] indicate a logarithmic-linear relationship between the number of cycles and discharge depth for alkaline cells. For the types of discharge depth anticipated in actual motive power service, such log-linear extrapolation predicts useful service lifetime of approximately 1000 cycles.

---

[1]H. T. Francis, Technology Handbook, Space Batteries, NASA SP 5004, Washington, 1964.

[2]W. W. Clark, W. G. Ingling, J. F. Luke, E. A. Roeger, Jr., Alkaline Battery Evaluation, Technical Documentary Report No. APL TDR 64-76 (1964).

The data do not indicate that variation in LiOH concentration influences either the capacity or lifetime of the nickel electrode. This is contrary to the findings of previous investigators[3,4]. Electrode design and test conditions are not equivalent, however, preventing direct comparison with previous work.

3.2.2 IRON ELECTRODE ELECTROLYTE EFFECTS

Nine 3-plate test cells for the negative plate comprised a central iron electrode similarly wrapped with K-501 separator material, with a nickel electrode on each side. These cells operated in excess electrolyte, with 1 cm space at the plate edges and 2-3 cm of electrolyte above the plates.

All cells were initially filled with 25 w/o KOH electrolyte having 15 g/ℓ of LiOH. After 35 cycles to stabilize cell performance, each cell electrolyte was changed to evaluate one of the KOH and LiOH levels previously stated. The cells were repetitively charge-discharge cycled by charging at the C/3 rate (8.3A) for 3.3 hours; then discharging at the C/3 rate to a 1.0 V cutoff. Cycling was continued through Cycle 355, at which time the cells were left on open circuit for approximately three months. After resumption of cycling through Cycle 358, all electrolyte was replaced with fresh material and some sediment shorts were removed. Continued cycling was carried out through Cycle 436, at which time the performance-versus-cycle life test was terminated.

Within the group of cells comprising 25 w/o KOH and 35 w/o KOH, (Figure 3.4), no significant difference in capacity maintenance could be detected, either due to KOH concentration or to LiOH content. At 45 w/o KOH, overall capacity was maintained best by the cell having a LiOH content of 25 g/ℓ. The cell with no LiOH developed internal shorting at approximately 250 cycles, a condition also evidenced by the cell comprising LiOH = 15 g/ℓ at approximately 380 cycles. Except for these two latter cells, all iron negative plates had a

---

[3] L. C. Turnock, Trans. Electrochem. Soc., 32, 405, (1917).

[4] K. Hofer, Batterien, 12, 247 (1943); 12, 257 (1944).

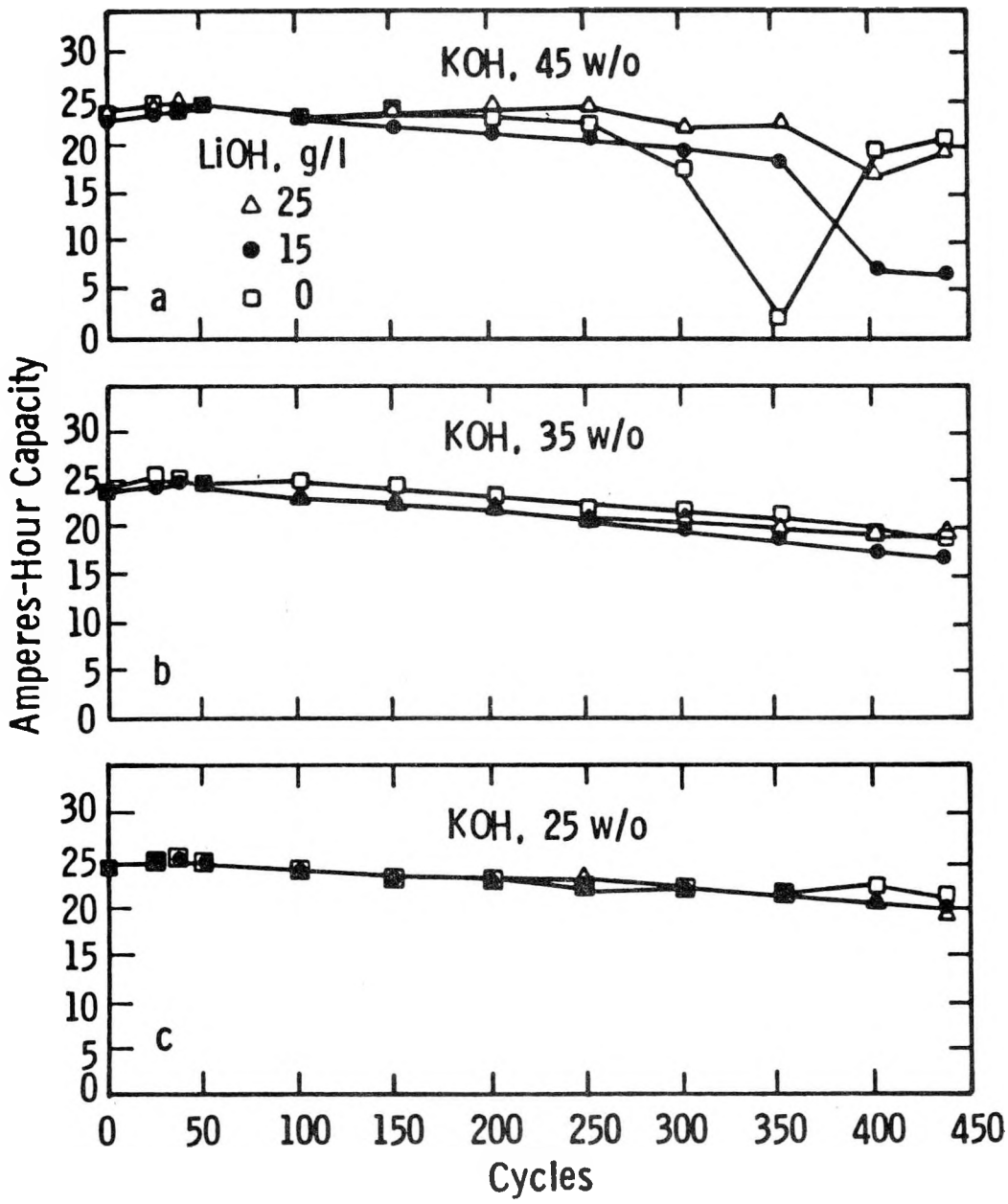

Figure 3.4. Iron Electrode Electrolyte Concentration Effects

charging efficiency of approximately 95 percent when discharged up to 80 percent of nominal C/3 capacity.

Iron-plate expansion did not depend significantly on KOH concentration. However, those cells employing KOH, plus LiOH, consistently displayed greater plate expansion than cells with only KOH as the electrolyte. Active material loss for all iron-plate test cells was independent of electrolyte composition parameters.

Iron electrodes perform well in 25 w/o KOH without showing any response to lithium at all. Capacity retention (approximately 15 percent capacity decline over the span of the test) was good for all of the specimens employing 25 w/o KOH. However, lithium did affect negative electrode expansion; apparently causing approximately double the electrode thickening compared to cell cycles with no added lithium.

Active material losses do not, however, reflect any response to the increased mechanical stresses in the iron electrodes with added lithium. In spite of expansion forces equivalent to that experienced by the nickels, the iron electrodes did not lose active material as dramatically as the nickels. The effect of this is the superior capacity maintenance of the irons relative to the nickels.

The lithium influence on the iron electrode may follow a mechanism analogous to the absorption-desorption behavior of K+ and Li+ in nickel oxyhydroxide. In a tightly-restrained stackup which is normally the case for a commercial cell, lithium could prevent iron electrode collapse with consequent loss of porosity and capacity.

Iron electrodes employing a steel fiber current collector design show optimum capacity maintenance in 25 w/o KOH under a stressful (100% DOD) charge-discharge cycling schedule.

Lithium is not required in cells employing a "loose" 3-plate stackup where shimming is provided for electrolyte volume control alone. However, lithium may function as an expander for the negative in restrained plate stackups, maintaining porosity and performance.

The specific role played by lithium, in a crystallographic sense, in the iron electrode requires further investigation for detailed understanding.

3.3 FULL-SIZE CELL TESTS

Testing of all cells is done with electrolyte circulation for the 100 percent DOD test cycles. Based on nominal capacity of 230 Ah, the cells have been charged at 83.3A/3.7h (300 Ah, in) and discharged at 83.3A/1.0 V per 100 percent DOD cycle.

Again, these tests use a circulated and temperature controlled electrolyte condition (30°C on charge and 40°C on discharge--bulk electrolyte temperature).

3.3.1 FULL-SIZE TEST RESULTS

Figure 3.5 shows the appearance of the present full-size cell that is used to evaluate the in-house state-of-the-technology. The 21-plate cell has barbed tube fittings, which secure the electrolyte circulation and exhaust gas manifolding as part of the electrolyte circulation and gas venting system.

Table 3.4 presents the nature of some of the full-size experimental and/or pilot line nickel-iron cells tested, or on test, to date.

Couloumbic efficiencies still have not been optimized in the test results reported in these tables, since the cells were cycled by in-house standard procedures, primarily to obtain the effects of variables in electrode and cell construction performance, as a function of cycling.

However, cell results have indicated the feasibility of attaining 50 to 60 Wh/Kg at the C/3 rate in full-size nickel-iron cells, having the design volumetric constraint and using EPP nickel and composite-type iron electrodes.

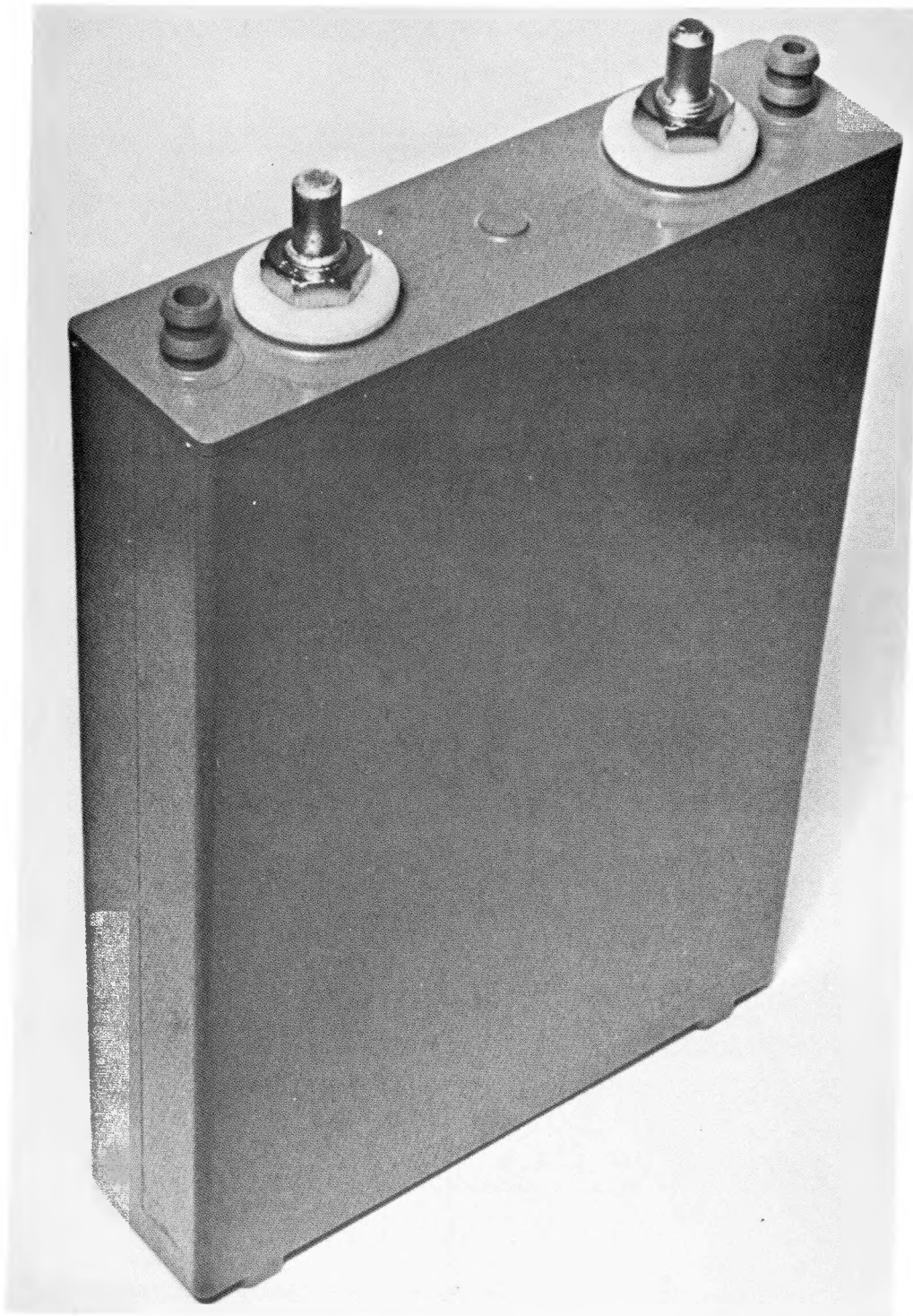

Figure 3.5. Nickel-Iron Cell Configuration

TABLE 3.4: CONSTRUCTION DETAILS OF FULL SIZE NICKEL-IRON CELLS

Cell Code	Construction Details Nickel Electrodes	Separator System Absorber, Barrier	Remarks
066CE	2.29 mm Thick, EPP, 2 Vertical Channels	K501	Needle punched nickel plaques (from vendor)
067CE	2.43 mm Thick, EPP, 2 Vertical Channels	K501	Higher fiber density, needle punched plaques (from vendor)
068CE	2.43 mm Thick, EPP, 2 Vertical Channels	K501	Higher fiber density, needle punched plaques (from vendor)
080CE	2.5 mm Thick, EPP, 2 Channels	K501	Mini-line run nickels, 3-hour nickel plating, 20 percent nickel pickup (throwing power evaluation)
082CE	2.28 mm Thick, EPP, 2 Channels	K501	Reactively-sintered fibers positives
083CE	2.25 mm Thick, EPP, 2 Channels	K501	650^{0} C H_2-treated positive fiber
091CE	2.61 mm Thick, EPP, 2 Channels	K501	Mg-doped nickel active material
093CE	Four Extra-Height Nickels, Three Extra Height Irons	K501	Gas pressure relief design
094CE	2.35 mm Thick, EPP, 2 Channels	K501	Reactively-sintered fibers + nickel replate
097CE	2.54 mm Thick, EPP, 2 Channels	K501	Reactively-sintered fibers + nickel replate, Run 8
098CE	2.54 mm Thick, EPP, 2 Channels	K501	Reactively-sintered fibers + nickel replate, Run 8
099CE	2.55 mm Thick, EPP, 2 Channels	K501	Reactively-sintered fibers + nickel replate, Run 8
103CE	2.57 mm Thick, EPP, 2 Channels	K501	Reactively-sintered fibers + nickel replate, Run 9
128CE	2.4 mm Thick, EPP, 2 Vertical Channels	SM 263.4, 3501	Cell from Module 6-1, tested at ANL/NBTL for 327 Cycles
169CE	2.51 mm Thick, EPP, 2 Vertical Channels	SM 263.4, 3501	Pilot line Cell
186CE	EPP, 2 Vertical Channels	SM 263.4, 3501	Pilot line cell
270CE	EPP, 2 Vertical Channels	SM 263.4, 3501	Pilot line cell
330CE	2.31 mm Thick, EPP, 2 Vertical Channels	49696, 3501	Needle punched nickel pilot line cell plaques (from vendor)
336CE	2.39 mm Thick, EPP, 2 Vertical Channels	K501	Serpentine wrapped pilot line cell
731CP	2.34 mm Thick, Pasted, 2 Channels	K501	Commercial green nickel hydrate
732CP	2.49 mm Thick, Pasted, 2 Channels	K501	Commercial green nickel hydrate
C-CE-01	2.9 mm Thick, EPP, 19-Plate	K501	Reactively-sintered corrugated fibers in positive plates

Cyclic life testing was conducted at 100 percent depth of discharge cycles at the C/3 drain rate and was further modified to permit electrolyte composition, circulation and temperature control.

Table 3.5 summarizes the best results obtained this year on full-size nickel-iron cells. Initial capacities of these cells ranged from 175 to 239 Ah at the C/3 drain rate. The better pilot line cells sustained up to 80 percent of their initial capacities after 325 cycles (Cell 128CE), 464 cycles (Cell 186CE) and 511 cycles (Cell 270CE). Maximum test cycles to date have been completed on Cells 169CE (556 cycles and 27 percent degradation), Cell 816CE (541 cycles and 24 percent degradation) and Cell 270CE (650 cycles and 28 percent degradation in capacity). Gravimetric energy density on these cells, based on an estimated 1086g contribution from electrolyte, case cover and terminals, ranged from 45 to 54 Wh/Kg at the C/3 drain rate for cells made with molded cases and covers. These cells ranged from 5.2 to 5.5 Kg per cells in total weight.

The module design of Figure 2.13 should effect a decrease in average weight of 9 and 14 percent in volume. This would improve the gravimetric energy density per cell to 49 to 59 Wh/Kg for the test cells described. A more detailed design configuration will be developed during FY 82 to confirm these improvements.

The best reactively-sintered Cell 094CE showed improvement over the best pilot line cells, with only 20 percent capacity decline after 650 cycles.

The cell featuring reactively-sintered positive plate fibers, plus the corrugated fiber design (C-CE-01) is performing well, with 9 percent capacity decline at over 400 cycles.

The cells employing pasted positive plates were 731 CP; 732 CP. Cell 731 achieved 684 cycles with 10 percent capacity decline, at which time an internal short developed. Disassembly of the cell determined this was caused by a sludge buildup across the tops of the plates. Cell 732 achieved 697 cycles with 25 percent capacity decline. Disassembly indicated a similar buildup of

TABLE 3.5: FULL-SIZE CELL TEST RESULTS

Cell/Monoblock/ Battery Description[a]	Initial Capacity[c] Ah	Wh	Initial Eff.,[c] % Ah	Wh	Life Characteristics Cycles[d,f]	% Decline[e] Capacity
066CE	195		63		286	44
067CE	199		65		482	49
068CE	196		64		638	58
080CE	159		48		371	35
082CE	193		58		330	48
083CE	227		68		421	58
091CE	175		53		89	42
093CE	222		67		146	50
094CE	203		61		650	20
097CE	203		61		515	31
098CE	202		61		35	26
099CE	201		60		515	32
103CE	216		65		44	25
128CE	239	289	-	53	(325) 413	(20) 80
169CE	225				(233) 556	(23) 27
186CE	189		57		(467) 724	(20) 57
270CE	223		56		(511) 1264	(20) 35
330CE	231		69		328	51
336CE	184		66		384	37
731CP	205		62		600	22
732CP	219		66		610	17
C-CE-01	200		60		>400	9

---

a. Special Feature, Components, Weight (kg) and Volume (l)
b. C/3 Discharge, 3-4 Hour Charge
c. Based on at Least Five Consecutive Cycles
d. "Greater Than" Symbols Denote Continuing Operation
e. Percent Decline from Initial
f. Data on Continuing Cells Effective December 31, 1981

sludge. After cleaning and repacking, this cell will be placed back on cycle-life test. The cells exhibited some increased pressure drop during life cycling.

Figure 3.6 shows the life-cycle history of Cell 270CE which eventually reached 1264 test cycles. This cell suffered an irretrievable loss of 10 Ah after a 2000h open circuit stand at 410 test cycles. At Cycle 650, the cell delivered 167 Ah, at Cycle 511 (including the 10 Ah loss) the cell was still at 80 percent of its initial capacity. Figures 3.7 through 3.11 provide additional performance data at various stages of cycle life.

3.3.2 LOW TEMPERATURE TESTS

Low temperature tests were performed on five cells that were grouped into a module configuration. Each of the cells had been previously bench tested, individually, for three cycles, to determine their capacities, with 30°C electrolyte circulation during charge and 40°C circulation during discharge. The first three cycles of the cells in the module configuration were run to confirm capacity, but with 30°C electrolyte circulation during charge and no circulation during discharge. In these initial ambient temperature cycles, no open circuit time existed between charge and discharge. In the next three cycles, charging was performed in ambient conditions with 30°C circulation, the module was then cooled to -5°C (typically over a 14 hour period), placed into a 0°C water/ice bath, and discharged with no circulation. Three additional test cycles were then run under ambient conditions to confirm capacity. The electrolyte concentration was then increased and the module test schedule was repeated.

In analyzing the data, open circuit losses in the cells at -5°C were assumed to be one-half those at 25°C (this tended to make the temperature effect seem greater). Average discharge potential dropped from 1.23V to 1.17V. Capacity at 0°C was still measured to 1.0V, where capacity losses ranged from 20 to 30 percent, with an averaged decrease of 25 percent. Energy loss averaged 29 percent at 0°C, compared with 25°C. This performance is much better than predicted at the onset of the program, where up to 40 percent loss in capacity was

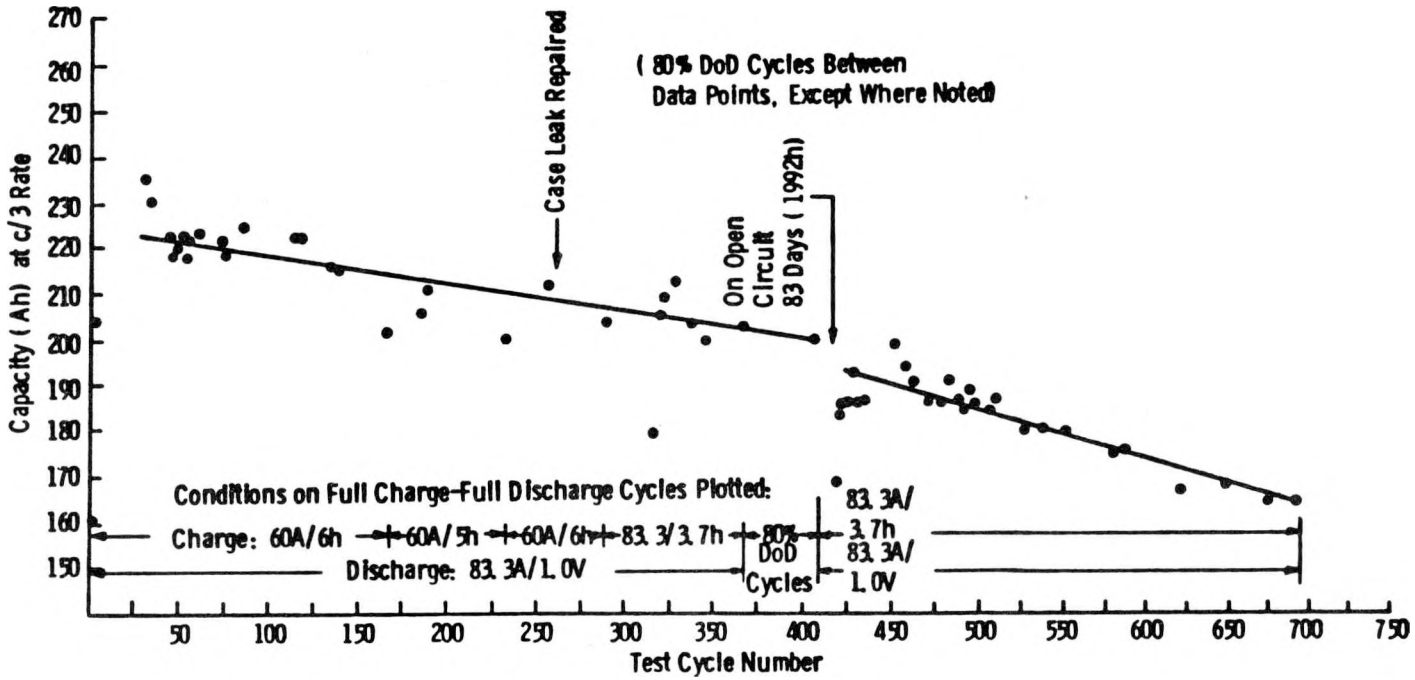

Figure 3.6. Cell 270 CE Life Test Results

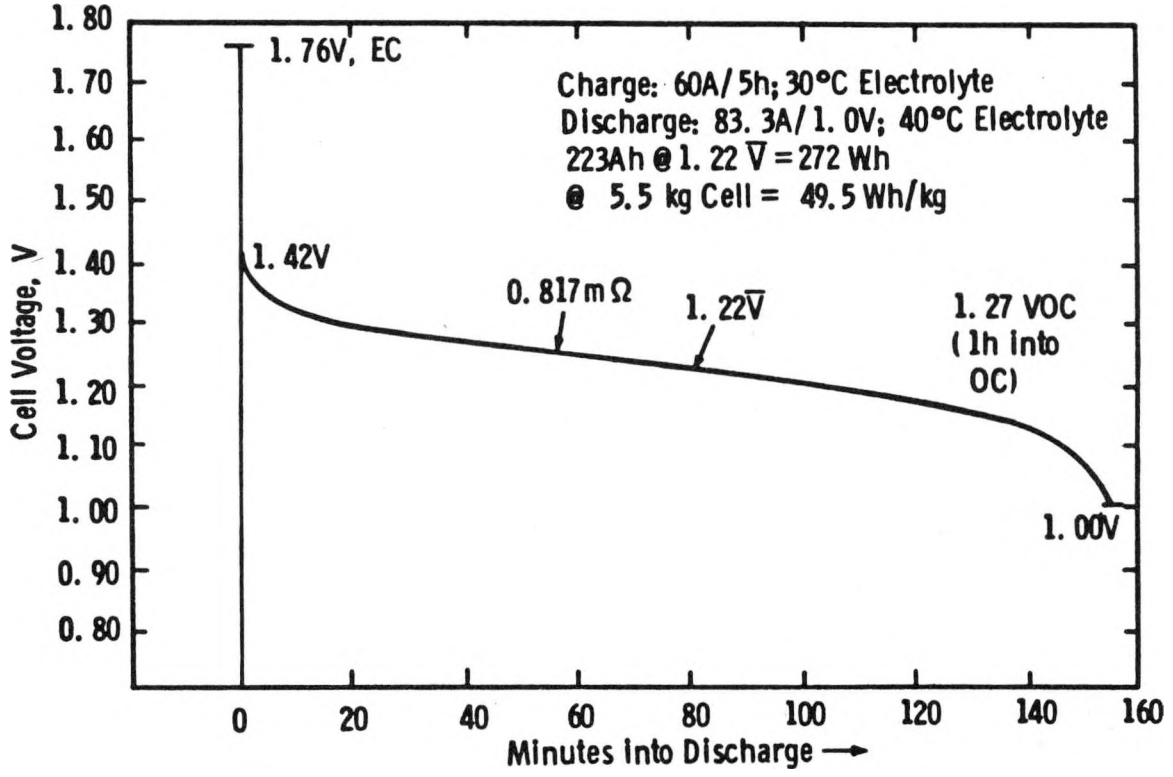

Figure 3.7. Cell 270 CE Cycle 52 Full Discharge Curve

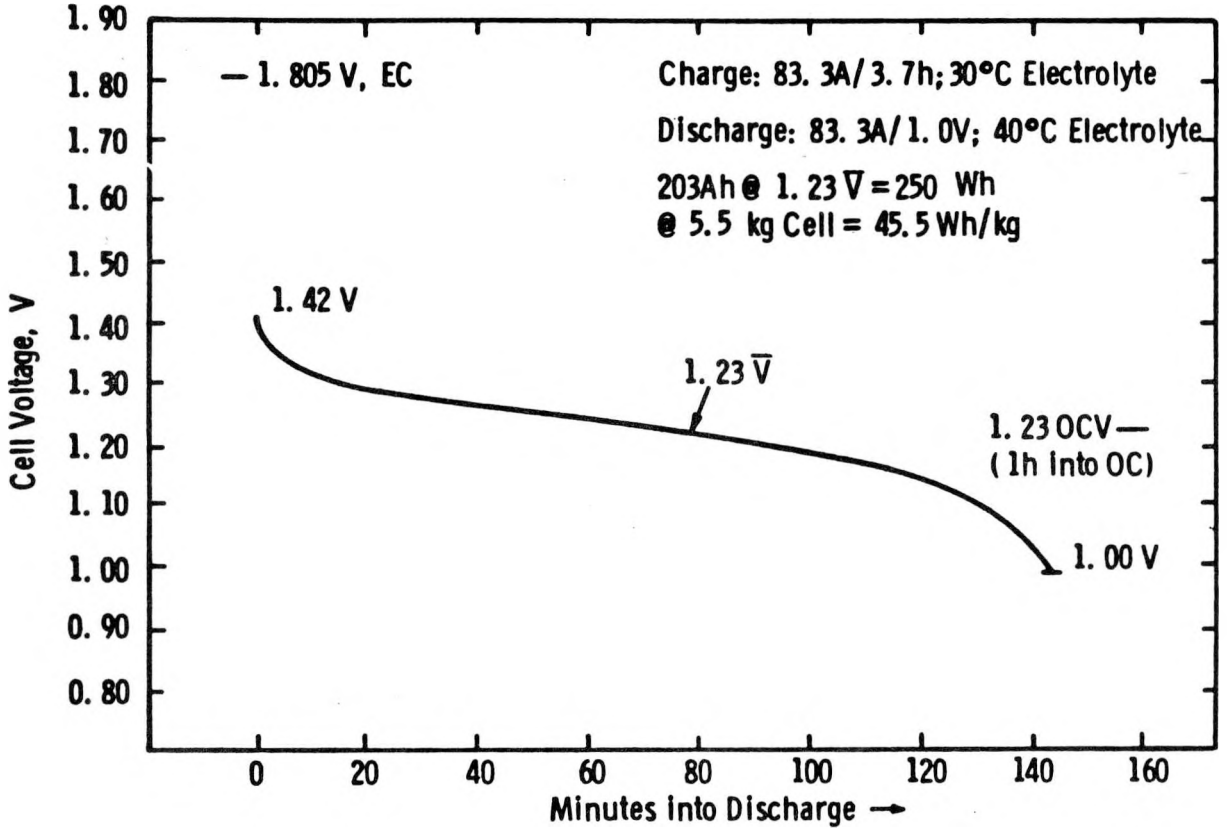

Figure 3.8. Cell 270 CE Cycle 366 Full Discharge Curve

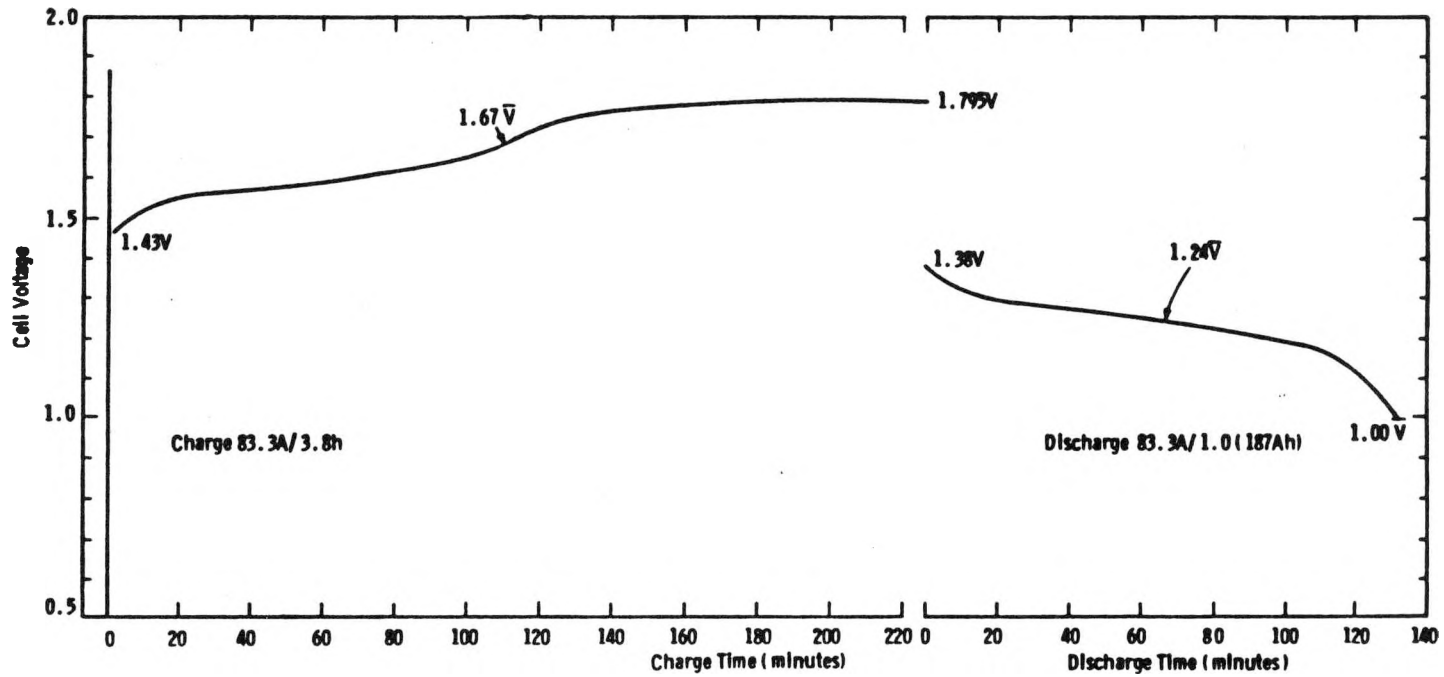

Figure 3.9. Cell 270 CE Cycle 510 Full Discharge Curve

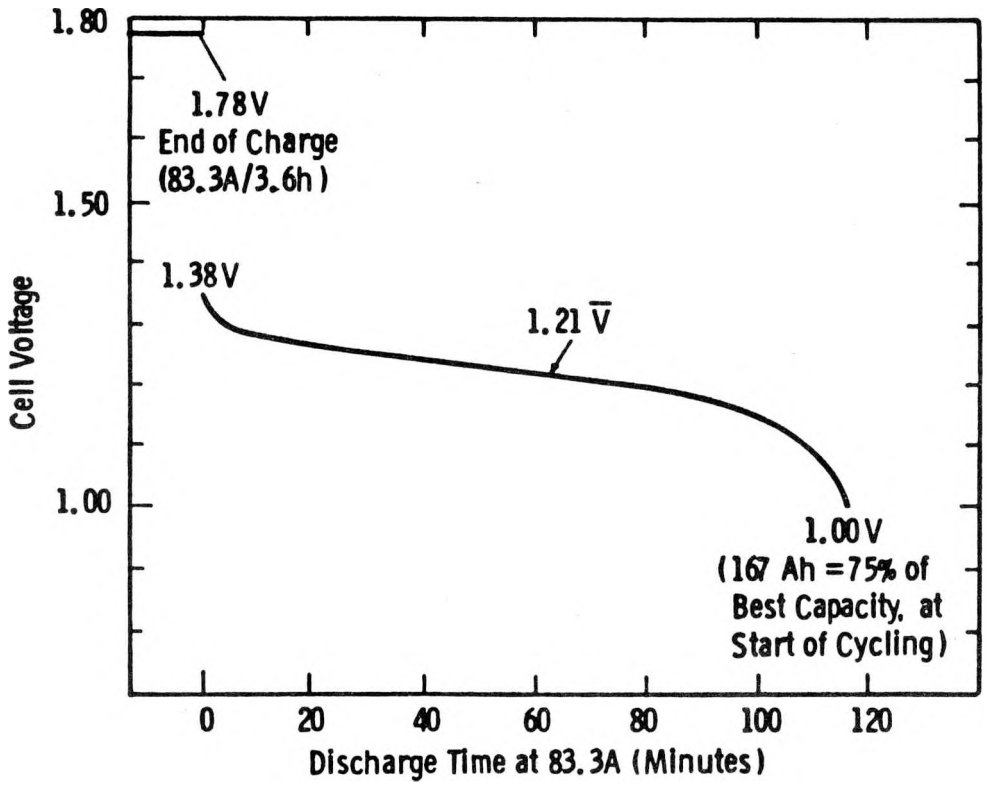

Figure 3.10. Cell 270 CE Cycle 659 Full Discharge Curve

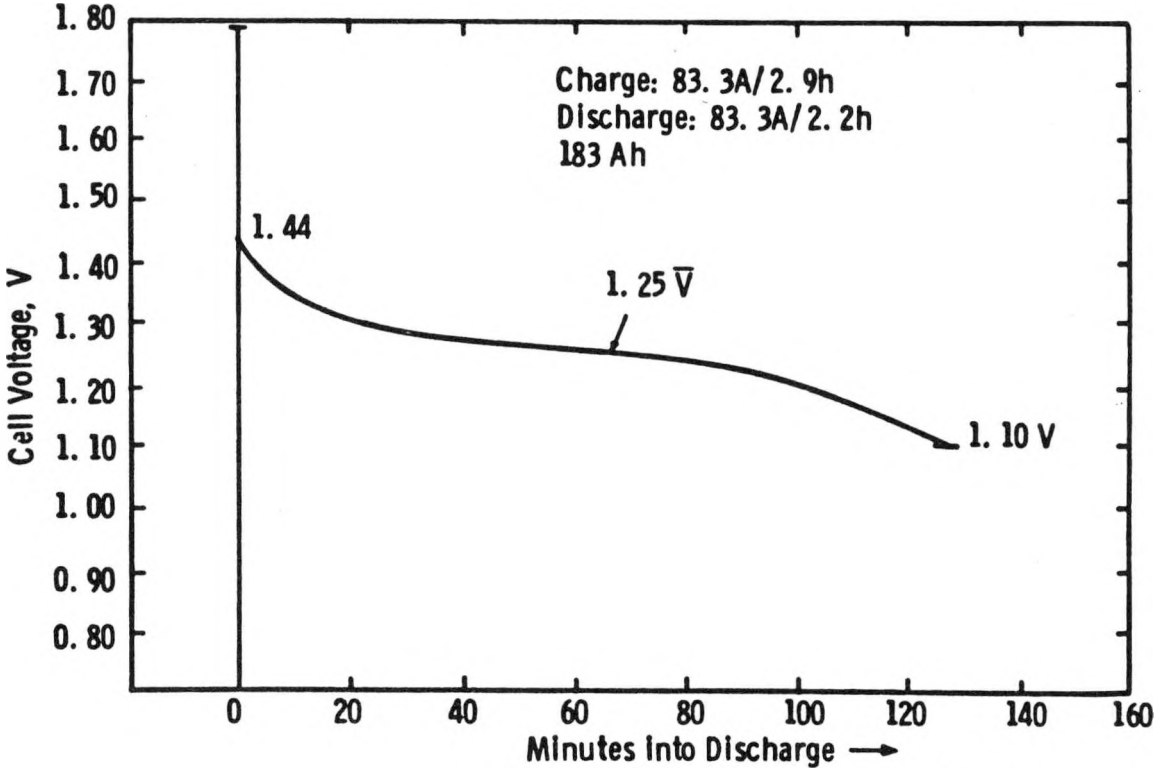

Figure 3.11. Cell 270 CE Cycle 366 80% Depth of Discharge

expected at 0°C, when compared with room temperature capacity. Other cell tests show even better low temperature performance. Only 12 percent decrease in capacity at 0°C and 25 percent decrease at 19°C at the C/3 rate. At the C rate, a 22 percent decrease in capacity was observed at 0°C. Figures 3.12 and 3.13 illustrate these effects.

3.3.3 DISCUSSION OF RESULTS

Initial capacity performance of full-size cells is on target, with 230 Ah per cell at the C/3 rate readily attainable within the cell design volumetric constraint. Gravimetric energy density of full-size cells having the design volumetric constraint, range from 49 to 61 Wh/Kg in finished cells, more typically, 50-54 Wh/Kg. This value can be improved approximately 9 percent with the concepted 6-cell monoblock design. Extended cyclic capability has also been demonstrated, with some cells operating 500 to 800 cycles to date. Low temperature (0°C) performance has exceeded expectations. However, cyclic life test capacity stability is below expectations, with long-cycle test cells showing about 21 percent to 35 percent loss, based on initial capacity. The test cells have shown 20 percent loss in initial capacity at 464 cycles (Cell 186CE) and 511 cycles (Cell 270CE).

Several factors can contribute to nickel-iron cell capacity loss, during long time cycling: (1) stack electrolyte starvation, (2) fiber metal grid corrosion, (3) internal gas pressure on charging, (4) deactivation of the active material, and, (5) excessive CO_3 pickup in the electrolyte.

Stack electrolyte starvation can be caused for several reasons. The first can be due to insufficient porosity in the electrode active material, limiting wicking of electrolyte. This condition, in turn, can cause localized overheating on fast charge (as at the C/3 rate), with irreversible damage to active material and/or poor charge acceptance. Nickel electrode charge acceptance is best at 35-45°C. Dimensional change, due to structural change in the active material during charge-discharge, results in swelling of the nickel electrode in the thickness direction.

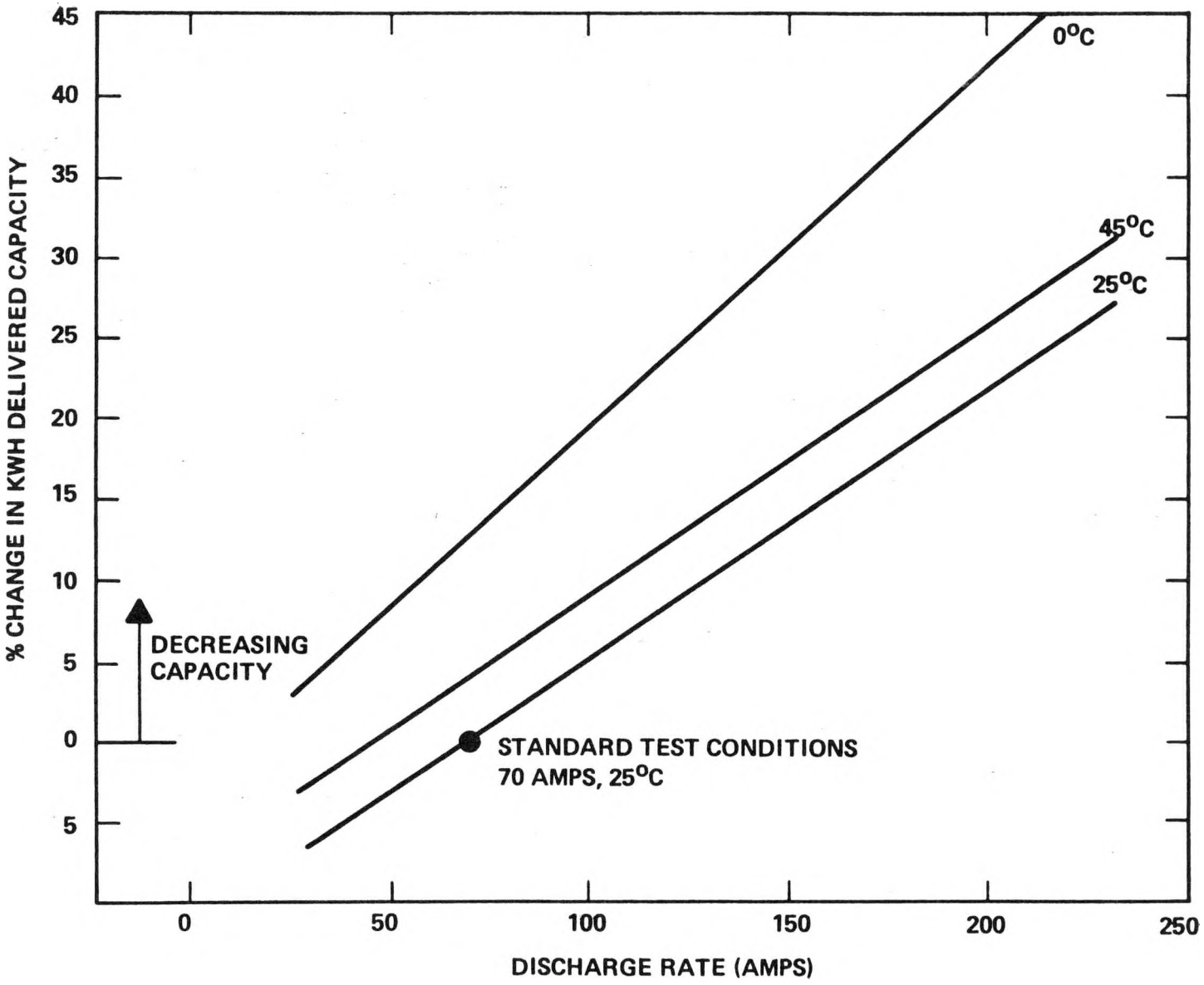

Figure 3.12. Thermal Effects on Wh Capacity

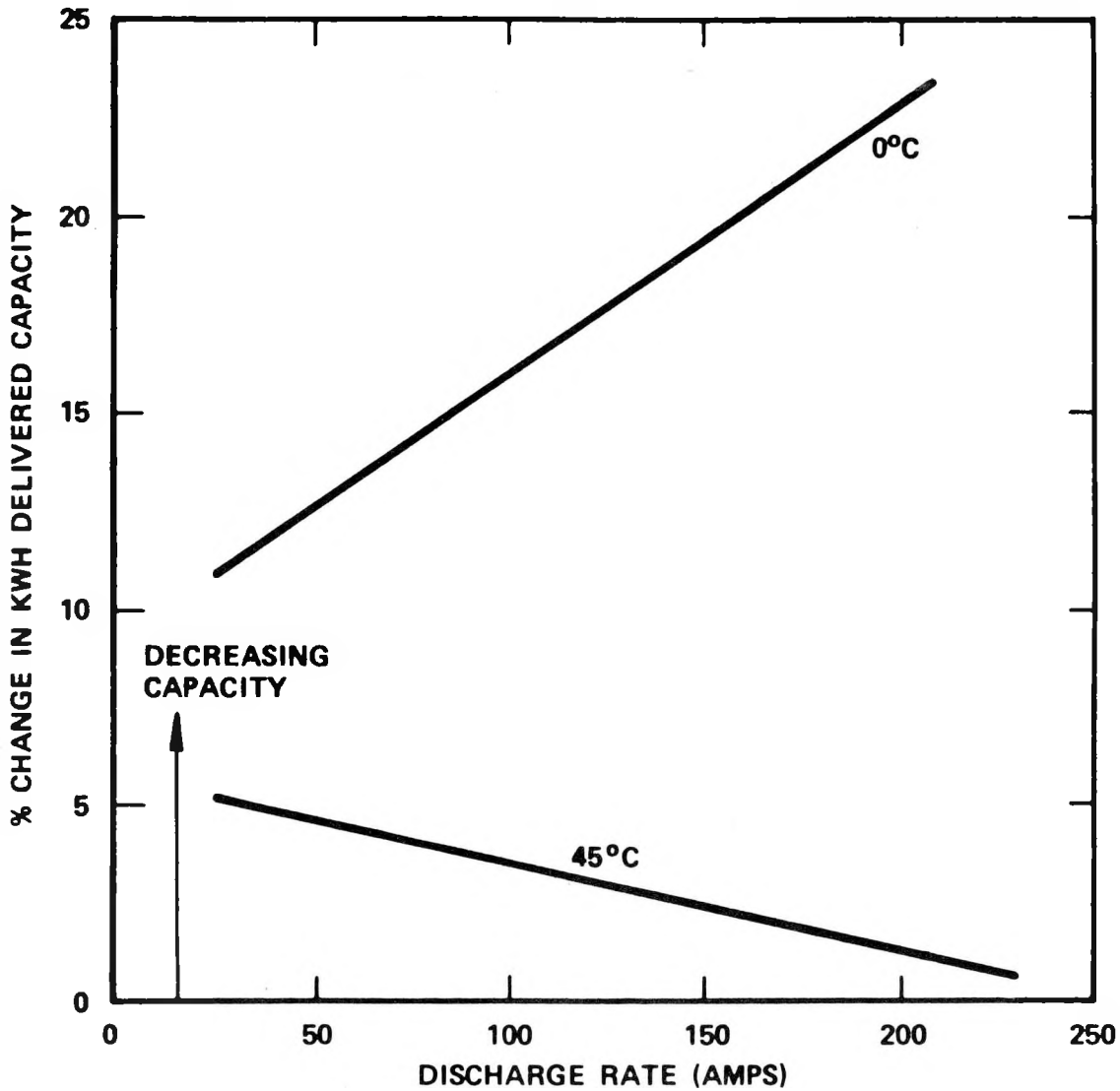

Figure 3.13. Thermal Effects Normalized to 25°C

This swelling can compress and reduce the wicking capability of the separator between the plates, causing localized dry out regions and, possibly, overheating of the active material on charge. It has been determined that a 42 percent volumetric increase is associated with the charge-to-discharge cation (K^+ and Li^+) movement -- in (charge) and out (discharge) of the active material and this, largely, contributes to the dimensional instability of the nickel electrode in the thickness direction.

This swelling, as a function of charge-discharge cycling, is the most critical factor affecting performance and life of cells that contains nickel electrodes. Sintered nickel powder plaques have been developed and used for many years in the industry, (especially for nickel-cadmium batteries) to provide a rigid structure that will resist thickness swelling, but, such structures are inherently expensive, when aimed at a selling price of $80/KWh (1980) in a nickel-iron battery. For this reason, this solution to the nickel electrode swelling problem has been discounted.

Loss of collector grid integrity can be another cause of capacity loss during cyclic life testing of nickel-iron cells. Increasing the mean fiber diameter, nickel plating at higher w/o pickup, relative to the grid, and reactively sintering the nickel electrode and replating with additional nickel are all potential solutions to this problem and are all being actively pursued. Cells with extreme cycling still have displayed nickel electrodes with good structural integrity (>300 cycles), so that grid collector failure does not seem to be a predominant factor, if any, in loss of capacity with cycling.

Deactivation of the nickel electrode active material can occur for several reasons. These include, physical detachment from the grid current collector, (by internal gas pressure and/or corrosion of the grid) thermal damage, dryout and, possibly, loss of water of hydration from the active material. These factors are best controlled by maintaining electrolyte availability, by controlled electrode porosity and electrolyte flow channel control. Thermal damage can be avoided by electrolyte availability during charge and discharge, electrolyte flow on charge, gas bubble release and back-wicking of electrolyte on

discharge. Detachment of active material usually relates to fiber grid corrosion and/or mechanical breakdown of bonds between the fibers (usually a localized condition, only, but significant enough to show up in capacity loss in the electrode and cell).

Carbonate buildup in the electrolyte can occur if it is exposed to air and absorbs carbon dioxide. Maximum permissible concentration is about 50g/l K_2CO_3 in the electrolyte, at which level the electrolyte must be changed. At higher concentration, lower capacity and lower discharge voltage can result, probably due to carbonate having an adverse effect on the iron electrode. Carbonate buildup is avoided by operation in an essentially closed loop system. Gas produced during charge is vented through an isolating water bubbler, which also served to shield the electrolyte reservoir from direct contact with the atmosphere.

In summary, the loss in cyclic capacity of the nickel-iron cells appears to be due, principally, to nickel electrode active material swelling, which is irreversible and can lead to electrode dryout, overheating on charge and permanent deactivation of active material in overheated regions. This problem is being addressed in several areas...optimization of pore volume/active material/grid volume, gassing control, strengthening the grid itself, utilization of grid designs aimed at maintaining thickness integrity and utilization of a paste formulation nickel active material, whose density and chemistry may produce less overall electrode swelling.

3.3.4 CELL POST OPERATION EXAMINATION

Three modules from the first 2 x 4 battery were returned by JPL after thirteen cycles because they had developed defective cells. Two cells appeared to have internal shorts and three had very high charge voltages. The three cells which had been observed to have high charge voltages (172CE, 219CE, 221CE) were found to have inlet tubes blocked with epoxy. Shorts were found in the other two cells (138CE, 146CE). Both shorts were at the top of a positive electrode. The separator, which had been accidentally folded down on assembly, left the top of the electrode bare, allowing the positive electrode to contact and short

to the adjacent negative electrode. Conditions which caused these failures have been alleviated by changing the method of sealing inlet tubes and by using a serpentine wrap to assemble separators.

Module 6-1 was delivered to ANL/NBTL for testing in July 1979. Prior to shipment the capacity of the module was 239Ah to 6.0V at the C/3 rate. Cell 102CE failed at Cycle 34 and Cell 120CE failed at Cycle 100. Each cell was bypassed when it failed so that cycling of the remaining cells could continue. Four cells were tested for a total of 327 cycles, when Cell 107CE failed. Typical capacities obtained at NBTL were:

Cycle	Initial	150	200	250	300	327
Ah	215-220	180	172	165	157	161

The three cells 102CE, 120Ce and 107CE failed because of shorts between adjoining plates. In Cell 102CE the short was due to separator meltdown at the nickel tab region, during TIG welding of the electrode tab to the post comb. The short in Cell 120CE, which occurred at the bottom of the stack, may have been caused by a sharp edge or fiber penetrating through the separator bag that sealed the iron plate.

A new method of fabricating the comb, using bar stock, helps prevent separator meltdown at the electrode tab region. Inspection of electrode edges before assembly insures that no fiber or sharp sheared edge protuberences exist to cause shorts. Serpentine separator wrapping (now being used) will avoid shorts caused by faulty bag sealing.

Table 3.6 summarizes procedures that are used in post operation examination of nickel-iron cells. Table 3.7 summarizes some of the observations recorded during disassembly analysis.

3.4 MODULE TESTS

Figure 2.21 illustrates a typical module concept that was used to construct the batteries this year. It differs from the module constructed and used to build

TABLE 3.6: SUMMARY OF NICKEL-IRON CELL POST OPERATIONS EXAMINATION

Step	Action
(1)	record open circuit voltage
(2)	record cell weight
(3)	cut cell from module with hacksaw, cut open top of manifolds and inspect inlet and outlet tubes
(4)	pour out and bottle electrolyte for analyses, if desired
(5)	cut off case bottom with hacksaw, examine bottom of stack and channel openings, examine case bottom for sediment
(6)	cut off cell cover at joint with hacksaw
(7)	unbolt terminals and remove cover
(8)	examine tubes, separator posts/comb welds
(9)	cut off posts with hacksaw, directly below comb-visually inspect welds
(10)	cut off case body from stack with hacksaw, by cutting at one vertical edge where the most stack to case clearance exists--carefully pry off case from stack
(11)	cut stack binding tapes
(12)	carefully remove electrodes, checking separator external condition
(13)	inspect unbagged nickels, remove bags from outside and central iron and inspect
(14)	measure outer and centrally-located nickel and iron electrodes for thicknesses at corners and between flow channels
(15)	inspect separator layers removed from outer and central iron electrodes for appearance, dryness, overheating, sticking, strength
(16)	store iron and nickel electrodes in separate trays of electrolyte of the same composition as in the test reservoir
(17)	if electrodes are to be post tested for performance, allow excess electrolyte to drip off and seal in plastic bags until ready for 3-plate test assembly

TABLE 3.6: SUMMARY OF NICKEL-IRON CELL POST OPERATIONS EXAMINATION (Cont'd)

Step	Action
(18)	depending on observations, chemical and metallographic procedures may be used to evaluate electrolyte active material for clues to explain observed behavior of module; electrodes should be bagged if long storage periods (>1 day) are anticipated, prior to analyses
(19)	if iron electrodes are to be discarded, they should be allowed to completely oxidize, first in a hood, in a vertical position resting in a tray having 1/2" of water as a heat sink, at least a week, or until it is obvious they have oxidized; allow bottom part to oxidize during this period by inverting the plates

TABLE 3.7: POST OPERATIONS ANALYSIS PROCEDURE FOR NICKEL-IRON CELLS IN MODULES

Cell No.	Construction	Max. Cycle	Capacity Ah	Final Cycle	Final Capacity Ah	Performance	Observations
017CE	Kendall SP126 absorber	32	254	90	121	58 cycles to 100% capacity	Separator & plates in good condition
022CE	0.635 cm holes in nickel plates	20	233	56	182	31 cycles to 100% capacity	Nickel plates expanded to 3.05 mm
023CE	High density steel fibers	49	242	76	147	15 cycles to 100% capacity	Nickel plate channels blocked
025CE	Finer gage steel fiber	2	237	383	153	Cell restraints loosened	Nickel plates expanded to 3.17 mm
026CE	Kimberly-Clark S 49023 absorber	8	250	84	105	18 cycles to 100% capacity	Nickel plates expanded to 3.05 mm
030CE	K-C 49696 absorber No barrier	48	224	48	224	All cycles to 100% capacity	Plate & separators in good condition
031CE	Celgard K-501 Separator	6	246	45	214	All cycles to 100% capacity	Nickel plates soft
032CE	K-C S49023 absorber No barrier	6	212	48	210	All cycles to 100% capacity	Nickel plates tough
038CE	Cross fiber nickels K-C S49033 absorber	2	214	23		All cycles to 100% capacity	Nickel plates expanded to 2.96 mm
042CT	Thermal nickel	25	225	246	137	Loosening cell restraints gave slight improvement	2% iron in nickel active material
050CT	Barium in nickel active material	9	197	263	113	Cycled to 80% of rated capacity	Co in active material of one nickel plate
058CE	19 plates, K-C S 49696 absorber	31	212	130	131		Separators with black residue stuck to plates
060CE	Low porosity nickel plates	2	237	91	100	Low electrolyte flow	Plates and separators very dry
194CE	Celgard 3501 barrier Kendall 263.4 absorber	100	233	355	175	Cell case split on cycles 225, 348, 355	Plates and separators in good condition

the 2 x 4 battery (see Figure 2.7 of the FY '79 Annual Report) for JPL in 1979. Principal construction changes include: location of manifolding at the outside edges of the cell; flexible rubber inlet and outlet manifolds, which seal onto barbed posts coming out of the cell cover; flexible intercell cables that are of the shortest length possible and that are mechanically clamped onto the cell terminal posts.

3.4.1 TEST EQUIPMENT

Figure 2.15 illustrates the three station nickel-iron module tester. Modules are tested with electrolyte circulation on charge and with or without electrolyte circulation on discharge. Figure 3.14 provides a schematic of the electrolyte management system utilized for cyclic tests.

The function of the electrolyte management system (EMS) is to circulate electrolyte to transfer heat generated during the charge and discharge of the electrochemical reaction, carry off all gases, both hydrogen and oxygen, and provide an uniform supply of electrolyte for the reaction.

The EMS system is designed to control the maximum system temperature at 40°C. With a water circulation cooling unit. Appropriate alarms have been established. A low level in the reservoir will energize a yellow "low level" light on the panel to warn of an abnormally low electrolyte level in the reservoir. A red light on the panel will be energized and the pump will be stopped if dangerously low electrolyte level, low electrolyte flow, high pump temperature or an electrolyte spill condition exists. A relay contact will also open to signal the computer that a shutdown has occurred. During the charging operation, gas generated is directed through a separator chamber and a bubbler. This isolates the system from the atmosphere by preventing outside air from entering the system and minimizes carbonate buildup in the electrolyte.

The pump delivers 3.5 to 4.5 gph/cell. Integrally connected in the pump loop are pressure gauges and flow meters, to monitor the pressure and flow to each module. A common thermocouple is installed at the pump outlet to monitor

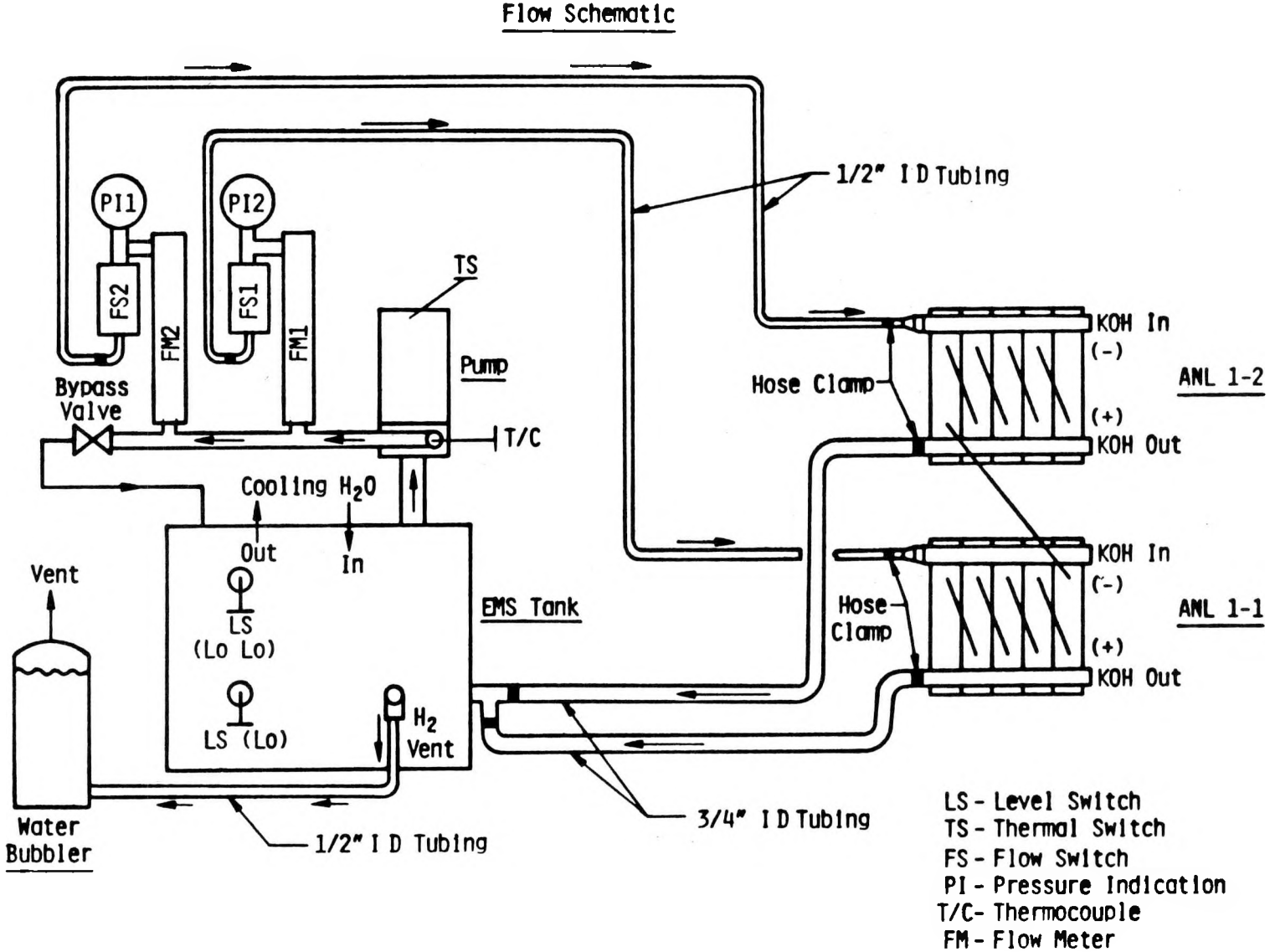

Figure 3.14. Module EMS Test Loop

electrolyte temperature. A bypass valve is incorporated at the end of the flow meter loop to regulate flow to the modules to control temperature.

All data generated at the level switches on the reservoir, flow meter sensors, and pump control are integrally connected to the alarm panel circuit shown in Figure 3.15.

3.4.2 MODULE TEST DATA

The test data generated for Module ANL-1 and ANL-2 are given in Table 3.7 and Table 3.8. The charge efficiency summarized for ANL-1 in Figure 3.9 indicates that the coulombic average efficiency is 72 percent and the watt hour average efficiency is 52.8 percent. Similar results are tabulated in Table 3.10 for ANL-2, giving 68.1 coulombic and 49.5 percent watt hour efficiencies.

The best nickel-iron module data is represented by Modules 5 and 7, which are tested at Argonne National Laboratories, National Battery Test Laboratory. These modules remain on test after 582 cycles at which time they have degraded about 17 percent from their initial capacity. Initial tests conducted by Westinghouse indicated these modules can deliver 53 Wh/Kg and 106-113 Wh/l based on a C/3 drain rate.

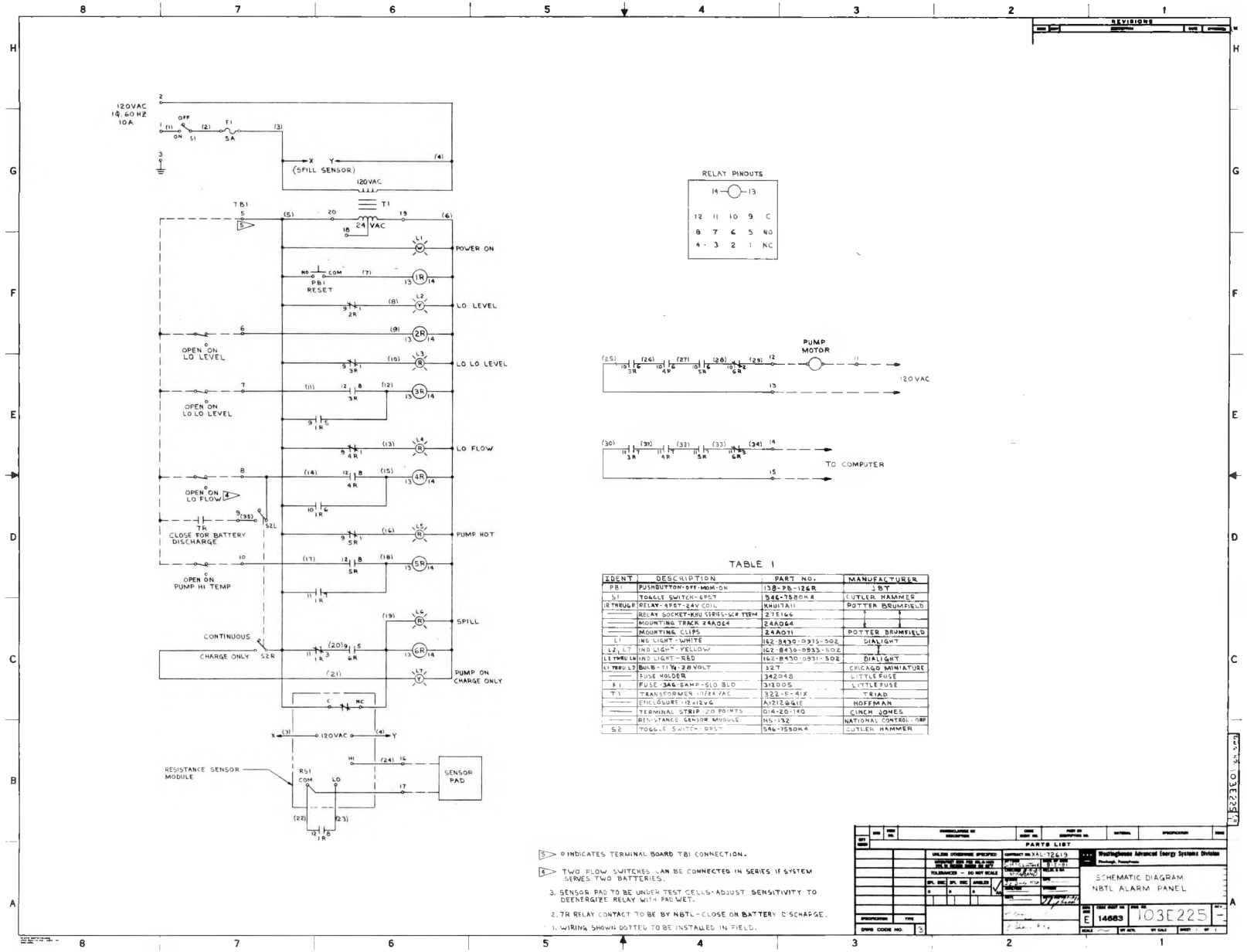

TABLE 1

IDENT	DESCRIPTION	PART NO.	MANUFACTURER
PB1	PUSHBUTTON-OFF-MOM-ON	138-PB-126R	LBT
S1	TOGGLE SWITCH-6PST	346-7880M4	CUTLER HAMMER
1R THRU 6R	RELAY-4PDT-24V COIL	KHU17A11	POTTER BRUMFIELD
——	RELAY SOCKET-KHU SERIES-SCR TERM	27E166	
——	MOUNTING TRACK 24A064	24A064	
——	MOUNTING CLIPS	24A031	POTTER BRUMFIELD
L1	IND LIGHT-WHITE	162-8430-0935-502	DIALIGHT
L2, L7	IND LIGHT-YELLOW	162-8430-0933-502	
L3 THRU L6	IND LIGHT-RED	162-8430-0931-502	DIALIGHT
1, THRU L7	BULB-T1¾-28 VOLT	327	CHICAGO MINIATURE
——	FUSE HOLDER	342048	LITTLE FUSE
F1	FUSE-3AG SAMP-SLO BLO	312005	LITTLE FUSE
T1	TRANSFORMER-117/24 VAC	322-F-41X	TRIAD
——	ENCLOSURE-12x12x6	A1212GGIE	HOFFMAN
——	TERMINAL STRIP-20 POINTS	014-20-140	CINCH JONES
——	RESISTANCE SENSOR MODULE	NS-132	NATIONAL CONTROL-NBP
S2	TOGGLE SWITCH-DPST	346-7530K4	CUTLER HAMMER

5> Ø INDICATES TERMINAL BOARD TB1 CONNECTION.

4> TWO FLOW SWITCHES CAN BE CONNECTED IN SERIES IF SYSTEM SERVES TWO BATTERIES.

3. SENSOR PAD TO BE UNDER TEST CELLS-ADJUST SENSITIVITY TO DEENERGIZE RELAY WITH PAD WET.

2. 7R RELAY CONTACT TO BE BY NBTL-CLOSE ON BATTERY DISCHARGE.

1. WIRING SHOWN DOTTED TO BE INSTALLED IN FIELD.

PARTS LIST

Westinghouse Advanced Energy Systems Division

SCHEMATIC DIAGRAM NBTL ALARM PANEL

CONTRACT No. XAL-72619

SIZE E | CAGE CODE NO. 14683 | DWG. NO. 103E225 | REV. -

DWG CODE NO. 3

M-F223E01 REV 0

Figure 3.15. Alarm Panel Schematic

TABLE 3.8: MODULE ANL-1 TEST DATA

MODULE ID ANL-1

WEIGHT 64 Lb

CELL CYCLE SUMMARY

Cell S/N	Pressure (PSI)	Ri (m Ω)	QC Capacity Ah	QC Capacity Cycles	MODULE CYCLES Cell Voltage at End of Discharge Cycle 1	2	3	4
1466	3.0	.73	235	8	1.03	0.97	0.99	
1464	0.9	.77	232	8	0.98	0.95	1.00	
1458	3.4	.74	242	8	1.05	1.04	1.06	
1443	2.4	.84	235	6	1.08	1.03	1.03	
1437	1.8	.81	232	6	1.08	1.02	1.04	

CHARGE CYCLE DATA	1	2	3	4
Open Circuit Voltage (Volts)	6.77	6.45	6.40	
Charge Current (Amps)	83.3	83.3	83.3	
Total Input (Ah)	336.0	333.0	333.0	
Charge Temperature Start (°F)	73.4	87.1	82.0	
End (°F)	89.6	95.0	95.0	
EMS PSID @ 4.5 gph (Psi) (EOC)	2.9	2.9	2.0	
Voltage - Start of Charge	7.58	7.7	7.81	
End of Charge	8.6	8.57	8.60	

DISCHARGE DATA	1	2	3	4
Discharge Current (Amps)	83.0	83.0	83.0	
Total Discharge Capacity (Ah)	247.0	242.0	239.0	
Module Voltage End of Discharge	5.28	5.01	5.07	
Discharge Temperature Start (°F)	87.8	93.2	90.0	
End (°F)	102.0	100.4	97.0	

TABLE 3.9: MODULE ANL-2 TEST DATA

MODULE ID ANL-2

WEIGHT 70 lb

CELL CYCLE SUMMARY					MODULE CYCLES Cell Voltage at End of Discharge Cycle			
Cell S/N	Pressure (PSI)	Ri (m Ω)	QC Capacity Ah	Cycles	1	2	3	4
1397	2.8	.76	228	10	1.01	1.10	1.07	
1395	3.0	.78	225	10	0.90	1.07	1.00	
1352	6.5	.74	226	10	-.21	0.96	Replaced	
1343	0.9	.79	224	10	0.95	1.08	0.98	
1342	1.3	.79	226	10	0.93	1.07	1.02	
1419	2.2	.70	218	21	-	-	1.09	

CHARGE CYCLE DATA	1	2	3	4
Open Circuit Voltage (Volts)	6.77	6.35	6.34	
Charge Current (Amps)	83.3	83.3	83.3	
Total Input (Ah)	336.0	333.0	333.0	
Charge Temperature Start (°F)	73.4	87.1	84.0	
End (°F)	89.6	95.0	94.0	
EMS PSID @ 4.5 gph (Psi) (EOC)	3.1	3.1	2.0	
Voltage - Start of Charge	6.77	6.35	7.88	
End of Charge	8.66	8.66	8.74	

DISCHARGE DATA	1	2	3	4
Discharge Current (Amps)	83.0	83.0	83.0	
Total Discharge Capacity (Ah)	239.0	222.0	221.0	
Module Voltage End of Discharge	3.59	5.23	5.16	
Discharge Temperature Start (°F)	87.8	93.2	90.0	
End (°F)	102.0	104.0	99.0	

TABLE 3.10: MODULE ANL-1 CHARGE EFFICIENCY

Cycle No.	Ampere Hours Input	Ampere Hours Output	Efficiency %	Watt Hours Input	Watt Hours Output	Efficiency %	Gravimetric Energy Density
1	336	247	73.7	2772.0	1482	53.5	
2	333	242	72.7	2747.5	1452	52.9	
3	333	239	71.8	2747.5	1434	52.8	
		Avg.	72.7	2757.5	1456	52.8	$\frac{WH}{Lb}$ 22.8 / / $\frac{WH}{Kg}$ 50.1

4.0 FUTURE WORK

The development program for FY 82 will be concentrated in the following key areas:

- Grid Structure Development
- Multicell Module Design
- Separator Evaluation
- Performance Evaluation
- Charge Optimization
- Module Fabrication and Development Support
- Program Management

The proposed task milestones are shown in Table 4.1.

4.1 GRID STRUCTURE DEVELOPMENT

The objective of this task is to evaluate improved fiber grid structures for both nickel and iron electrodes. The major thrust should concentrate on evaluation of alternative manufacturing processes for grid structures that have higher conductivity and reduced cost.

At a minimum, this evaluation will include the following:

- o Establish a development plan for the key elements of this task.
- o Assess applicability of the fiber mat structures being developed by National Standard Corporation for use as an electrode substrate and also for potential use as an iron electrode. Performance tests on electrodes and cells should be included in the evaluation.
- o Assess substitute materials for the EXMET presently utilized in the iron electrodes, concentrating on lower cost materials

TABLE 4.1: FY '82 PROPOSED TASK MILESTONES

ALTERNATIVE GRID STRUCTURE

- Establish Development Plan
- Initiate Three (3) Plate Tests
- Initiate Full-Size Cell Tests

MULTICELL MODULE DESIGN

- Establish Development Plan
- Select Concept for Detail Design
- Initiate Proof of Concept Test
- Complete Detail Design

SEPARATOR EVALUATION

- Initiate Cell Tests

PERFORMANCE EVALUATION

- Establish Test Plan
- Demonstrate 800 Cycles Life

CHARGE OPTIMIZATION

- Establish Test Plan
- Specify Charge Procedure

MODULE FABRICATION AND DEVELOPMENT SUPPORT

- Deliver Six (6) 5-Cell Modules to NBTL
- Deliver Four (4) 5-Cell Modules to NBTL

PROGRAM MANAGEMENT

- Submit Updated Program Management Plan
- Submit Summary Manufacturing Cost Analysis
- Submit Draft FY '82 Public Report
- Monthly Progress Reports

that can meet or exceed the present Ah/gm total electrode performance with equivalent or lower electrode resistance.

- Cost estimates of alternative materials shall be provided for pilot and projected commercial manufacturing quantities.

4.2 MULTICELL MODULE DESIGN

The objective of this task is to design a multicell modular package that will result in weight, volume, and cost reductions.

The performance objectives for the multicell modules are:

65 Wh/kg	Gravimetric Energy Density
135 Wh/l	Volumetric Energy Density
130 W/kg	Power Density at 50 percent DOD

The initial effort for this task shall include:

- Establish a design requirement document.
- Establish a development plan addressing the key engineering tasks associated with the initial design.
- Establish appropriate vendor contacts to provide inputs for design areas such as tooling, sealing, etc.
- Identify manufacturing development support required for modular assembly.
- Identify and initiate key materials tests for prototype current collectors, seals, package materials, etc.
- Provide cost estimates of the projected modular design and resultant manufacturing processes and compare to present costs.

4.3 SEPARATOR EVALUATION

The objective of this task is to identify and test alternate separators that show promise of lower resistance and/or lower cost.

Separators with and without barrier materials shall be tested in full size cells if the preliminary engineering evaluations identify the material as a suitable candidate.

4.4 PERFORMANCE EVALUATION

The objective of this task is to perform characterization and life cycle testing of electrodes, cells, modules and batteries, to assess performance levels and demonstrate cycle life objectives.

This task also provides test support for evaluations identified in the other development tasks, i.e., alternate grids, separators, etc.

4.5 CHARGE OPTIMIZATION

The objective of this task is to evaluate charge acceptance characteristics of the nickel-iron system and develop a charge procedure with a minimum watt hour charge efficiency of 70 percent.

This effort will be primarily conducted at the R&D Center under an IWR.

The objectives of this task are to provide modules for testing at NBTL and supply test articles for performance evaluation as required by the other tasks.

4.6 MODULE FABRICATION AND DEVELOPMENT SUPPORT

The objectives of this task are to provide modules for testing at NBTL and supply test articles for performance evaluation as required by the other tasks.

4.7 PROGRAM MANAGEMENT

The objective of this task is to provide overall control of the aforementioned tasks, including schedule and cost, control, and to coordinate these activities with other battery program R&D activities.

5.0 PUBLICATIONS AND PRESENTATIONS

The following publications and presentations have been generated since initiation of this contract.

FY 1979

1. "Westinghouse Iron-Nickel Battery Development," R. Rosey, ACS/CSJ Chemical Congress Symposium, April 1979.

2. "Westinghouse Iron-Nickel Battery Characteristics," R. Rosey Presentation at Second DOE/LLL Workshop on Energy Storage Systems for Automobile Propulsion - Electrochemical Panel, June 1979.

3. "Design of an Iron-Nickel Battery for Electric Vehicles," W. Feduska/ R. E. Vaille, ECS Battery Division Proceedings of the Symposium on Battery Design and Optimization, Vol. 79-1, Edited by S. Gross P. 299-310.

4. "An Advanced Iron-Nickel Battery for Electric Vehicle Propulsion," W. Feduska, et al, Electrochemical Society, October 1979.

5. "Fabrication of High Capacity Nickel Electrodes Using a Pasting Technique," J. Seidel/J. F. Jackovitz, Electrochemical Society, October 1979.

6. "Westinghouse Iron-Nickel Development Program," W. Feduska, panel presentation at Third DOE Battery and Electrochemical Contractors Conference - Session III Near Term Batteries, December 1979.

7. "Research, Development and Demonstration of a Nickel-Iron Battery for Electric Vehicle Propulsion - Annual Status Report for FY 1978," R. Rosey, et al, Public Report ANL Contract No. 31-109-38-4141.

FY 1980

1. "Fabrication of High Capacity Nickel Electrodes Using a Pasting Technique," J. Seidel/J. F. Jackovitz, Electrochemical Society, October 1979.

2. "Westinghouse Nickel Iron Battery Design and Performance," R. Rosey/ B. E. Taber, EV EXPO 1980, May 1980.

3. "An Advanced Technology Iron-Nickel Battery for Electric Vehicle Propulsion," W. Feduska/R. Rosey, Intersociety Energy Conversion Engineering Conference, August 1980.

4. "Annual Report for 1979 on Research, Development and Demonstration of Nickel Iron Batteries for Electric Vehicle Propulsion," Westinghouse Electric Corporation, R. Rosey et al, Public Report ANL Contract No. 31-109-38-4141, June 1980.

FY 1981

1. "Research, Development and Demonstration of a Nickel-Iron Battery for Electric Vehicle Propulsion - Annual Status Report for FY '80," R. Rosey et al, Public Report ANL Contract 31-109-38-4141, March 1981.

2. "Westinghouse Nickel-Iron Technology Features," R. Rosey, 4th DOE Battery and Electrochemical Contractors Conference, June 1981.

3. "Vibrational Spectra of Nickel Hydroxide and Higher Nickel Oxide," J. F. Jackovitz, Westinghouse Internal Publication, September 1981.

4. "Westinghouse Nickel-Iron Battery Performance - 1981," R. Rosey, EVC Symposium VI Proceedings, October 1981.

5. "Alkaline Nickel Electrode Voltage versus Current Performance," N. J. Maskalick, Electrochemical Society Nickel Electrode Symposium Proceedings, October 1981.

6. "Spectroscopic Study of Nickel Electrode Reactions," J. F. Jackovitz, J. Seidel, Electrochemical Society Nickel Electrode Symposium Proceedings, October 1981.

6.0 ACKNOWLEDGEMENTS

The members of the program team who contributed to the work described in this report, and their major areas of responsibility are:

AESD

O. Alfonso	Quality assurance, control and engineering.
A. M. DiCroce	Electrical testing systems, module life test system design and construction, systems testing.
E. D. Goslin	Manufacturing, engineering.
M. Jacobson	Manufacturing and pilot line operation management.
F. P. Malaspina	Product and process development management.
O. V. Montefusco	Electrode plaque process development, EPP pilot line process.
B. R. Nair	Electrolyte management system design.
C. Quinter	Manufacturing, cost analysis, facilities engineering.
R. E. Sabolcik	Pilot line technician supervision.
J. Seidel	Composite iron electrode and process, pasted nickel electrode and process, advanced concept cells.
B. M. Woodle	Component, cell, module and battery design, battery auxiliary systems design.

R&D CENTER

J. F. Jackovitz	Composite iron electrode, pasted nickel electrode.
N. J. Maskalick	EPP nickel electrode process development, advanced EPP concepts.
E. A. Pantier	Pasted nickel electrode development.